UNIVERSIDADE DE SÃO PAULO

SAMUEL SANCHEZ QUEIROZ JARDIM

Tri-reforming of CO_2-rich natural gas: equilibrium analysis and reactor technology evaluation

São Paulo
2020

SAMUEL SANCHEZ QUEIROZ JARDIM

Tri-reforming of CO_2-rich natural gas: equilibrium analysis and reactor technology evaluation

Versão Corrigida

Dissertação apresentada à Escola Politécnica da Universidade de São Paulo para obtenção do título de Mestre em Ciências.

São Paulo
2020

SAMUEL SANCHEZ QUEIROZ JARDIM

Tri-reforming of CO_2-rich natural gas: equilibrium analysis and reactor technology evaluation

Versão Corrigida

Dissertação apresentada à Escola Politécnica da Universidade de São Paulo para obtenção do título de Mestre em Ciências.

Área de Concentração: Engenharia Química

Orientador: Prof. Dr. Rita Maria de Brito Alves
Co-orientador: Dr. José Eduardo Alves Graciano

São Paulo
2020

Este exemplar foi revisado e corrigido em relação à versão original, sob responsabilidade única do autor e com a anuência de seu orientador.

São Paulo, _____ de _____ de _____

Assinatura do autor: _____

Assinatura do orientador: _____

Catalogação-na-publicação

Jardim, Samuel
Tri-reforming of CO2-rich natural gas: equilibrium analysis and reactor technology evaluation / S. Jardim -- versão corr. -- São Paulo, 2020.
94 p.

Dissertação (Mestrado) - Escola Politécnica da Universidade de São Paulo. Departamento de Engenharia Química.

1.Tri-reforming of methane 2.Tri-reforming reactors I.Universidade de São Paulo. Escola Politécnica. Departamento de Engenharia Química II.t.

ACKNOWLEDGEMENTS

I would like to thank God for the gift of life and the inspiration to proceed in this master and also acknowledge the love and support of my family.

My thanks also go to my supervisors, Prof. Ph.D. Rita Alves and Ph.D. José Eduardo, for their advice, assistance, and guidance throughout the development of this master thesis. I also thank my friends and colleagues in the laboratory, for their fellowship, help, advice, and support.

In particular, I acknowledge the financial support of CNPq (Conselho Nacional de Desenvolvimento Científico e Tecnológico) throughout these 2 years of master research. In addition, I would like to thank the sponsorship of Shell and FAPESP through the "Research Centre for Gas Innovation - RCGI" (FAPESP Proc. 2014/50279-4), hosted by the University of São Paulo, and the strategic importance of the support given by ANP (Brazil's National Oil, Natural Gas, and Biofuels Agency) through the R&D levy regulation. I could not forget to mention the University of São Paulo and Escola Politécncia for this opportunity.

"Order, proportions, harmony delight us;
painting and music are samples of these:
God is all order;
he always keeps truth of proportions,
he makes universal harmony;
all beauty is an effusion of his rays."
G. W. Leibniz (Theodicy)

ABSTRACT

JARDIM, S.S.Q.. *Tri-reforming of natural gas rich in CO_2: equilibrium analysis and reactor technology evaluation.* Universidade de São Paulo, 2019.

The tri-reforming of methane was studied for converting natural gas, rich in CO_2, into syngas suitable for the industry. The reaction was evaluated at typical industrial pressure by performance indicators, such as carbon dioxide conversion, syngas yield, syngas ratio, and coke production. Three possible reactor configurations were investigated and compared, seeking industrial applicability and good performance, encompassing the membrane, autothermal and heated reactors. The study employed two approaches: (i) analysis of reaction equilibrium and (ii) simulation of first-principle reactor models. The tri-reforming equilibrium was analyzed varying the chemical composition and temperature at 25 bar, either in adiabatic or isothermal conditions. In turn, the reactor simulations evaluated the behavior of each specific configuration and compared their performance, addressing issues such as coke deposition and temperature profile. The equilibrium data showed the need for high concentration of oxygen in the feed to drive the adiabatic reaction, around 50% of O_2/CH_4 in molar proportion, thus, demanding a special reactor to manage the temperature. The adiabatic data also revealed a trade-off between carbon-dioxide conversion and syngas ratio. However, when the reaction temperature was maintained by an external heat source, the trade-off disappears and performance is enhanced. Concerning the reactor simulations, the results indicated that membrane reactors (for oxygen distribution) for tri-reforming are unsuitable for the industry due to problems with coke deposition. In addition, the reactor comparison showed an outperformance of the heated over the autothermal reactor. It had superior syngas yield and carbon dioxide conversion in the two cases tested. However, when the furnace emission of CO_2 was accounted, the overall conversion of the heated reactor was inferior to the autothermal one. Up to 52% of carbon dioxide conversion was attained by tri-reforming as well as 83% of syngas yield. In summary, the results from the equilibrium data and reactor simulations endorsed the expectations concerning the applicability of tri-reforming to convert syngas from resources concentrated in CO_2, with the caveat concerning temperature and solid carbon deposition.

Keywords: Tri-reforming of methane. Carbon dioxide conversion. Tri-reforming reactors.

RESUMO

JARDIM, S.S.Q.. *Tri-reforming of natural gas rich in CO_2: equilibrium analysis and reactor technology evaluation.* Universidade de São Paulo, 2019.

A tri-reforma do metano foi estudada visando a conversão de gás natural concentrado em CO_2 em gás de síntese (*syngas*) para aplicação industrial. A reação foi avaliada a típicas pressões industriais por indicadores de performance, como conversão de dióxido de carbono, rendimento, razão de gás de síntese e produção de coque. Três possíveis configurações de reatores foram investigadas e comparadas, buscando aplicação industrial e boa performance, abrangendo o reator de membrana, o reator autotérmico e o reator aquecido. O estudo abordou o tema em duas frentes: (i) análise de equilíbrio da reação e (ii) simulação de modelos fenomenológicos dos reatores . O equilíbrio da tri-reforma foi analisado variando-se a composição química e a temperatura a 25 bar, seja em condições adiabáticas ou isotérmicas. As simulações dos reatores avaliaram o comportamento específico de cada configuração, assim como compararam a sua performance, a deposição de coque e o perfil de temperatura. Os dados do equilíbrio mostraram a necessidade de uma grande concentração de oxigênio na alimentação para sustentar a reação adiabática, cerca de 50% molar em relação ao metano. Portanto, fez-se necessário a utilização de reatores especiais para controlar a temperatura. Os dados de equilíbrio também revelaram um *trade-off* entre a conversão de dióxido de carbono e a razão de syngas. Entretanto, quando a temperatura foi sustentada por uma fonte externa de calor, tal *trade-off* desapareceu e a performance foi melhorada. Em relação às simulações dos reatores, os resultados indicaram que a configuração de reator de membrana (para distribuição de oxigênio) é inadequada para aplicação industrial, devido a problemas com a formação de coque. Comparando-se os reatores, o reator aquecido superou o autotérmico em desempenho, considerando os dois casos operacionais testados, tanto na conversão de dióxido de carbono quanto no rendimento de syngas. Contudo, quando a emissão de CO_2 no forno é contabilizada, a conversão total do reator aquecido foi menor do que a do autotérmico. Conversão de até 52% de CO_2 foi obtida pelo tri-reformador, bem como 83% de rendimento do gás de síntese. Os resultados obtidos por equilíbrio e simulações endossaram a expectativa em relação a aplicabilidade da tri-reforma para converter gás natural de fontes ricas em CO_2, com ressalvas em relação à temperatura e ao depósito de coque.

Keywords: Tri-reforma do metano. Conversão de dióxido de carbono. Reatores de tri-reforma.

LIST OF FIGURES

LIST OF TABLES

LIST OF ABBREVIATIONS AND SYMBOLS

Abbreviations

ANP	Agência Nacional do Petróleo, Gás Natural e Biocombustíveis
BR	Bourdouard reaction
CCM	Catalytic combustion of methane
CTM	Coke oven gas
CTM	Water gas shift
DME	Dimethyl ether
DMR	Dry methane reforming
FT	Fischer-Tropsch
GTL	Gas-to-liquids
KOGAS	Korean Gas Corporation
LBFC2828	Water gas shift
LSCF6428	Water gas shift
MD	Methane decomposition
NG	Natural Gas
POM	Partial oxidation of methane
SMR	Steam methane reforming
syngas	Synthesis gas
TRM	Tri-reforming of methane

Symbols

F_i	Molar flow of specie i
X_i	Conversion of specie i
$\Delta H°$	Enthalpy of reaction at standard conditions
ΔH_{TRM}	Reaction enthalpy of TRM

$\delta_{membrane}$	Membrane thickness
$\dot{m}$	Mass flow
η	Viscosity
η_q	Effectiveness factor for reaction q
μ	Chemical potential
$\nu_{i,q}$	Stoichiometric coefficient of specie i in reaction q
$\nu_{i,q}$	Stoichiometric coefficient of specie i
ρ	Density
b	chemical element vector
C	Chemical formula matrix
ξ_q	Extent of reaction q
ζ	Energy transfer efficiency in the reformer reactor
A_t	Cross section area
B_0	Darcy's permeability constant
c_p	Mass heat capacity
D	Diameter
G	Gibbs energy
h	Partial enthalpy
H_{TRM}	Reaction enthalpy of TRM per CH_4 mol converted
J	Molar permeation flux
K_i	Adsorption constant of specie i
K_q	Equilibrium constant of reaction q
k_q	Pre-exponential rate constant of reaction q
MW_i	Molecular weight
n_i	Molar number of specie i
P	Pressure

q''	Heat flux
Q_{comb,CO_2}	Fire energy of the furnace side in the reformer
Q_{TRM}	Heat duty of TRM
R	Universal constant of gases
r_q	Reaction rate of reaction q
S	Selectivity
T	Temperature
V	Volume
Y	Yield
y	Mass fraction
z	Axial coordinate

CONTENTS

1 INTRODUCTION

1.1 INTRODUCTION

Natural Gas is a hydrocarbon mixture mainly composed of methane and is used as an energy source or as raw material for the industry. It is the third most consumed energy source in the world and it is expected to surpass coal as the second after 2030 (5, 6). It emits less greenhouse gases when burnt, it is cleaner than other fossil fuels such as oil and coal and is largely available (7). Natural gas is also used as raw material to obtain valuable industrial products, such as synthetic oil, methanol, hydrogen, and ammonia.

However, some resources provide natural gas of low quality, largely composed of contaminants which restrain its commercialization in the fuel and industrial markets. Carbon dioxide, one of the undesirable components, lowers the calorific power of NG and demands expensive separation units prior to commercialization or industrial employment. Natural gas from biodigesters, for instance, are often composed of 50% in volume of carbon dioxide. In Brazilian exploration sites, the CO_2 composition varies from 8 and 18%, and, in some cases, up to 79% (8) but ANP restricts to 3% the carbon dioxide composition in commercial NG. In addition, the Brazilian NG is usually associated with oil sites (77% of production in 2017), which means that it is often a by-product in exploration. When not commercialized, it is flared, re-injected in the well or even vented. For instance, in 2017, more than 25% of the explored NG was re-injected in the fields and ca. 3% was vented or flared (9).

Natural gas is important for energy and chemical industries but contamination by carbon dioxide makes commercialization difficult, particularly when the market is incipient, as in Brazil. Therefore, the production cost and waste would substantially decrease if technologies that use NG rich in CO_2 were applied without previous separation.

In this scenario, the tri-reforming of methane (TRM) emerges. It is a synergistic combination of reactions that convert both methane and carbon dioxide into synthesis gas (*syngas*, a mixture of H_2 and CO), which is the conventional intermediate to the production of methanol, synthetic oil and dimethyl ether (DME). There are reported conversions of CO_2 and CH_4 up to **80 %** and **95%** in catalytic experiments (4), respectively. TRM combines the reforming reactions of methane (reactions 1.1), steam (SMR) and dry reforming (DMR) and catalytic combustion of methane (CCM). The association of endothermic and exothermic reactions enables adiabatic operation, which reduces the reactor size. Furthermore, it may produce syngas ratio in the range of 1.0 - 2.5, suitable for GTL (Gas-To-Liquid) plants. Compared to steam and dry reforming, TRM is less prone to coke formation because water and oxygen are both carbon oxidants. Therefore, not only is TRM a promising reaction to

produce syngas for GTL, but also to abate CO_2 from NG.

$$SMR:\ CH_{4\,(g)} + H_2O_{\,(g)} \overset{Ni\ cat}{\rightleftharpoons} 3\,H_{2\,(g)} + 1\,CO_{\,(g)} \qquad \Delta H° = 206.3\,kJ/mol \quad (1.1a)$$

$$DMR:\ CH_{4\,(g)} + CO_{2\,(g)} \overset{Ni\ cat}{\rightleftharpoons} 2\,H_{2\,(g)} + 2\,CO_{\,(g)} \qquad \Delta H° = 247.3\,kJ/mol \quad (1.1b)$$

$$CCM:\ CH_{4\,(g)} + 2\,O_{2\,(g)} \overset{Ni\ cat}{\longrightarrow} 2\,H_2O\,(g) + 1\,CO_{2\,(g)} \qquad \Delta H° = -891\,kJ/mol \quad (1.1c)$$

However, TRM is a recent technology that still does not have reported employment in the industry. Since its first proposal by Song and Pan(4), many researchers have developed catalysts and studied possible reactors. It is still a topic for exploration. TRM was analyzed accessing reaction equilibrium data, particularly at atmospheric pressure. However, TRM is expected to reduce its performance at elevated pressure. Thus, if a typical pressure of industrial reformers (20 - 30 bar) is applied, how would TRM behave? Furthermore, how would the difference between an adiabatic and a non-adiabatic operation be?

Another concern is about reactors. Since TRM combines strong endothermic with fast exothermic reaction, reactor design and operation are challenging. Simulations of adiabatic packed-bed reactors have revealed the presence of dangerous hot spots that make it unsuitable for industrial applications. As an alternative, a membrane reactor was proposed by the scientific literature to control the exothermic reaction rate by a slow oxygen distribution. However, aspects of carbon dioxide conversion, coke deposition and oxygen partition were not evaluated. Reactor configurations other than adiabatic packed-bed reactors also need to be accounted for, such as the steam and autothermal reformers.

In this sense, the present study explores some of the gaps presented in the scientific literature. It analyzes TRM under conventional industrial pressure, investigating and comparing possible reactors by a first-principle approach. It is divided into three main parts: (i) Review, (ii) Methods and Models and (iii) Results and Discussions. The first part provides a concise review of TRM reactions and membranes for oxygen distribution. It also discusses the state of the art in modeling and simulation. The second part describes the methods and models employed. Finally, the last part discusses the results of simulations in reaction equilibrium and reactors for TRM.

1.2 OBJECTIVES

The main objective is to explore the applicability of tri-reforming of CO_2-rich natural gas at industrial conditions. The specific objectives are:

I. Evaluating the influence of operational conditions on TRM at usual industrial pressure of reformers, concerning

i. CO_2 conversion,

ii. syngas yield and composition,

iii. coke yield;

II. Investigating and comparing three configurations of reactors, seeking

i. the best conversion of NG feed rich in CO_2,

ii. best productivity.

Part I

Review

2 BACKGROUND

This chapter provides background information about tri-reforming of methane and the conventional reforming reactors, before a deeper analysis of the equilibrium data. The first section overviews reactions, catalysts, and mechanisms of tri-reforming. The second section concisely describes two conventional reactors for methane reforming, steam, and autothermal reformer. The last section deals with a membrane for oxygen distribution. Two types of membrane are discussed, the dense and the porous ceramic. The porous ceramic will be applied to the membrane reactor model to permeate oxygen into the catalytic bed.

2.1 TRI-REFORMING OF METHANE

2.1.1 Reactions

Before studying TRM by equilibrium data, it is worth mentioning important reactions that occur simultaneously in the catalytic bed (equations 2.1).

$$SMR:\ CH_{4\,(g)} + H_2O_{\,(g)} \overset{Ni\ cat}{\rightleftharpoons} 3\,H_{2\,(g)} + 1\,CO_{\,(g)} \qquad \Delta H° = 206.3\,kJ/mol \quad (2.1a)$$

$$DMR:\ CH_{4\,(g)} + CO_{2\,(g)} \overset{Ni\ cat}{\rightleftharpoons} 2\,H_{2\,(g)} + 2\,CO_{\,(g)} \qquad \Delta H° = 247.3\,kJ/mol \quad (2.1b)$$

$$POM:\ CH_{4\,(g)} + 0.5\,O_{2\,(g)} \overset{Ni\ cat}{\longrightarrow} 2\,H_{2\,(g)} + 1\,CO_{\,(g)} \qquad \Delta H° = -35.6\,kJ/mol \quad (2.1c)$$

$$CCM:\ CH_{4\,(g)} + 2\,O_{2\,(g)} \overset{Ni\ cat}{\longrightarrow} 2\,H_2O\,(g) + 1\,CO_{2\,(g)} \qquad \Delta H° = -891\,kJ/mol \quad (2.1d)$$

$$WGS:\ H_2O_{(g)} + CO_{\,(g)} \overset{Ni\ cat}{\rightleftharpoons} H_{2\,(g)} + CO_{2\,(g)} \qquad \Delta H° = -41\,kJ/mol \quad (2.1e)$$

$$MD:\ CH_{4\,(g)} \overset{Ni\ cat}{\rightleftharpoons} 2\,H_{2\,(g)} + C_{\,(s)} \qquad \Delta H° = 74.6\,kJ/mol \quad (2.1f)$$

$$BR:\ 2\,CO_{\,(g)} \overset{Ni\ cat}{\rightleftharpoons} CO_{2\,(g)} + C_{\,(s)} \qquad \Delta H° = -172.4\,kJ/mol \quad (2.1g)$$

Water Gas Shift (WGS) reaction (reaction 2.1e), for example, is responsible for adjusting the syngas composition (syngas ratio). Processes that require high hydrogen concentration, as ammonia plants often employ specific WGS reactors to convert the syngas CO into H_2 and CO_2. Another important reaction is the Catalytic Combustion of Methane (reaction 2.1d), which is supposed to occur rather than *direct* partial oxidation (POM). The observed POM (reaction 2.1c) would be, according to this hypothesis, the *indirect* result of CCM followed by SMR and DMR (reactions 2.1a and 2.1b). Methane Decomposition (MD) and Bourdouard Reaction (BR), in turn, are crucial to reactors (reactions 2.1f and 2.1g) because they produce the solid carbon that deposits on the catalyst surface, deactivating it. As a result, their suppression is crucial for long term operations.

A common characteristic of reforming reactions is their severe operational temperature. They are carried out at temperatures above 700 °C, which require special material structures,

such as refractory chambers and special metal alloys. The requirement for high temperature can be explained by Figure 1. The reforming reactions, SMR and DMR, become spontaneous only at temperatures higher than 600°C. Not only they require high temperatures to operate but also require substantial heat supply due to their endothermicity.

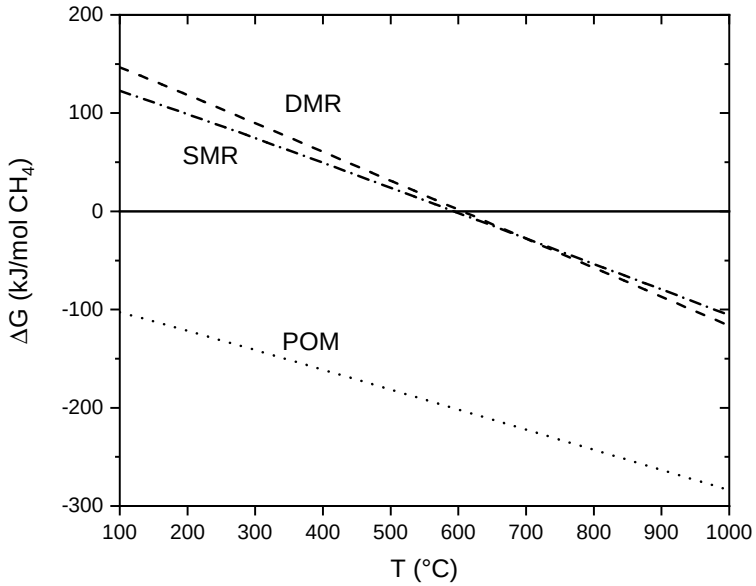

Figure 1 – Variation of ΔG of TRM reaction as a function of temperature in the form of an Ellingham - type diagram.

Source: The author's.

2.1.2 Catalysts

The transitional metals Ni, Pd, Pt, Ir, Rh catalyze reforming reactions, including tri-reforming. Noble metals have higher activity and are stabler but their elevated cost hinders industrial application. Nickel, instead, is much cheaper and widely used in reformers, albeit less active and more susceptible to coke deposition. In conventional steam reformers, Nickel supported on Al_2O_3 catalysts are commonly employed, offering continuous operation over 5 years (> 50,000 h) (10). In autothermal reformers, which subject catalysts to higher temperature and pressure, Ni supported in a magnesia-alumina has shown high stability and activity (11). Song and Pan(4) demonstrated that Ni/MgO, Ni/MgO/CeZrO and Ni/Al_2O_3 catalysts are active and selective for TRM. New catalysts and promoters for TRM are in an active field of research, which seeks improvements in activity, selectivity and coke suppression. A collection of them can be found in the review by Amin et al.(12).

2.1.3 Mechanism

Tri-reforming of methane does not have a detailed mechanistic study yet. However, mechanisms for DMR and SMR can serve as a guide to understand how reforming reactions

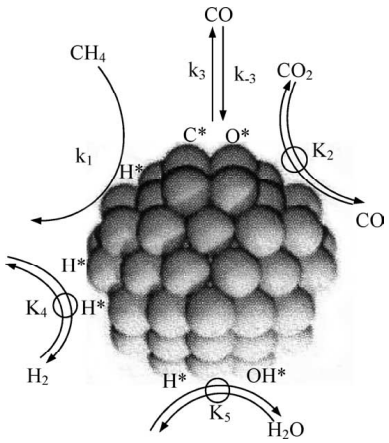

Figure 2 – Reforming mechanism on metal surface.

Source: (13).

occur. In this brief overview, the mechanism proposed by Wei and Iglesia(13) is described, despite many others being available in the scientific literature.

$$CH_4 + 2* \rightarrow CH_3^* + H^* \tag{2.2a}$$
$$CH_3^* + * \rightarrow CH_2^* + H^* \tag{2.2b}$$
$$CH_2^* + * \rightarrow CH^* + H^* \tag{2.2c}$$
$$CH^* + * \rightarrow C^* + H^* \tag{2.2d}$$
$$CO_2 + 2* \rightleftharpoons CO^* + O^* \tag{2.2e}$$
$$C^* + O^* \rightleftharpoons CO^* + * \tag{2.2f}$$
$$CO^* \rightleftharpoons CO + * \tag{2.2g}$$
$$H^* + H^* \rightleftharpoons H_2^* + * \tag{2.2h}$$
$$H_2^* \rightleftharpoons H_2 + * \tag{2.2i}$$
$$H^* + O^* \rightleftharpoons OH^* + * \tag{2.2j}$$
$$OH^* + H^* \rightleftharpoons H_2O^* + * \tag{2.2k}$$
$$H_2O^* \rightleftharpoons H_2O + * \tag{2.2l}$$

The mechanism of SMR and DMR can be divided into three main steps: (i) reactants adsorption, (ii) surface reaction and (iii) desorption, as shown in Figure2 and Equations 2.2, where * is the reactive site and N* is the adsorbed chemical component. Methane is chemically adsorbed by two vacant sites on the metallic surface, resulting in a transition state ($H_3C^* - H^*$). The hydrogen-carbon bond is broken and the first hydrogen is abstracted from methane (reaction 2.2a). This step is suggested to be the slowest and the **determinant**

in the overall reaction. The sequential hydrogen extractions occur faster until elemental carbon is formed (reactions 2.2a - 2.2d). However, adsorbed oxygen, derived from water and carbon dioxide (reactions 2.2e and 2.2j), reacts with carbon (reaction 2.2f), resulting in CO, which further desorbs. Conversely, the adsorbed hydrogens, from water and methane, react with each other, forming the hydrogen molecule. Most elementary steps are fast and near to equilibrium, except the first hydrogen abstraction (reaction 2.2a) and the carbon monoxide formation (reaction 2.2f).

In POM, three different mechanisms may occur depending upon the coverage of catalytic sites, according to Chin and Iglesia(14). For small oxygen coverage, the mechanism is similar to the SMR and DMR; methane decomposition is followed by the oxidation reactions. However, when the oxygen coverage is substantial, new intermediate species may appear, such as CH_3^* and OH^* or CH_3O and OH^*.

2.1.4 Reaction Kinetics

Despite many kinetic models for SMR and DMR, there is not a complete set of validated kinetic equations for TRM, despite efforts in the literature (4, 15). Since the reaction system can be described by at least three independent reactions, a set composed of well-known equations for SMR and CCM is often used for TRM and POM reactions (16, 17, 18, 19). The same strategy is adopted here, using the kinetic rates of Xu and Froment(2) and Trimm and Lam(3).

Xu and Froment developed intrinsic kinetics for SMR in 1989, which is well validated and widely used in the literature. The experiments were conducted at a pressure range of 3 - 15 bar and temperature of 573 to 848 K with $Ni/MgAl_2O_3$ catalyst pellet (0.18-0.25 mm). The reactions rates for SMR (r_1), SMR2 (r_2) and WGS (r_3) are shown in Table 1 and the adsorption and kinetic parameters in Tables 2 and 3.

Trimm and Lam performed a kinetic study for the Catalytic Combustion of Methane on a Pt/Al_2O_3–based catalyst (3), in the temperature range of 773 to 873 K. To apply them in Ni-based catalyst, the adsorption parameters must be adapted. The kinetic parameters and reaction rates for CCM are in Tables 2 and 3.

Using a set composed of different kinetics to model TRM has some drawbacks. Some adsorption factors are absent. For example, SMR kinetics does not consider the adsorption of oxygen or carbon dioxide and CCM lacks the adsorption terms of other components besides methane and oxygen. Moreover, the experiments were done in different conditions. The SMR rates present partial pressure of hydrogen in the denominator, which constrains the feed to have at least small concentration to avoid infinity rates. In practice, hydrogen

Table 1 – Reaction rates used for TRM. Reactions SMR, SMR2, WGS are derived from (2) and CCM from (3).

Reaction	**Rate**
$CH_{4\,(g)} + H_2O_{\,(g)} \overset{Ni\ cat}{\rightleftharpoons} 3\ H_{2\,(g)} + 1\ CO_{\,(g)}$	$r_{SMR1} = \frac{k_1}{P_{H_2}^{2.5}}\left(P_{CH_4}P_{H_2O} - \frac{P_{H_2}^3 P_{CO}}{K_1}\right)\cdot\frac{1}{\alpha^2}$
$CH_{4\,(g)} + 2H_2O_{\,(g)} \overset{Ni\ cat}{\rightleftharpoons} 4\ H_{2\,(g)} + 1\ CO_{2\,(g)}$	$r_{SMR2} = \frac{k_2}{P_{H_2}^{3.5}}\left(P_{CH_4}P_{H_2O}^2 - \frac{P_{H_2}^4 P_{CO_2}}{K_2}\right)\cdot\frac{1}{\alpha^2}$
$H_2O_{(g)} + CO_{\,(g)} \overset{Ni\ cat}{\rightleftharpoons} H_{2\,(g)} + CO_{2\,(g)}$	$r_{WGS} = \frac{k_3}{P_{H_2}}\left(P_{CO}P_{H_2O} - \frac{P_{H_2}P_{CO_2}}{K_3}\right)\cdot\frac{1}{\alpha^2}$
	where $\alpha = 1 + K_{CO}P_{CO} + K_{H_2}P_{H_2} + K_{CH_4}P_{CH_4} + K_{H_2O}\frac{P_{H_2O}}{P_{H_2}}$
$CH_{4\,(g)} + 2\,O_{2\,(g)} \xrightarrow{Ni\ cat} 2\ H_2O\ (g) + 1\ CO_{2\,(g)}$	$r_{CCM} = \frac{k_{1a}P_{CH_4}P_{O_2}}{(1 + K_{CH_4}P_{CH_4} + K_{O_2}P_{O_2})^2} + \frac{k_{1a}P_{CH_4}P_{O_2}}{1 + K_{CH_4}P_{CH_4} + K_{O_2}P_{O_2}}$

is always present because feed is often partially composed of a recycling stream. Also note that the SMR2 is a linear combination of the SMR and WGS, although the SMR could be described only by two reactions. Concerning errors in the adaptation of Pt to Ni-based catalysts for CCM, they are not expected to significantly affect the predictions because the combustion is extremely fast compared to other rates.

Table 2 – Kinetic parameters of TRM derived from (2) and (3).

Reaction rate	Equilibrium constant, K_j	k (mol/kgcat s)	E (kJ/mol)
SMR1	$K_I = exp\left(\frac{-26,830}{T}\right) + 30.114$ bar^2	1.17e+15 bar$^{0.5}$	240.10
SMR 2	$K_{II} = K_I \cdot K_{III}$ bar^2	2.83e+14 bar$^{0.5}$	243.90
WGS	$K_{III} = exp\left(\frac{4,400}{T} - 4.036\right)$ bar^2	5.43e+05 bar^{-1}	67.13
CCM		a: 8.11e+15 bar^{-2} b: 6.82e+15 bar^{-2}	86.00 86.00

Source: (2, 3).

Table 3 – Van't Hoff parameters for specie absorption for the kinetics of TRM.

Components	$K_{a,i}$ (bar^{-1})	Δ H$_i$ (kJ/mol)
CH_4	6.65e-04	-38.28
CO	8.23e-05	-70.65
H_2	6.12e-09	-82.9
H_2O	1.77e+05	88.68
CH_4 (combustion)	1.26e-01	-27.3
O_2 (combustion)	7.78e-07	-92.8
$K = K_{a,i} \cdot exp\left(\frac{-\Delta H}{RT}\right)$		

Source: (2, 3, 17).

Diffusion resistance in catalyst porous is severe in reformers. Xu and Froment(20) calculated the effectiveness factor for the three reaction rates in a conventional catalyst pellet. The

intrinsic reaction rates were reduced by almost 100 times ($\eta \sim 1E-02$) due to intra-particle diffusion. Even though some authors ignored intra-particle resistance, most of them obtained values in the same range as Xu and Froment, as shown by Pantoleontos, Kikkinides and Georgiadis(21). For catalytic partial oxidation (POM), Groote and Froment(17) suggested average values for the four reactions: $\eta_{SMR1} = 0.07,\ \eta_{SMR2} = 0.06,\ \eta_{WGS} = 0.7,\ \eta_{CCM} = 0.05$. The effectiveness factors were close to Xu and Froment and were used extensively in POM and TRM simulations (22, 23, 24, 25, 26, 19). For autothermal and secondary reformer catalysts, even lower effective factors were calculated, reducing intrinsic rates by almost 1000 times (27, 28).

2.2 CONVENTIONAL REFORMERS

In order to evaluate possible configurations of TRM reactors, it is important to know how two of them already operate in the industry. This section briefly describes the conventional steam methane reformer and autothermal reformer.

Steam Methane Reformer and Autothermal are well-established technologies for converting methane into syngas. Conventional steam reformers are composed of a large furnace that provides heat to packed bed tubes, where the reactions occur. In turn, autothermal reactors operate adiabatically, comprising two internal sections for reaction, one for homogeneous and another for catalytic reactions. The operation of the reformer unit is intrinsically dependent on downstream processes. For example, Fischer-Tropsch and Methanol require the syngas ratio of around 2, but DME and higher alcohols demand the syngas ratio of around 1. In large scale natural gas conversion plants, up to 60% of the capital investments are destined to syngas production and cleaning units (29). Therefore, improvements in the reactor design would result in a large impact on methanol, Ficher-Tropsch and DME plants.

2.2.1 Steam Methane Reformer

Steam reforming of methane is a strongly endothermic reaction that converts steam and methane to obtain syngas with H_2/CO around 3 (reaction 1.1a). The conventional reactor comprises fixed bed tubes with Ni-based catalyst, heated up by an external furnace. Figure 3 shows a schematic configuration of the reformer reactor and Figure 4, a typical steam reformer unit. The reactor operates at pressures above 20 bar and temperature varying between 500 to 900 °C (10). Feed proportions between 2.5 and 3 of H_2O/CH_4 are usually applied because the reforming reactions are prone to deposit coke on the catalyst surface (10). The reactor is often composed of thermal resistant tubes (Ni alloy), with 15 m in height and 0.12 m in diameter (30).

Heat transference is crucial to conventional reformers. Energy is transferred to tubes by

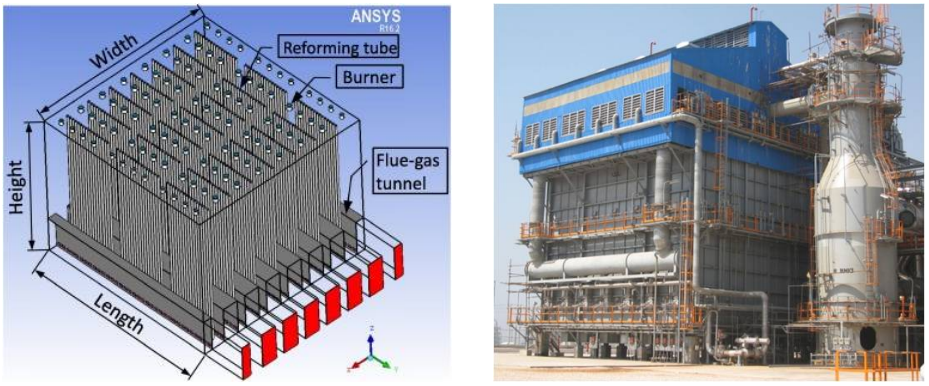

(a) Virtual representation (b) Industrial

Figure 3 – Conventional steam methane reformer

Source: (31, 32)

radiation, burning a mixture of CH_4, air, H_2, CO_2, CO. About 50% of the firing heat is effectively transferred to reaction (29). As a consequence of the operation severity, the lifetime of the metallic tube material is very sensitive to the temperature of its wall (33). The tube temperature restricts operation, limiting wall temperature to 950 °C in the old metals alloys and up to ca. 1050 °C in the new ones (11).

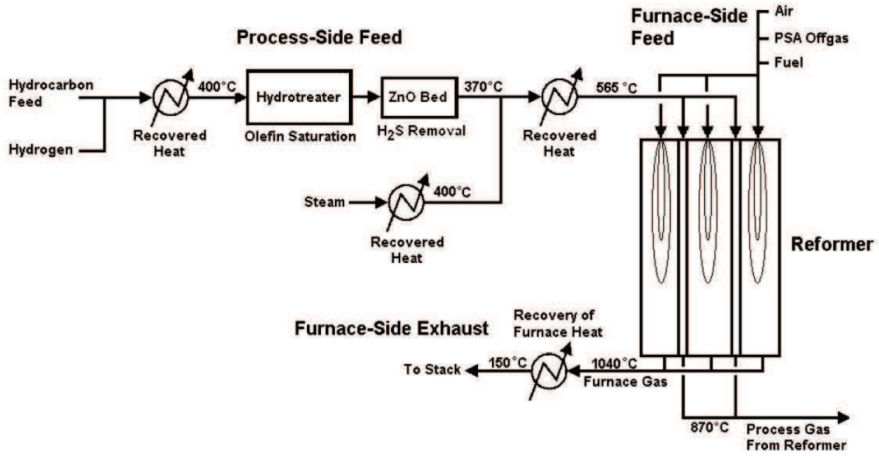

Figure 4 – Representative process diagram of a conventional SMR unit.

Source: (34)

2.2.2 Autothermal Reformer

Autothermal reforming is a combination of SMR and homogeneous POM. The reactor is smaller than a conventional steam reformer (Figure 5) and the syngas ratio obtained is around 2. The adiabatic reactor is composed of two chambers. The refractory chamber is for the homogeneous partial oxidation of methane and is followed by a catalytic section where SMR occurs. The important issue in the homogeneous chamber is to produce turbulent

flames that mix the reactants and prevent soot. With oxygen feed of O_2/ CH_4 0.55-0.6, the temperature can reach 2000 °C in the core flame and 1100-1400°C in the inlet of the catalytic section (11). The catalytic bed is composed of Ni on magnesia-alumina spinels and the reaction is controlled by film diffusion. Although an autothermal is much smaller than a steam reformer, demanding less capital investment, the requirement of an oxygen plant may reduce the economic advantages. Up to 40% of the costs of an ATR plant is estimated to relate to the oxygen unit (29).

(a) Virtual representation (b) Industrial

Figure 5 – Conventional autothermal reformer

Source: (35, 36)

2.3 MEMBRANES FOR OXYGEN DISTRIBUTION

Membrane reactors are used to deliver or to withdraw chemical species in the reaction mixture, boosting performance and controlling kinetics. Among many applications, membranes can improve selectivity, control reaction rates and also shift reaction equilibrium. In this work, a membrane is used to distribute oxygen to the reaction mixture. Two types of ceramic membranes accomplish this objective, the **dense** perovskite membranes (perfect selective) and **porous** alumina membranes (high permeable). This section briefly describes their main features and discusses which is more suitable for the membrane reactor.

2.3.1 Dense Membranes

Due to its ionic and electronic conductivity, dense perovskite membranes have been studied for oxygen separation units, solid oxide fuel cells, and membrane reactors. The oxygen permeation is enhanced at high temperatures, which makes it also suitable for oxidative reactions (exothermic). Air Products, for example, developed oxygen separation units based on wafer membranes modules and Praxair coupled oxidative process with perovskite membrane modules (37, 38, 39, 40).

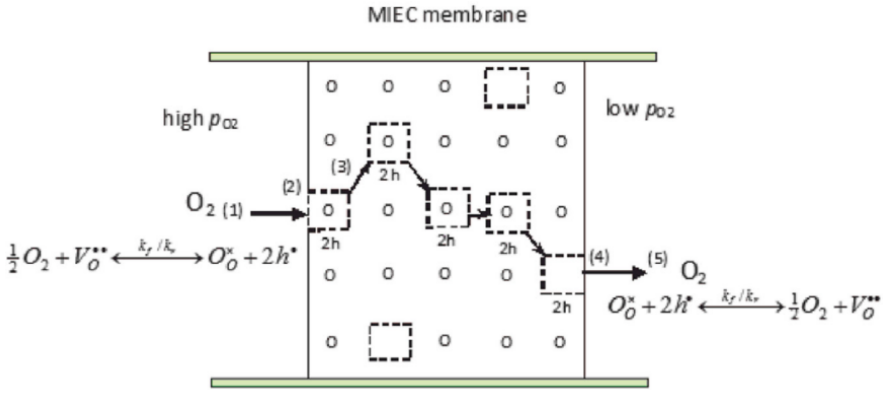

Figure 6 – Illustrative scheme of oxygen permeation through perovskite membranes (□ - oxygen vacancy, o - lattice oxygen, h-electron hole).

Source: (41)

Perovskites are especially useful for oxygen separation because their lattice structure can conduct ions and electrons. They are composed of different oxides in an ABO_3 structure. The A- cation site is large (size of 1.10-1.8 Å) and it is often composed of lanthanide, alkaline or alkaline-earth metals (La and Sr, for instance). The B-site is smaller (0.62-1 Å) and may be composed of Fe and Co, for example. The perovskite is doped by cations with similar size but different valences to produce ion vacancies. The oxygen vacancies are more prone to exist than cation-deficiencies. Under a chemical potential gradient and sufficient temperature, oxygen transport occurs by a hopping mechanism (Figure 6), in which it transfers successively to the near vacant site producing a flux inside the membrane (41).

Although perovskites are perfect selective to oxygen and operate at high temperatures, they are susceptible to mechanical and chemical instabilities that hinder their commercialization and use in reactive systems. Large gradients of temperature or vacancy concentration (gradient of oxygen partial pressure) can cause unbalanced volume expansion; consequently, mechanical stresses. Additionally, in a strongly reducing atmosphere (syngas in this case), perovskite can react and change its chemical and lattice structure, consequently, reducing the permeation rate and generating mechanical stresses. For this reason, many developed materials failed in experimental tests, such as $Ba_{0.5}$ $Sr_{0.5}$ $Ca_{0.8}$ $Fe_{0.2}$ $O_{(3-\delta)}$, $BaTi_{0.2}$ $Ca_{0.5}$ $Fe_{0.3}O_{(3-\delta)}$ (42). Efforts for mechanical and chemical stabilization have been made in the literature, with the inclusion of compatible inert support, different doping cations, and assembly of several perovskites. A review of dense membranes for oxygen separation and technological applications can be found in (41).

Not only should the membrane be mechanically stable, but it must also deliver a minimum amount of oxygen to the process. It was estimated that 3.5 mL/cm^{2}min (2.06e-6 mol/cm^{2}s) was necessary for current technological applications (43, 44). Particularly two dense membranes were experimented in POM and TRM reactions, LBCF2828 ($La_{0.2}$ $Ba_{0.8}$

$Co_{0.2}$ $Fe_{0.8}$ $O_{(3-\delta)}$) and LSCF6428 ($La_{0.6}$ $Sr_{0.4}$ $Co_{0.2}$ $Fe_{0.8}$ $O_{(3-\delta)}$) (45, 46). LSCF presented permeability in the range of 0.05 to 0.23 mL/cm^{2}min and LBCF2828 varied from 0.3 to 0.5 mL/cm^{2}min, below the estimated required values. The LBCF2828 proved to be resistant in the POM with more than 850 h of operation, delivering moderate flux. Note that the mathematical model developed byTsai et al. applies to bulk limited transfer (thick membranes) and not to surface limited (small thickness) transfer, as used in some papers (47, 23). In addition, LBCF6428 was also studied for POM and separation (48, 46) but the flux was also insufficient for membrane reactors (below 0.3 mL/cm^{2}min).

2.3.2 Porous Membranes

Porous membranes can also distribute oxygen, providing higher flux than dense ceramic at the lack of selectivity expense. For example, α- alumina porous membrane, which is commonly used in liquid microfiltration and ultrafiltration (0.2-3 μm of mean pore diameter), can be used as an inert gas distributor in packed bed reactors, particularly in oxidative reactions (49, 50, 51). The α-alumina porous membrane is chemically inert, thermally stable[1], easy to make and commercially available (52, 53). Due to the high gas fluxes, it is generally modified to conform the permeability and permselectivity required by the reactions (54, 51). Porous membranes usually have low selectivity because the separation is geometrical rather than chemical. Depending on the pore size, different flow regimes can occur, such as Knudsen flow, which may separate components by kinetic size. To provide high fluxes to the TRM reactor, a macroporous membrane is chosen with laminar flow. In this regime, the permeation is non-selective and is driven by a pressure gradient in the membrane, similar to a porous bed. The major drawback concerning the **macroporous** membranes as distributors is the backflow of reactants towards the retentate side. However, a large pressure drop across the membrane is often sufficient to prevent the by-pass of reactants and to minimize back-diffusion.

2.3.3 Considerations

Since dense perovskite membranes presented in the literature suffer from stability problems and often do not provide enough permeability, it is difficult to use them in reactors of the industrial size. The chemical and thermal stability, ease of construction and modification and, especially, the high permeation fluxes make the porous membrane more applicable than dense membranes, for the required conditions. Therefore, for the application proposed here, α-alumina porous membrane is used. However, a separation unit of oxygen would be necessary to provide pure oxygen to pass through the membrane since the porous membrane is not selective.

[1] Melting point = 2072 °C

3 LITERATURE REVIEW

Song(55) was the first to propose TRM as a useful reaction to convert methane and carbon dioxide from flue gases into syngas for the industry. In 2004, Song and Pan, in a more detailed paper, studied the feasibility of TRM, its catalysts and possible kinetics. They tested the activity of Ni catalysts in several support materials. In addition, the authors observed a reduction of carbon deposition due to oxygen and water when compared to DMR. They obtained methane and carbon dioxide conversions of 95% and 80% at 800-850 °C and 1 atm. Since then, catalysts, reactors, and processes schemes have been explored. Despite recent advances, there is no active industrial operation of TRM yet, only a report of a pilot plant and a demonstration unit in Korea (56).

In this scenario, this chapter reviews the recent advances in Tri-Reforming of Methane. It encompasses simulations in reaction equilibrium, reactors and process design. Out of scope are the recent developments in catalysis, kinetics and reaction mechanisms.

3.1 REACTION EQUILIBRIUM

Zhang et al. investigated TRM by a thermodynamic approach (1). They explored conversions, production of hydrogen and coke, varying feed composition and temperature. The analysis mainly focused on atmospheric and isothermal conditions. The authors minimized the total Gibbs energy by the nonstoichiometric approach using the Peng-Robinson equation of state. They observed that high temperatures and low pressures were beneficial to TRM. Indeed, the best conditions occurred at low pressures, temperatures above 850 °C and ratio lower than 0.5 for CO_2: CH_4 and H_2O: CH_4. Maximizing the hydrogen production, they obtained CO_2 conversion of ca. 90%. The optimized molar feed was CH_4: CO_2: H_2O: O_2 = 1: 0.291: 0.576: 0.088 at 850 °C and 1 atm.

Challiwala et al. made a similar study, exploring the influence of process variables in performance at atmospheric pressure and fixed temperature (57). They also evaluated the deviation of the ideal gas behavior at pressures up to 20 bar and claimed that Peng-Robinson is more suitable to model the thermodynamic behavior than Redlich-Kwong and Soave-Redlich-Kwong. In addition, they maximized CO_2 conversion, attaining 47.84 % and energy demand of 180 kJ/mol of CH_4 for feed mole ratio of CH_4: CO_2: H_2O: O_2 = 1: 1: 0.4: 0.1 at 1 bar and 750 °C.

In contrast to other approaches, Yan et al.(58) used the equilibrium constant method to examine two distinct behaviors of TRM, whether in the presence or absence of solid carbon. The simulations occurred at atmospheric pressure and constant temperature of 676.85 °C. They concluded that feed of CH_4: CO_2: H_2O: O_2 = 1: 0.45: 0.45: 0.31 was sufficient to

supress coke and to achieve reasonable conversions.

3.2 REACTORS

In 2011, Arab Aboosadi, Jahanmiri and Rahimpour(24) optimized feed conditions of a packed bed reactor to obtain syngas suitable for methanol plants with maximum hydrogen production. The proposed reactor comprised 184 metallic tubes with 2 m of length and 0.125 m of diameter, filled with NiO-Mg/Ce–ZrO_2/Al_2O_3 catalyst. The model consisted in 1D plug-flow, ideal gas behavior without pressure drop. The kinetics of TRM were derived from SMR and CCM (2, 3). Due to the absence of industrial data for TRM, they compared their model results with data from industrial steam reformers. The optimization resulted in methane conversion of 97.9 % and syngas ratio (H_2: CO) of 1.7. The optimum feed was CH_4: CO_2: H_2O: O_2 = 1: 1.31: 2.46: 0.47 at 826.85 °C and 20 bar. Nevertheless, the simulations showed a dangerous hot spot in the inlet zone, over 1370 °C, probably resulting in catalyst deactivation.

Khajeh, Arab Aboosadi and Honarvar(59) proposed and optimized a fluidized bed for the methanol process. The optimized inlet conditions were similar to the packed-bed of Arab Aboosadi, Jahanmiri and Rahimpour but the outcome was slightly superior. The methane conversion and syngas ratio were 99.4% and 1.84 for the fluidized bed, against 97.9 % and 1.7 for the packed bed. Although the reactor offered better thermal control and lower pressure drop, it was unable to prevent hot spot. Additionally, the two reactors obtained a small CO_2 conversion.

Chein and Hsu investigated a tubular packed bed reactor for TRM at adiabatic conditions and elevated pressure (20 bar). They fed the reactor with biogas (CO_2: CH_4 = 0.5), air and water(60). The authors analyzed the syngas production, methane and carbon dioxide conversion, varying the feed conditions. Contrasting with other papers, the authors studied the CO_2 conversion and highlighted the requirement of large oxygen concentration to convert CO_2 and CH_4. They also noted the trade-off between CO_2 conversion and syngas ratio but the implications of hot spot and carbon deposition were neglected.

In 2009, KOGAS (Korean Gas Corporation) planned a Dimethyl Ether (DME) plant for the Asian market (Korea, Japan, China, and India) that would use a tri-reforming unit to convert natural gas into syngas (56). Pilot tests were divided into three stages: a burner, pilot plant, and a demonstration unit. The tri-reformer unit consisted basically of a pre-reformer and a tri-reformer. The TRM was designed similar to an autothermal reformer, with a chamber for combustion and other for catalytic reforming. The first-principle model employed kinetics for combustion from Smith et al.(61) and for reforming reactions from Xu and Froment(2) and Trimm and Lam(3). The model was adjusted with pilot plant data

and the results compared to equilibrium.

To control the thermal behavior and improve performance, Rahimpour, Arab Aboosadi and Jahanmiri(23) proposed a dual membrane reactor. The reactor configuration was composed of two concentric tubes, where the catalytic bed was placed in the annular space and each membrane in the tubular walls. The outer membrane was made of Pd for H_2 removing, whereas the inner membrane was made of dense perovskite ($La_0.2Ba_0.8Fe_0.8CoO3 - \delta$) for oxygen injection. While the air stream was flowing in the inner tube, oxygen was continuously and selectively removed through the perovskite membrane and added into the catalytic bed. The performance of the dual membrane reactor was compared to the common packed-bed reactor. The dual membrane reactor achieved higher conversions and hydrogen production, and prevented the hot spot formation.

3.3 PROCESSES USING TRM

Zhang, Zhang and Benson(62) proposed a DME process that used a TRM unit for syngas production. The conceptual process consisted in a unit of TRM, DME and purification. They used thermal power effluents as the process feed to obtain a syngas ratio of 1 in the TRM reactor. The DME, at 280 °C and 60 bar, was modeled with a kinetic approach whereas the TRM was modeled as an equilibrium reactor, operated at 900 °C and 20 bar. The authors optimized the energy integration and saved 33% of utility cost compared to the base case.

Zhang et al.(63) analyzed the operational cost of a methanol plant using a TRM fed by a thermal power effluents. The TRM reactor operated at 850 °C and 1 atm, modeled as an equilibrium reactor. Minimizing the utility costs, the economic analysis showed a profit of US$ 33.4 millions/year and US$ 0.9/h for each kilogram of CO_2 converted.

Qian et al. also proposed a methanol plant, coupling of a CTM (Coal To Methanol) plant to an industrial waste of COG (Coke-oven Gas), including a TRM reactor in the process (64). Modeled as equilibrium reactor, the TRM reactor produced syngas, fed by methane stream from the COG effluents and CO_2 from coal gaseification process. The new proposed process increased 11.4% in energy efficiency and 4.3% of carbon utilization compared to the conventional CTM plant.

Some Fischer-Tropsch processes also included a reactor of TRM for syngas production. In the process proposed by Damanabi and Bahadori(65), carbon dioxide production was 24.4% lower than the conventional process and its emission were reduced by half, with an increase of gasoline productivity more than 100%. Graciano, Chachuat and Alves(66) included a plug flow TRM reactor in a Fischer-Tropsch plant. The CO_2-rich NG stream

entered in a pre-reformer followed by an adiabatic tubular packed bed reactor operated at 5 bar. They maximized the hydrogen production at a minimum of 25% of CO_2 conversion. The reactor converted 98.7% of methane at feed molar composition of CH_4: CO_2: H_2O: O_2 = 1: 0.625: 0.39: 0.52. A parametric study indicated that feeds around 50% of oxygen are generally required for adiabatic performance. In addition, it showed a trade-off between water in the feed and carbon dioxide conversion. The FT process achieved 54% of carbon conversion efficiency, despite the 30% CO_2 content in the NG.

3.4 SUMMARY OF THE LITERATURE REVIEW

TRM showed to be an useful reaction to convert methane and carbon dioxide. According to equilibrium data, TRM has high conversions and yields, generally above 80%. Additionally, simulations showed that introduction of a TRM unit in several GTL processes implied in economic savings and carbon dioxide abatement.

However, the literature in reaction equilibrium focused on operations at atmospheric pressure rather than usual pressure of syngas units. For instance, conventional steam and autothermal reformers operate with pressures above 20 atm in order to save capital and operational costs with larger equipment (65). If pressure grows, performance may decline substantially. For example, Figure 7 shows carbon dioxide conversion and syngas yield as function of pressure, using the optimized feed of Zhang et al.(1). As pressure increases, syngas yield and carbon dioxide reduce from 90% to ca. 40% at 30 bar. Therefore, analyzing equilibrium data only at atmospheric pressure may be misleading.

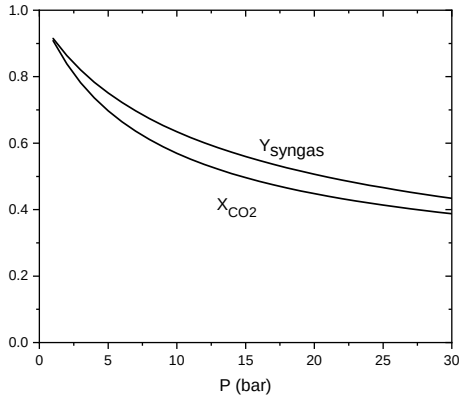

Figure 7 – Pressure effect on syngas yield and CO_2 conversion in isothermal TRM. CH_4: CO_2: H_2O: O_2 = 1: 0.291: 0.576: 0.088 at 850 °C.

Source: Own authorship.

On the other hand, the reactor configurations explored in the literature were mainly packed-bed and fluidized bed, with predominance of the former (Table 4), and all of them were operated at adiabatic conditions. The conventional tubular packed-bed reactors showed

harmful hot spots. Additionally, most of the papers despised carbon dioxide conversion and coke deposition.

Table 4 – Summary of reactor models for TRM in literature.

Authors	**Configuration**	**Reference**
Arab Aboosadi, Jahanmiri and Rahimpour	Packed-bed tube	(24)
Khajeh, Arab Aboosadi and Honarvar	Fluidized-bed	(59)
Farniaei et al.	Coupled reactors	(22, 16)
Chein and Hsu	Packed-bed tube	(60)
Rahimpour, Arab Aboosadi and Jahanmiri	Dual membrane packed-bed reactor	(23)
Farniaei et al.	Coupled Membrane Reactor	(22)
Cho et al.	Autothermal Reactor	(56)
Graciano, Chachuat and Alves	Packed-bed tube	(66)

In this scenario, the present investigation aims to provide broader information on TRM, completing the gaps currently presented in the scientific literature. The performance of TRM is evaluated, regarding conversions, productivity, CO_2 abatement and coke production. The equilibrium performance is analyzed in both conditions, adiabatic and isothermal, at 25 bar. Additionally, three different reactor configurations are simulated, analyzed and compared.

Part II

Methods and Models

4 METHODS AND MODELS

This chapter describes the models and methods employed in the study of TRM. To represent the industrial pressure of reformers, all the models fixed the pressure to 25 bar, which is in the industrial range for syngas units (20-35 bar). In the analysis of reactors, the pressure will be varied to examine its effect on performance. To explore TRM, equilibrium and kinetic approaches were used, resulting in two groups of models: (i) Reaction Thermodynamic Equilibrium and (ii) Reactors, as shown in Figure 8.

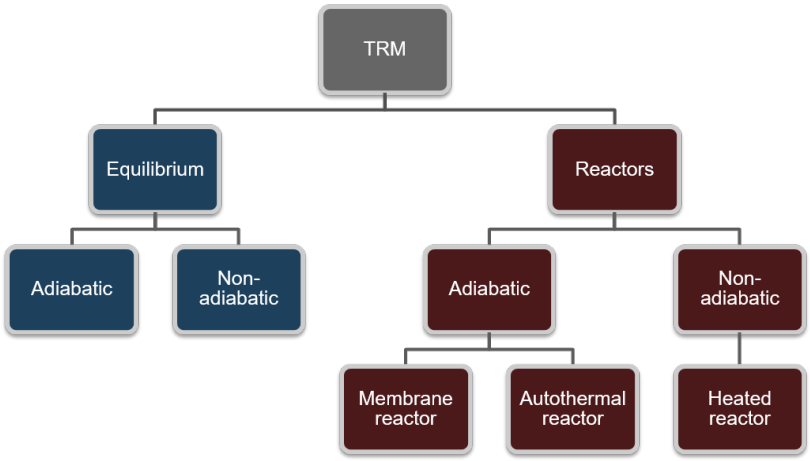

Figure 8 – Modeling strategy.

Source: The author's.

Reaction Thermodynamic Equilibrium The purpose of the model is to investigate TRM at industrial pressure, identifying optimum operational regions, limitations, typical conversions of carbon dioxide and general productivity. The model provides equilibrium composition and temperature as a function of the feed at adiabatic or at fixed temperatures.

Reactors The goal is to explore the advantages and disadvantages of each reactor configuration as well as compare their technical performance to be applied in the industry. Three reactors models were simulated:

1. **Membrane Reactor (MR)** The goal is to represent membrane reactors that distribute oxygen to prevent hot spot. The model provides composition and temperature profiles as a function of feed and oxygen permeation flux.
2. **Autothermal Reactor (ATR)** The purpose is to resemble the reactor configuration of autothermal reformers, the combustion, and catalytic chambers. The model supplies composition and temperature profiles in both sections.

3. **Heated Reactor (HR)** The objective is to resemble the reactor configuration of industrial steam reformer tubes, where heat is supplied to the catalytic packed bed. The model provides composition and temperature profiles.

This chapter is organized as follows. Firstly, the performance metrics are defined. The second section describes the methods and models for the analysis of reaction equilibrium. Finally, the three reactor models are characterized as well as the analytic methods.

4.1 METRICS

In a reactive system covering several variables and parameters, it is useful to concentrate information into few indicators. They should consider the performance of reactants, products, and reactions. However, it is necessary to establish firstly a fixed set of independent reactions. In the case of TRM, given the seven reactive species, CH_4, CO_2, H_2O, O_2, CO, H_2 and C, only four reactions are stoichiometrically independent. Then, the chosen reactions to represent TRM throughout this study are:

$$SMR:\ CH_{4\,(g)} + H_2O_{\,(g)} \overset{Ni\ cat}{\rightleftharpoons} 3\,H_{2\,(g)} + 1\,CO_{\,(g)} \qquad \Delta H° = 206.3\,kJ/mol \tag{4.1a}$$

$$DMR:\ CH_{4\,(g)} + CO_{2\,(g)} \overset{Ni\ cat}{\rightleftharpoons} 2\,H_{2\,(g)} + 2\,CO_{\,(g)} \qquad \Delta H° = 247.3\,kJ/mol \tag{4.1b}$$

$$CCM:\ CH_{4\,(g)} + 2\,O_{2\,(g)} \overset{Ni\ cat}{\longrightarrow} 2\,H_2O\,(g) + 1\,CO_{2\,(g)} \qquad \Delta H° = -891\,kJ/mol \tag{4.1c}$$

$$MD:\ CH_{4\,(g)} \overset{Ni\ cat}{\rightleftharpoons} 2\,H_{2\,(g)} + C_{\,(s)} \qquad \Delta H° = 74.6\,kJ/mol \tag{4.1d}$$

Considering the metrics, the conversion reports reactant consumption and is defined as

$$X_i = 1 - \frac{F_i}{F_{0,i}} \qquad\qquad i = \{CO_2,\ CH_4,\ H_2O\}\ . \tag{4.2}$$

where F_i denotes the molar flux of specie i. The study focused on methane and carbon dioxide conversion. Water conversion is less important because it is plainly available in the process and it is easy to separate. Throughout the study, oxygen conversion is considered to be equal to one. It is also important to point out that the conversion may have negative values because some reactants act as products depending upon certain operational conditions.

Yield and selectivity, in turn, measure productivity and waste of raw material. The yield indicates how much was produced in relation to the maximum **stoichiometrically** possible, given the initial amount of reactants. It is defined for syngas and coke as

$$Y_{syngas} = \frac{(F_{H_2} + F_{CO}) - (F_{0,H_2} + F_{0,CO})}{4 \cdot F_{0,CH_4}} \tag{4.3}$$

$$Y_{coke} = \frac{F_C}{F_{0,CH_4}}\ . \tag{4.4}$$

On the other hand, selectivity indicates how much the desired product was formed in relation to all (competitive) products. Not only gives information about product preference but also about waste of raw material. In this sense, the selectivity of syngas is calculated as:

$$S_{syngas} = \frac{(F_{H_2} + F_{CO}) - (F_{0,H_2} + F_{0,CO})}{4 \cdot (F_{0,CH_4} - F_{CH_4})} \,. \tag{4.5}$$

The maximum value is one, which means that all converted raw material was transformed into the desired product. In the case of TRM, syngas selectivity lower than 1 means that methane was also converted into carbon dioxide, water and/or coke.

To study the performance of specific reactions, an yield indicator is defined based on the extent of reaction. It provides information about the amount reacted in relation to the maximum **stoichimetrically** possible. The reaction yield is defined as follows:

$$Y_q = \frac{\xi_q}{n_{0,limited\ reactant}} \tag{4.6}$$

where, for closed systems, the extent of reaction is defined as

$$n_i = n_{0,i} + \sum^{q} \nu_{i,q} \xi_q \,. \tag{4.7}$$

ξ_q, $\nu_{i,q}$ and n_i denote the extent of reaction q, stoichiometric coefficient of specie i in reaction q and number of specie i in mol, respectively. Note that the extent and yield may assume negative values, which means that the reverse reaction is taking place.

Three additional metrics are necessary to complete the analysis: syngas ratio, TRM enthalpy and total carbon dioxide conversion. The syngas ratio is a requirement of the downstream process and is defined as

$$H_2/CO = \frac{F_{H_2}}{F_{CO}} \,. \tag{4.8}$$

The TRM enthalpy is the heat required by the TRM reaction divided by the amount of methane converted,

$$H_{TRM} = \frac{\Delta H_{TRM}}{F_{0,CH_4} - F_{CH_4}} \,. \tag{4.9}$$

The total carbon dioxide conversion includes conversion inside the reformer tubes and also in the furnace of the heated reactor model (HR). It is calculated as:

$$X_{CO_2}^{\text{total}} = 1 - \frac{F_{CO_2} + \dfrac{Q_{TRM}}{\zeta \cdot Q_{comb,CO_2}}}{F_{0,CO_2}} \,, \tag{4.10}$$

where Q_{TRM} is the TRM heat duty, Q_{comb,CO_2} is the heat of combustion of a typical furnace fuel and ζ is the efficiency of the energy transfer between the furnace and the process gas. The furnace heat (Q_{comb,CO_2}) is 800.77 MJ/kmol of CO_2, which corresponds to the burning enthalpy of reformer fuel at constant 524 K and 132.4 kPa (34); the efficiency is 50%, the approximated value of a conventional steam reformer in ammonia plants (67).

4.2 REACTION EQUILIBRIUM MODEL

The reforming reactions are limited by equilibrium and very influenced by temperature, pressure and feed compositions. Since the catalytic reactions reach values near to equilibrium (4), analyzing equilibrium data is more general and suitable for different types of reactors. Moreover, it is faster than analyzing several reactors, varying in geometrical configuration, kinetics, catalytic loading, and operational restrictions.

The thermodynamic system was considered to be multicomponent, isobaric and free from electric, superficial and field forces. Species adsorptions on catalyst surface were despised. The equilibrium states were calculated by the minimization of the total Gibbs energy, subjected to the conservation equations of mass and energy, as follows:

$$min\, G(T, P, n_i) = \sum^{i} \mu(T, P, n_i) \cdot n_i \tag{4.11a}$$

s.t.:

$$\sum^{i} C_{ci} \cdot \delta n_i = \sum^{i} A_{ci} \cdot n_i - b_c = 0 \tag{4.11b}$$

$$\Delta P = 0 \tag{4.11c}$$

$$H_0 - H(T, P, n_i) = H_0 - \sum^{i} h_i(T, P, n_i) \cdot n_i = 0 \qquad \text{(adiabatic)} \tag{4.11d}$$

or

$$\Delta T = 0 \qquad \text{(isothermal)}, \tag{4.11e}$$

(4.11f)

where C_{ci} is the entry of the chemical formula matrix, i. e., it is the number of c element atoms in the i component, and b_c is the total number of c element. G, H and μ denote the Gibbs energy, enthalpy and chemical potential, respectively.

The minimization covered seven gaseous species (CH_4, CO_2, H_2O, O_2, CO, H_2, N_2) and solid carbon (C), which represents the coke. The simulation was performed by an equilibrium reactor model (RGibbs) of Aspen Plus® V8.8, using the Peng-Robinson equation of state (57).

The TRM was evaluated varying initial composition and temperature at a fixed pressure of 25 bar. The initial molar composition was described as a proportion, in percentage, between the reactant (water, oxygen or carbon dioxide) and methane feed. The water feed ranged from 0 to 300% and carbon dioxide up to 200 %, which is the composition range of some NG resources (8). Oxygen ranged from 0 to 60 %, which is the usual limit applied in autothermal reformers. When TRM is non-adiabatic, the equilibrium temperature varied

from 700 up to 1000 °C [1].

4.3 REACTORS

4.3.1 Membrane Reactor Model

The membrane reactor model aims to represent reactors for TRM that add oxygen through membranes. Two types of oxygen flux were considered uniform and variable. The model of uniform flux evaluated the impact of oxygen distribution in the performance metrics, equilibrium and in the temperature profile. The second model explores the effect of a non-uniform flux of oxygen in TRM, particularly of a α-alumina membrane. Both models employed a basic configuration that consists of a packed bed tube with a membrane as the tube wall. From an external pressurized shell, pure oxygen flows into the catalyst side through the membrane, as depicted in Figure 9 (51, 68).

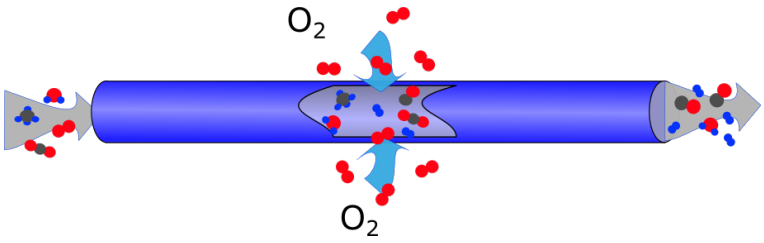

Figure 9 – Illustrative scheme of a membrane reactor for oxygen distribution.

Source: The author's.

A 1D pseudo-homogeneous model was developed, assuming:

- steady-state regime;
- plug-flow;
- uniform distribution in the cross-section area;
- the heat conduction in the wall is despised;
- pseudo-homogeneous reactions;
- no diffusion in the axial direction;
- constant effectiveness factor.

[1] The limit temperature of the current tubes in steam reformers is 1080 °C (11).

Considering a differential volume, the molar balance is given by

$$\frac{dF_i}{dz} = A_t \rho_{bed,app} \sum^{q} \nu_{i,q} r_q + J_i \, \pi D \tag{4.12}$$

and the energy balance, by

$$\frac{dH}{dz} = J_{O_2} \, h_{O_2} \, \pi D, \tag{4.13}$$

where z, A and D are the axial length of the tubular reactor, the cross-section area and the internal diameter of the tube. Additionally, $\rho_{bed,app}$, r_q and J_i denote the apparent density of the catalytic bed, the reaction rate of reaction q and the molar flux of specie i (only O_2 in the case).

Uniform Flux: the model considers constant oxygen flux along the reactor axis and despises pressure drop. An additional variable, **oxygen partition**, was used to study the oxygen distribution, which is the proportion between oxygen that flows through the membrane and the total oxygen added,

$$O_2^{partition} = \frac{F_{O_2}^{membrane}}{F_{O_2}^{total}}. \tag{4.14}$$

Variable flux: the second model assumes an inert porous membrane made of α-alumina, which delivers a non-uniform flux along the reactor. The α-alumina is chemically inert, thermal stable and it has been applied to distribute oxygen in oxidative reactions, as seen in section 2.3. Oxygen permeation **is not selective** through the porous membrane and is modeled by Darcy's equation (equation (4.15)) of flow in porous media (69). In this model, the pressure drop in the catalytic bed is calculated by Ergun's equation (equation 4.16).

$$J_{O_2} = \frac{B_0 \, \rho_{gas}}{\eta \, \delta_{membrane}} (P_{shell} - P_{tube}) \tag{4.15}$$

$$\frac{dP}{dz} = -\frac{\dot{m}}{\rho_{gas} D_p} \left(\frac{1-\phi}{\phi^3} \right) \left[\frac{150(1-\phi)\eta}{D_p} + 1.75\dot{m} \right] \tag{4.16}$$

B_0, $\delta_{membrane}$ and η denote the Darcy's permeability, the membrane thickness and the gas viscosity; $\dot{m}$, ϕ, ρ_{gas} and D_p are the mass flow, void fraction, gas density and the particle diameter.

The resultant mass and energy equations were implemented in Aspen Custom Modeler® (ACM), using the Peng-Robinson equation of state to predict the thermodynamic behavior. The system of differential-algebraic equations was discretized by the backward finite difference method with 300 internal nodes, 150 for the initial 0.5 m and 150 nodes for the last 5.5 m, and solved by a Newton-like method. The parameters for the membrane reactor are shown in the Table 5. The effect of membrane support layers are despised. The intrinsic kinetics of Xu and Froment(2) and Trimm and Lam(3) and the constant effectiveness factor

of Groote and Froment(17) were used (see section 2.1.4). The feed pressure and temperature are set to 25 bar and 700 °C, the methane molar flow is 5 kmol/h and the temperature of the oxygen in the shell is set to be equal to feed.

Table 5 – Membrane reactor parameters.

F_{CH_4}	(kmol/h)	5
P_0	bar	25
P_{shell}	bar	29
T_0	°C	700
L	(m)	6
D	(m)	0.1
D_p	(m)	0.015
ρ_{cat}	(kg cat/m^3)	2100
ϕ	-	0.43
B_0	($\times 10^{-16} m^2$)	1.65
$\delta_{membrane}$	mm	1.5

4.3.2 Autothermal Reformer

The model of autothermal reactor was divided into two consecutive models, homogeneous and catalytic, as depicted in Figure 10 . The homogeneous model used a developed Python program to deal with natural gas combustion. It receives data from a feed stream in the Aspen Plus® program, simulates the homogeneous reactions and, then, outputs the thermodynamic data into the feed stream of the catalytic reactor. The catalytic model employed the RPlug in Aspen Plus® to conduct the reforming reactions SMR and DMR.

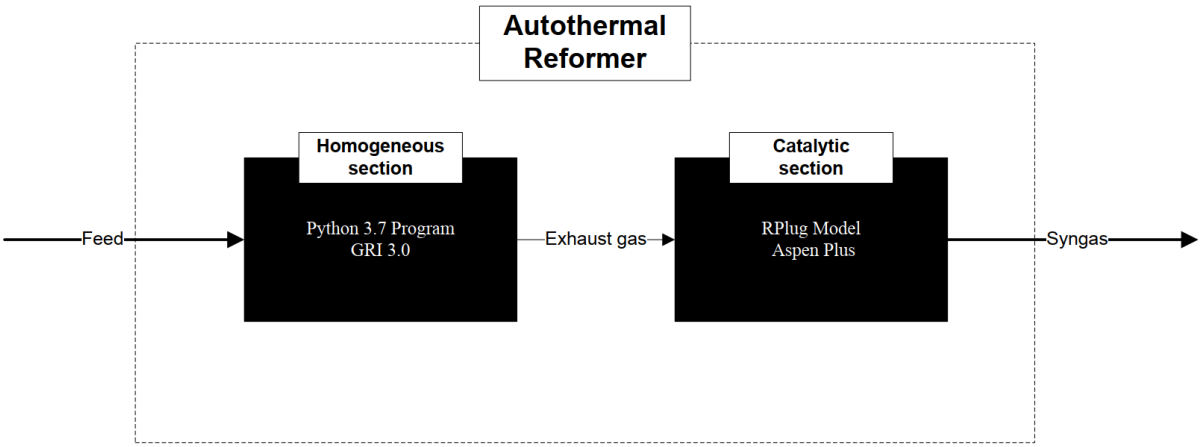

Figure 10 – Illustrative scheme of the autothermal model.

Source: The author's.

The impact of pressure on performance is evaluated by equilibrium and kinetic approaches. The geometric configuration and volume flow in the feed are maintained constant, during

pressure variation. The calculated residence time is defined as the time in the reactor necessary to convert 95% of the methane expected in the equilibrium.

4.3.2.1 Combustion Section

In an industrial autothermal reformer, the combustion chamber is carefully designed to provide a proper mixture of the gases and to prevent soot production. However, the present model does not intend to replicate the complex fluid dynamics around the burner neither the radiation effects in the refractory vessel. In the literature, different models were applied to the combustion section, including PFR, equilibrium, and CFD. Considering that industrial geometry is not available in the open literature and the design detail is out of scope, a CFD model is an inadequate choice. In its turn, an equilibrium reactor would be too unrealistic because the *homogeneous* reforming reactions are too slow to attain equilibrium. Therefore, a homogeneous PFR model was chosen, similarly as in Cho et al.(56). The model consists of an ignition problem, where the composition and temperature profiles are simulated. Its assumptions were:

- steady-state regime;
- plug-flow;
- no diffusion in the axial direction;
- adiabatic and isobaric operation;
- ideal gas behavior.

The mass balance for a specie i was

$$\dot{m}\frac{dy_i}{dV} = \sum^{q} \nu_{iq} r_q \cdot MW_i \tag{4.17}$$

and the energy conservation equation was

$$\frac{dT}{dV} = -\frac{\sum^{i} \tilde{h}_i \sum^{q} \nu_{iq} r_q}{\dot{m} \cdot c_p}, \tag{4.18}$$

where y_i, V, MW_i and c_p denote the mass fraction of specie i, the volume of the reactor, the molecular weight of specie i and the molar heat capacity, respectively.

The kinetic model is crucial to adequately model the homogeneous section. Simplistic models containing three or four lumped chemical reactions are restricted to the empirical data and do not behave well in extrapolations (as occurs in TRM conditions), despite

simpler to implement and faster to simulate (70, 71). For this reason, a complete and well-validated kinetic model for homogeneous combustion of methane was applied, the GRI 3.0 mechanism (61). It considers 53 chemical species and 325 homogeneous reactions.

To solve the resultant differential-algebraic equation system involving the complex combustion mechanism, a script in Python 3.7 was developed. Using the Aspen Plus® COM interface, the program is able to transfer data between the Aspen simulation objects, such as streams and reactors, and those in the local Python program. In this manner, it receives data from a feed stream from Aspen Plus®, solves the equations of the combustion model and outputs stream data to Aspen Plus®, integrating the homogeneous and catalytic model as depicted in Figure 10.

The full GRI 3.0 mechanism, as well as the thermodynamic data of all species, were managed by Cantera packages available on Python(72). The conservation equations were integrated by a multi-step BDF algorithm in the Scipy package (73). Although the kinetics comprised 53 species, there were only six relevant components during the simulation (CH_4, CO_2, H_2O, O_2, CO, H_2). Other chemical species appear as trace, except acetylene that is slowly consumed after ignition. Since the ignition time varies greatly with feed composition and temperature, criteria to establish a mean (and general) residence time is necessary. As proposed by (56), two criteria are adopted here: depletion of (i) oxygen and (ii) saturated hydrocarbons, acetylene; resulting, in a mean residence time ca. 1.3 s.

4.3.2.2 Catalytic Section

The exhaust gases from the homogeneous section flow to the catalytic reactor, where the reforming reaction occurs. The adiabatic catalytic model assumed:

- steady-state regime;
- plug-flow;
- pseudo-homogeneous reactions;
- no diffusion in the axial direction;
- constant effectiveness factor.

Considering a differential volume of the reactor, the molar balance is given by

$$\frac{dF_i}{dz} = A_t \rho_{bed} \sum^{q} \nu_{iq} r_q \tag{4.19}$$

and the energy balance,

$$\frac{dH}{dz} = 0\,. \tag{4.20}$$

The intrinsic kinetics adapted from Xu and Froment(2) and Trimm and Lam(3) were used together with the effectiveness factor of Groote and Froment(17), similar to the membrane reactor model. It was used the RPlug module of Aspen Plus® with Peng-Robinson equation of state. The reactor parameters are shown in Table 6.

Table 6 – Geometric parameters of the fixed bed reactor for TRM.

D	(m)	3.45
$L_{catalytic}$	(m)	4
D_p	(m)	0.015
ρ_{app}	(kg cat/m^3)	2100
ϕ	-	0.43

4.3.3 Heated Reactor

To complete the analysis concerning possible reactors for TRM, a reactor that operates non-adiabatically is necessary. In this sense, a model was developed to analyze the main features of a heated tubular packed bed reactor, resembling those in conventional steam reformers. A 1D PBR model was used, assuming:

- steady-state regime;
- plug-flow;
- uniform distribution in the cross-section area;
- no diffusion at the axial direction;
- pseudo-homogeneous reactions;
- constant effectiveness factor along the reactor;
- constant heat flux on the tube wall

The specie i molar balance is given by

$$\frac{dF_i}{dz} = A_t \rho_{bed,app} \sum^{q} \nu_i r_q \tag{4.21}$$

and the energy balance, by

$$\frac{dH}{dz} = q'' \cdot \pi D, \tag{4.22}$$

where q'' is the heat flux across the tube.

The pressure drop was calculated by the Ergun equation (equation 4.16). The intrinsic reaction rate of Xu and Froment(2) and Trimm and Lam(3) was used with the effectiveness factor calculated by Groote and Froment(17). The model was solved by the RPlug of Aspen Plus® V9.0 with the Peng-Robinson equation of state and its parameters are shown in Table 7

Table 7 – Geometric parameters of the fixed bed reactor for TRM.

L	(m)	12
D	(m)	0.1
D_p	(m)	0.015
ρ_{app}	(kg cat/m^3)	2100
ϕ	-	0.43

The impact of pressure on performance is evaluated by equilibrium and kinetic approaches. The geometric configuration and volume flow in the feed are maintained constant, during pressure variation. The calculated residence time is defined as the time in the reactor necessary to convert 95% of the methane expected in the equilibrium.

4.3.3.1 Comparison Conditions

To compare the performance of the autothermal and heated reactor configurations, feed conditions must be determined. For both configurations, the inlet conditions are chosen to give the best carbon dioxide conversion, subjected to the absence of coke production and 25 bar, and limited to 900°C. Two conditions were analyzed, TRM producing syngas ratio of 2.0 (case 01) and 1.0 (case 02). The feed conditions were obtained by optimizing an equilibrium reactor model in Aspen Plus® V8.8, using the SQP algorithm. The feed compositions for comparison are shown in Table 8.

Table 8 – Feed conditions for performance comparison between the autothermal and heated reactor configurations.

	Molar Composition CH_4: CO_2: H_2O: O_2	
Case	1	2
Autothermal reactor	1: 0.5: 1.17: 0.45	1: 1.5: 0.83: 0.54
Heated reactor	1: 0.5: 1.16: 0.1	1: 1.5: 0.82: 0.1

Part III

Results and Discussion

5 THERMODYNAMIC REACTION EQUILIBRIUM

Tri-reforming of methane is a promising reaction to convert both methane and carbon dioxide, particularly with NG rich in CO_2. The equilibrium data is useful to study the behavior of the reactive system in a wide range of conditions. Since the catalysts of TRM closely follow the equilibrium, the analysis can give useful insights about reactor operation and industrial applicability. Rather than the current scientific literature, the present chapter explores TRM at 25 bar, typical pressure of industrial reformers, and also includes adiabatic operation. The study is guided by the performance indicators, discerning optimum regions and possible limitations of TRM. The first section deals with adiabatic conditions and the second with constant temperatures.

5.1 ADIABATIC EQUILIBRIUM

The synergistic combination of endothermic and exothermic reactions enables TRM to operate adiabatically, not requiring large furnaces in contrast with what occurs in steam reformers. The enthalpy restriction changes the relative influence of species in performance when compared to isothermal reactions. Therefore, the following sections investigate the behavior of TRM, focusing on the oxygen and steam requirement for converting methane and carbon dioxide into syngas.

5.1.1 Adiabatic Temperature

Unlike the analysis of isothermal equilibrium, the equilibrium temperature is not directly known, it varies with initial composition, temperature, and pressure. Figure 11 shows the equilibrium temperature as a function of water and oxygen feed.

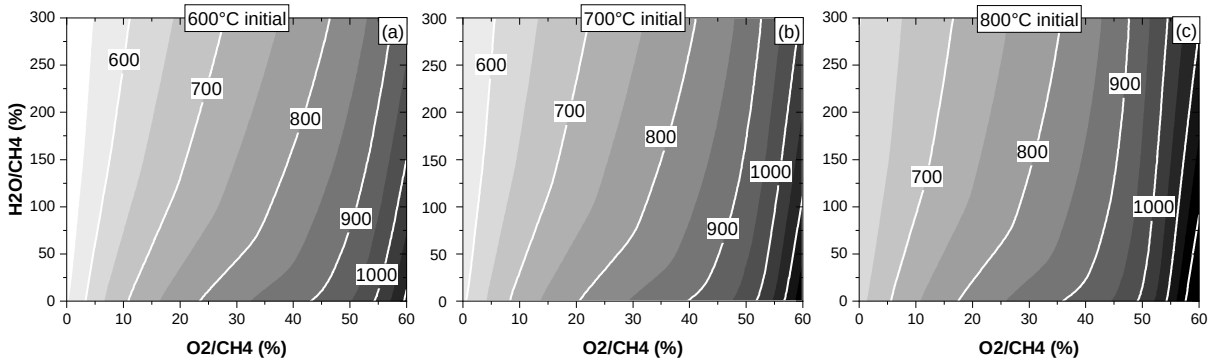

Figure 11 – Adiabatic temperature of TRM at CO_2/CH_4 = 50%, 25 bar and initial temperature of (a) 600, (b) 700, (c) 800 °C.

Source: The author's.

The adiabatic temperature ranged from 600 to 1200 °C. Temperature beyond 800 °C, which is beneficial to reforming reactions, is attained by oxygen feed exceeding 40%. In this initial compositional range, the adiabatic temperature is more sensitive to oxygen, i.e., small oscillations in the feed may drive the reaction to high temperatures (1100 °C). As a consequence, TRM reactor demands a strict control system so that operational runaways may be prevented.

The adiabatic temperature ranged from 600 to 1200 °C and values greater than 800 °C were attained at oxygen feed exceeding 40%. Beyond this feed proportion, adiabatic temperature becomes more sensitive to oxygen. Oscillations in oxygen feed may lead to dangerous temperatures in the reactor which, as a consequence, requires a strict feed control system. The contour lines reveal a particular inflection when the system is fed by a small concentration of water. In those conditions, the production of carbon solid is spontaneous and less endothermic than reforming reactions, leading to an increase in temperature.

The results also showed that the contour lines were close to orthogonality or, equivalently, the gradient was almost parallel to the oxygen axis. This means that oxygen is the key reactant for the adiabatic temperature, and, consequently, to adiabatic performance of TRM. In turn, water does not substantially impact temperature. For each oxygen mole converted, CCM gives off more than the double of the required energy to convert water into SMR [1], which may explain the difference in influence. Obviously, feed temperature also plays an important role in providing the energy required by TRM, as seen in Figure 11 (a), (b) and (c). Therefore, proper heat integration previous to the reactant mixture is crucial in order to provide sufficient temperature for a good performance. Although high temperatures are beneficial to TRM, the reactor materials may not be able to resist. For example, the metal in the conventional steam reformers can operate up to 1000°C and Ni melts at ca. 1400°C. Therefore, good energy management is crucial for the reactor.

5.1.2 Syngas Yield, Syngas Selectivity, and Methane Conversion

Yield and selectivity are key measures for reaction productivity. As methane conversion is correlated to both, it is useful to investigate them simultaneously. Figure 12 shows yield, conversion, and selectivity as a function of water and oxygen feed at temperatures of 600, 700 and 800 °C.

Figure 12 (a), (b), (c) show that both water and oxygen positively affect syngas yield. However, since TRM is mostly driven by temperature, oxygen plays a more important role than water. Feed temperature also contributed to the improvement of the reforming reactions and,

[1] In standard conditions, the reaction enthalpy of CCM and SMR is -445.5 kJ/ mol of O_2 and 206.3 kJ/mol of H_2O

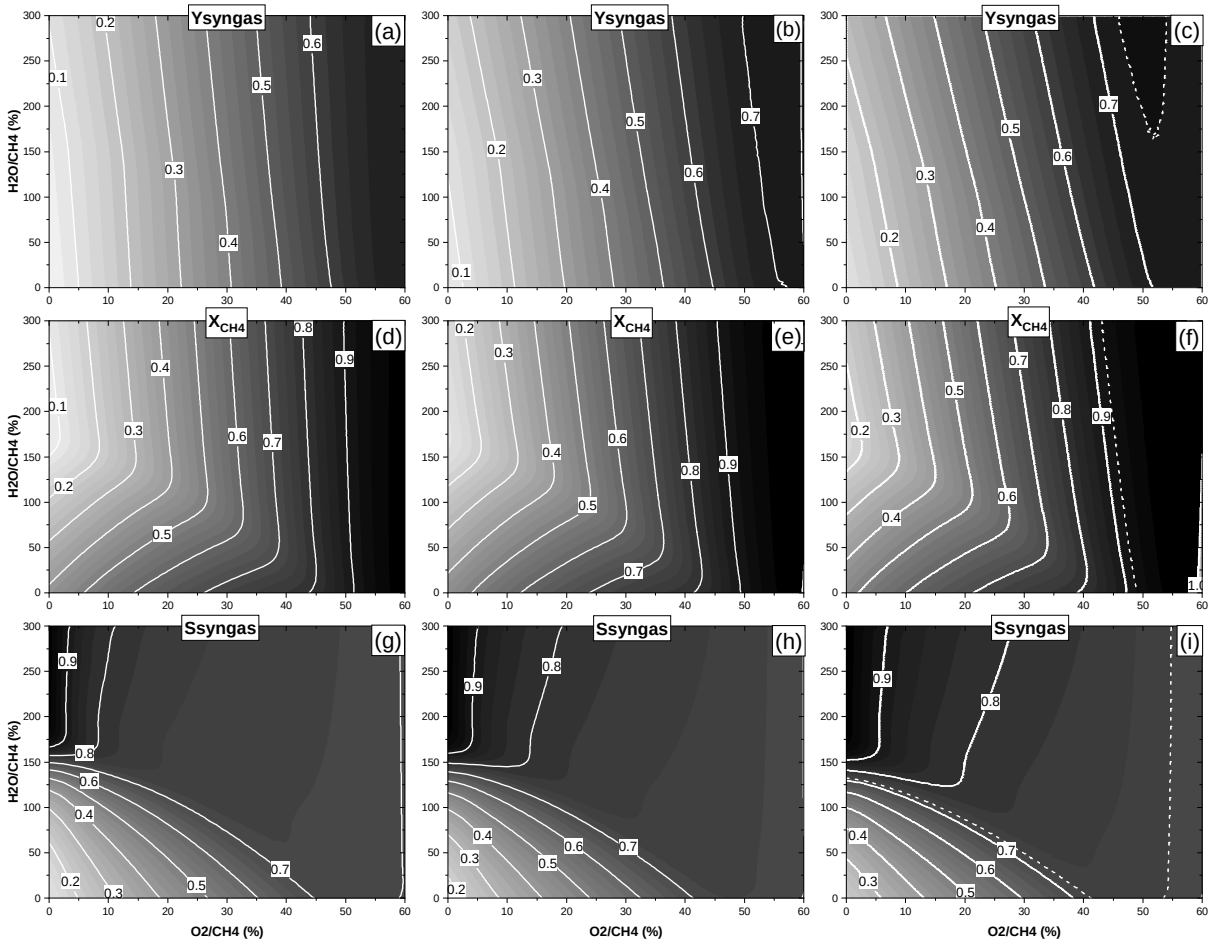

Figure 12 – Syngas yield at CO_2:CH_4 = 50% and initial temperature of (a) 600, (b) 700, (c) 800 °C at 25 bar. Methane conversion at initial temperatures of (d) 600, (e) 700, (f) 800 °C. Syngas selectivity at initial temperatures of (g) 600, (h) 700, (i) 800 °C.

Source: The author's.

consequently, the syngas yield. Syngas yield ranged from 0 to ca. 0.7 with a maximum between 50% and 60% of oxygen (easily seen in Figure 12 (c)). Oxygen concentration greater than 60% does not improve selectivity, it only raises the temperature; therefore, it should be avoided. Therefore, if high productivity per pass is desired, oxygen feed should be in the range between 45 and 60 %.

Likewise yield, methane conversion is substantially driven by oxygen (Figure 12 (d), (e) and (f)). A feed of oxygen greater than 55% completely consumes the methane. Variations in water feed are not important as long as coke is absent. The production of coke bends the contour lines, suggesting that methane decomposition converts more methane than SMR at lower temperatures [2].

Unlike most indicators, syngas selectivity is negatively affected by oxygen (Figure13 (g),

[2] Although the analysis on regions of coke may be done in equilibrium, the applicability is tiny because, in those conditions, the catalyst is likely to be deactivated

(h) and (i)). As it grows, selectivity reduces slightly in the range of 0.8 to 0.7. Although oxygen elevates temperature, it decreases selectivity by the production of CO_2 and H_2O (CCM). Conversely, reforming reactions enhance selectivity, although they decrease adiabatic temperature. The results support the conclusion that excess of oxygen, more than 60%, is unnecessary because methane is practically depleted and selectivity decreases.

5.1.3 Syngas Ratio

The syngas ratio is determinant to produce methanol, DME and synthetic hydrocarbons. Ratios around 2 are suitable for methanol and Fischer-Tropsch reactions whereas values low as 1 are adequate for DME plants. The adiabatic equilibrium results for syngas ratio are depicted in Figure 13.

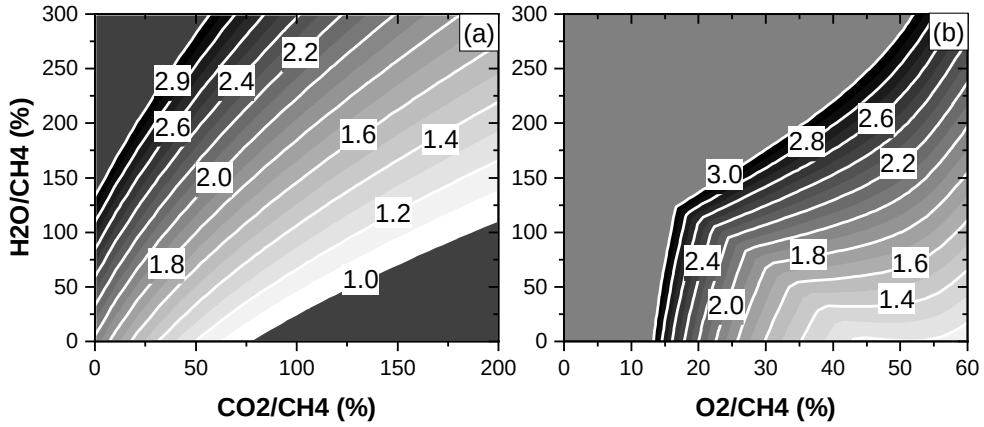

Figure 13 – Syngas ratio (H_2 : CO) at (a) 50% of O_2: CH_4 , (b) 50% of CO_2: CH_4 and 700 °C of initial temperature and 25 bar. In (b), ratios higher than 3.0 are not shown for the sake of clarity.

Source: The author's.

The syngas ratio is mainly determined by the relation between water and carbon dioxide. Figure 13 (a) shows that it ranges mostly between 1 to 3, the stoichiometric values obtained in DMR and SMR. If more water is fed than carbon dioxide, syngas ratio is raised and if it is less, the opposite occurs. For example, to obtain the syngas ratio around 2.0, the necessary feed proportion is around H_2O: CO_2 = 2: 1, whereas for ratios of 1, it inverts to H_2O: CO_2 = 1: 2. Oxygen, in turn, reduces the ratio (Figure 13 (b)) because DMR is more sensitive to temperature than SMR (shown in section 5.1.6).

5.1.4 Solid Carbon Yield

Coke production is one of the major concerns in syngas units. In conventional steam reformers, the proportion between water and methane in the feed is between 2 and 3 to avoid coke deposition and deactivation of the catalyst. Therefore, it is crucial for TRM to

verify whether coke is thermodynamically stable during reactor operations. Figure 14 shows coke yield as function of the oxidizing agents, O_2 and H_2O.

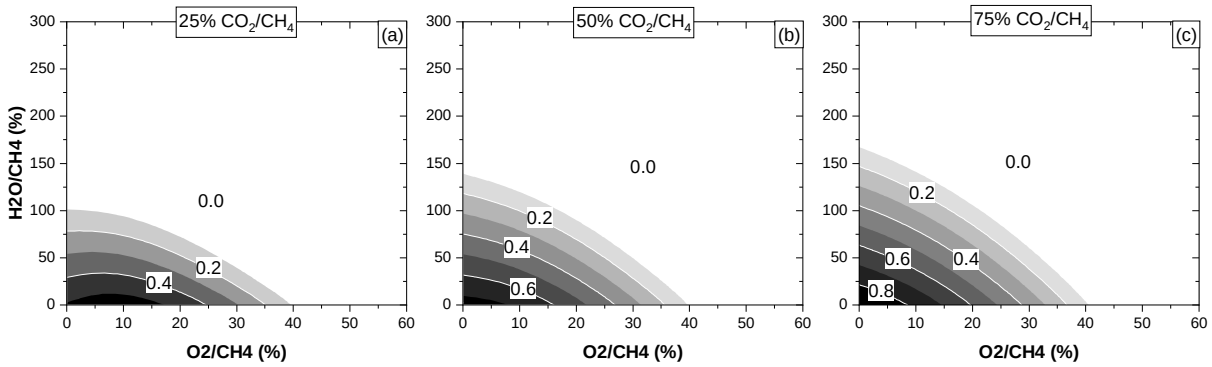

Figure 14 – Coke yield at (a) 25%, (b) 50%, (c) 75% of CO_2: CH_4 , 700 °C of initial temperature and 25 bar.

Source: The author's.

The white region represents equilibrium states that are free of coke, and the dark ones mean that coke production is spontaneous. TRM produces coke when oxidants are in low concentration or when the temperature is low. In adiabatic operation, the zone of coke increases with carbon dioxide addition, as shown in Figure 14 (a), (b), (c). Generally, an oxygen feed greater than 45% guarantees the absence of solid carbon, independently of steam. Note that this region also corresponds to the best syngas yield. Unlike oxygen, the minimum amount of water to guarantee the absence of coke is intrinsically dependent on carbon dioxide feed. For example, it is ca. 150% at 50% of CO_2 and 100% at 25% of CO_2.

5.1.5 Carbon Dioxide Conversion

For syngas processes that use natural gas rich in CO_2, a fair conversion is essential to prevent overload in separation units and recycles. The results of CO_2 conversion are shown in Figure15 as a function of water, oxygen and carbon dioxide.

In TRM, carbon dioxide conversion can be either positive or negative depending upon the initial state. Figure 15 (a) shows that the conversion varies from negative values below -1 up to 0.5, depending upon the feed of carbon dioxide and water. Since the oxygen is fixed at 50%, it is guaranteed that the results are not influenced by coke.

The reagents, water, and carbon dioxide influence the conversion in two distinctive ways. The increase of carbon dioxide and decrease of water enhance conversion when it is negative but, when the conversion is positive, only the reduction of water is relevant. In all cases, reducing the feed of water is beneficial because it competes directly with DMR for the methane molecule.

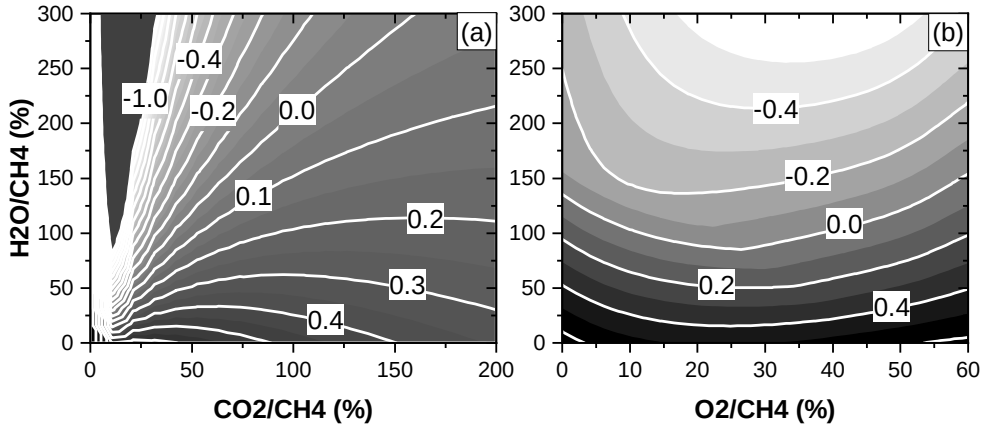

Figure 15 – Carbon dioxide conversion at (a) 50% of O_2/CH_4, (b) 50% of CO_2/CH_4 and 700 °C of initial temperature and 25 bar. In (b) lower values than -0.8 are not shown for the sake of clarity.

Source: The author's.

Conversely, oxygen has a low influence on the conversion of CO_2, as shown in Figure 15 (b). In TRM, it is responsible for raising the temperature, producing carbon dioxide and water by CCM, instead of converting CO_2. In both cases, the results indicate that TRM can only convert 40% or more of the CO_2 if the water feed is inferior of 50% in relation to methane. This feed is much lower than the industrial standards, suggesting that TRM with high conversion of CO_2 tends to dry reforming with an oxidation reaction.

5.1.6 Reaction Yield

The discussion on performance indicators has so far inferred explanations based on the behavior of the constituent reactions of TRM. However, an explicit analysis of the individual reactions is necessary to support those claims. In this sense, the individual yields of SMR and DMR are calculated as a function of oxygen and shown in Figure 16.

At the adiabatic conditions (Figure 16 (a)), oxygen enhances both reactions due to the temperature rise. The yield of DMR grows at a faster rate than SMR yield, from negative values up to 50% at 60% of oxygen. The yield of SMR also grows, but, around 50% of oxygen, it inflects in a decreasing fashion. At a fixed temperature of 900 °C (Figure 16 (a)), oxygen negatively influences the yield of SMR whereas the yield of DMR is practically unaffected. Since, in isothermal simulations, oxygen does not affect temperature, it only is responsible for producing water and carbon dioxide by CCM. Therefore, it may explain why SMR is more impacted by oxygen than DMR, the double of water molecules are produced than carbon dioxide. Additionally, it also explains the behavior of the syngas ratio and carbon dioxide conversion when oxygen feed increases. Since SMR is hindered whereas DMR is unaffected by oxygen, the syngas ratio is reduced and CO_2 conversion is boosted, as discussed in the sections 5.1.3 and 5.1.5.

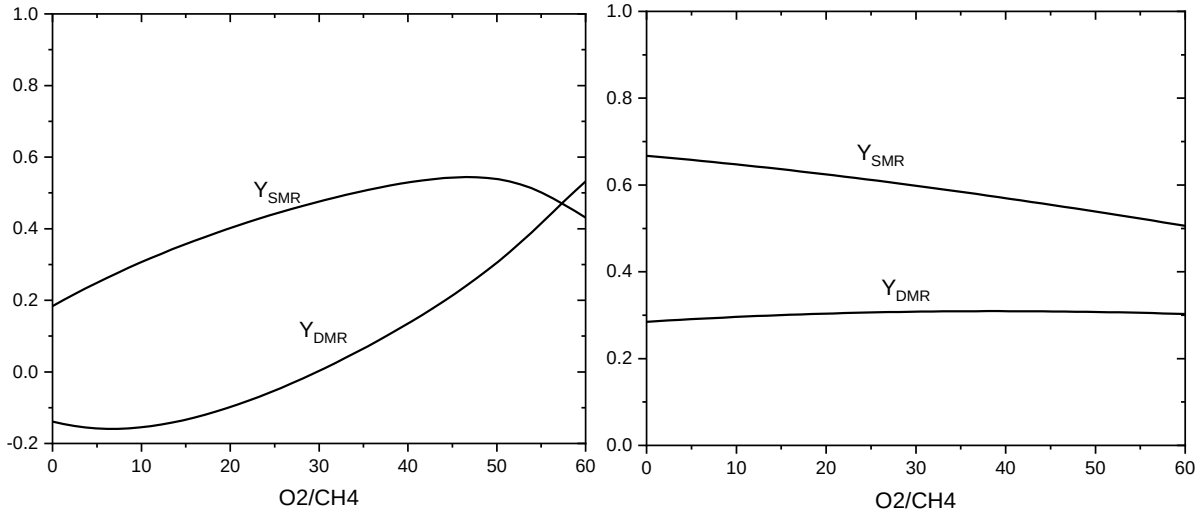

(a) adiabatic (b) at fixed 900 °C

Figure 16 – Yields of SMR and DMR at feed composition of CH_4: CO_2: H_2O = 1: 1.75: 0.5 at 700°C and 25 bar.

Source: The author's

5.2 ISOTHERMAL EQUILIBRIUM OF TRM

Due to its versatility, TRM can be operated adiabatically or non-adiabatically. Song and Pan(4) first proposed the operation of TRM similar to conventional steam reformers. heated by an external source. The TRM has advantages over conventional SMR and DMR on syngas ratio flexibility and coke prevention. In order to verify the benefits of this kind of operation, this section investigates TRM by its main performance indicators at industrial pressure of 25 bar.

5.2.1 Heat of Reaction

Tri-reforming is distinct from steam or bi-reforming reactions due to the presence of oxygen as a reactant. It acts as a strong oxidizer of methane and carbon, elevating the temperature due to CCM. The energy requirement for the reaction reduces as a function of oxygen. Figure 17 shows this trend at three temperatures.

The reaction enthalpy decreases with oxygen, ranging from + 225 (as a bi-reforming reaction) to -100 kJ/mol. The adiabatic point occurs at ca. 30, 42 and 45% of oxygen feed for 800, 900 and 1000 °C, respectively. Given isothermal conditions, the required energy for TRM becomes more sensitive as temperature reduces. For example, changing the supplied oxygen from 10 to 20%, the required energy reduces ca. 75 kJ/mol at 800 °C against 50 kJ/mol at 900 °C.

Given a fixed heat flux, the higher the temperature increases the more it becomes sensitive

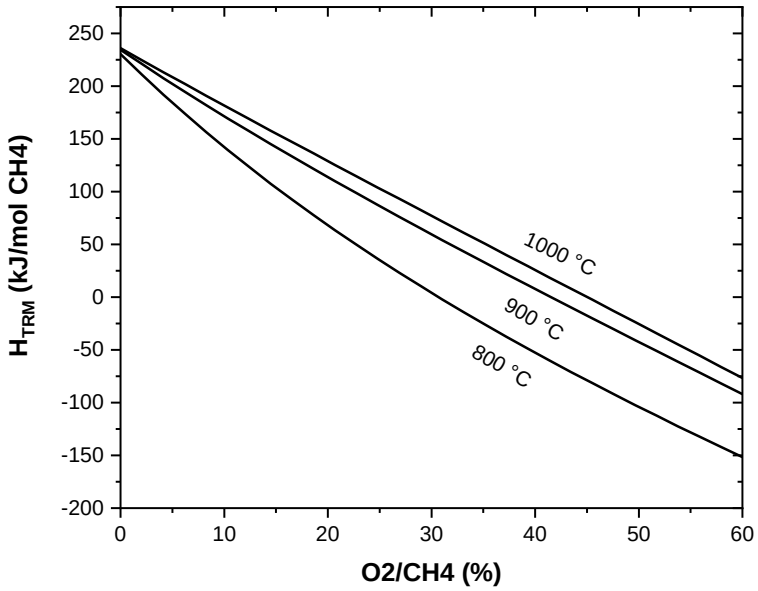

Figure 17 – Heat of reaction at constant temperatures of (a) 800 °C, (b) 900 °C, (c) 1000 °C at 25 bar, H_2O/CH_4 = 150 % and CO_2/CH_4 =50%.

.

Source: The author's.

to oxygen. Curves 900 and 1000 °C are much closer to each other than 800 to 900 °C. For example, given a heat supply of 100 kJ/mol, a change by 5% in oxygen is enough to drive the temperature from 900 to 1000 °C. This conclusion is the same found in the equilibrium data of adiabatic temperature (section 5.1.1). From a level of around 45% of oxygen, the adiabatic temperature is very sensitive to oxygen. As a consequence, oscillations in oxygen addition at this level can drive the reactive mixture to harmful temperatures.

Despite the benefits of the reduction in heat demand, oxygen feed may imply hot spot formation inside the catalytic bed. Using the information, in advance, from section 6.1 about oxygen distribution, which suggests that 20% of oxygen is sufficient for hot spots formation, the oxygen feed will be restricted to 10% in the following analysis.

5.2.2 Syngas Yield and Methane Conversion

When compared to adiabatic operation, TRM productivity is much higher at heated conditions. Figure 18 depicts syngas yield and methane conversion as a function of water and carbon dioxide.

As shown in Figure 18, syngas yield varies between 0.2 and 0.9 and conversion, from 0.4 to 1. Both water and carbon dioxide have a positive influence on syngas production and methane conversion. Note that carbon dioxide becomes more influential as temperature increases, converting more methane by DMR. To attain the best yields, excess of reactants are necessary, which means that the sum of water and carbon dioxide feeds must be greater

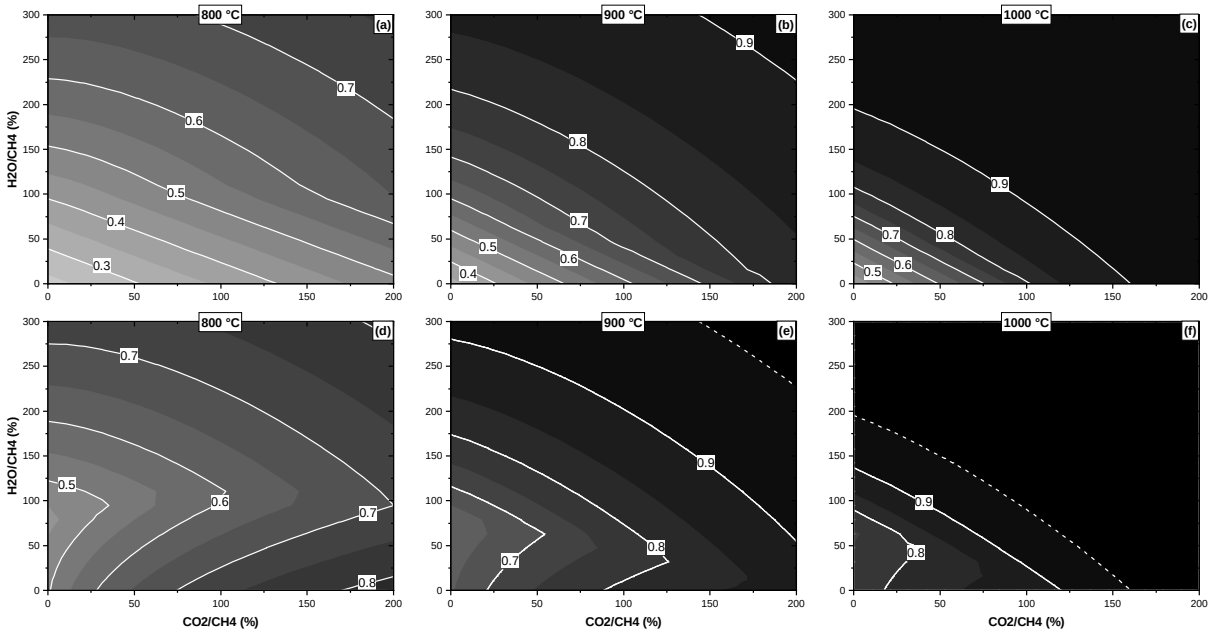

Figure 18 – Syngas yield (a, b, c) and methane conversion (d, e, f) at equilibrium temperatures of 800 °C, 900 °C, 1000 °C and 25 bar for 10% of O_2/CH_4 .

Source: The author's.

than 100% in relation to the methane feed. As a consequence, the total conversion of both reactants is not attained.

In addition, temperature plays a crucial role in syngas production. The results showed that the maximum yield grows from ca. 70% at 800 °C to 90% at 900 °C. For example, at CH_4: CO_2: H_2O = 1:0.5: 1.5 yield is ca. 90% at 1000 °C and 75% at 900 °C. The results suggest that, in order to substantially enhance productivity, it is more relevant to improve the resistance of reactor materials against temperature than optimizing the feed composition.

5.2.3 Coke Yield

Coke yield is an important indicator of possible catalyst deactivation. Figure 19 shows the coke production as a function of the feed of water and carbon dioxide.

The white region represents feed conditions whereby coke is thermodynamically unfavorable to form. Water and carbon dioxide can suppress coke formation, but they act differently depending on the temperature. The results show that water is the most relevant coke suppressant. For example, at 800 °C, water feed greater than 100 % in relation to methane is enough to restrain coke. However, carbon dioxide shows a different pattern. The suppression effect follows the reactivity of carbon dioxide, consequently, the higher the temperature less coke is produced. In this sense, the more the temperature rises, the more water and carbon dioxide are reactive and the smaller the plume of coke becomes. As a general conclusion, to efficiently

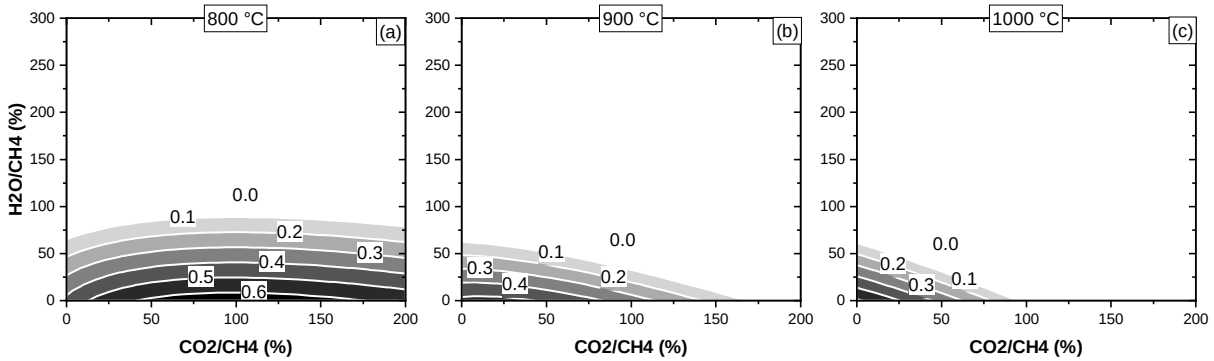

Figure 19 – Coke yield at equilibrium temperatures of (a) 800 °C, (b) 900 °C, (c) 1000 °C and 25 bar, 10% O_2/CH_4 and 700 °C of inlet temperature.

Source: The author's.

operate the reactor, the water level must be monitored to avoid coke deposition, regardless of the carbon dioxide feed.

5.2.4 Carbon Dioxide Conversion

Two types of conversion are shown in Figure 20 as a function of inlet water and carbon dioxide feed at three different temperatures. The first indicator, carbon dioxide conversion (X_{CO_2}), considers the conversion of the process gas (inside the tubes) (Figure 20 (a), (b), (c)) and the second indicator, total carbon dioxide conversion ($X_{CO_2}^{total}$) (Figure 20 (d), (e) and (f)) adds an estimation of the CO_2 emitted in the furnace.

Carbon dioxide conversion presents similar patterns to the adiabatic TRM. At negative values (CO_2 feed proportion greater than 15%), both co-reactants are important. To improve conversion, it is necessary to increase CO_2 feed or/and decrease the water supply. In the region of positive conversion, steam influence is predominant; conversion is improved if steam feed decreases. Compared to adiabatic operation, the conversion is much higher because the external furnace provides the necessary energy to maintain the temperature, and the small oxygen feed does not compete with SMR and DMR. Once more, temperature plays a crucial role in carbon dioxide conversion. For example, with feed composition of CH_4: H_2O: CO_2: O_2 = 1: 1.5: 0.5: 0.1, conversion goes from ca. 10% to 30% and 50%, at 800, 900 and 1000 °C respectively.

However, when the furnace emission of CO_2 is included in the calculations, the overall conversion drops drastically. For example, at 900 °C, while conversion in the catalytic bed is ca. 0.7, the overall conversion is around 0.25. Moreover, the influence of temperature is lower. While the maximum conversion varies between 0.6 to 0.8 from 800 to 1000 °C, the maximum total conversion is almost the same, ca. 0.25. The total conversion attained is much lower than in the adiabatic operation. As a conclusion, if the total conversion in

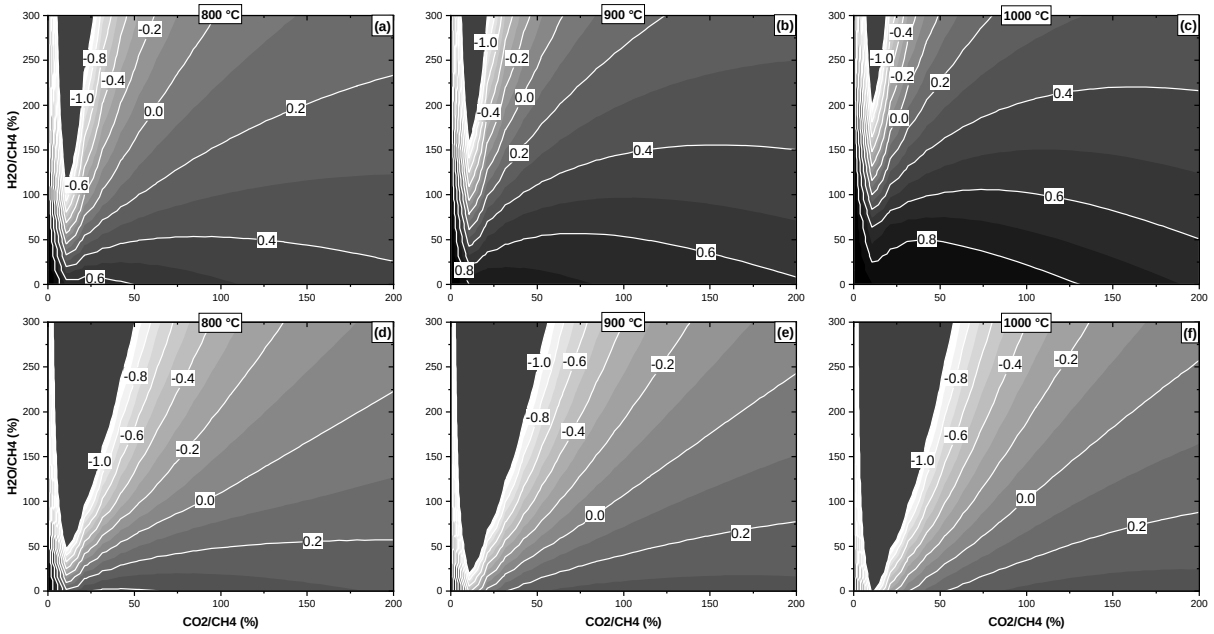

Figure 20 – Carbon dioxide conversion in the catalytic bed at equilibrium temperatures of (a) 800 °C, (b) 900 °C, (c) 1000 °C and 25 bar, 10% O_2/CH_4 and 700 °C inlet temperature. Carbon dioxide conversion of the overall reformer, including the carbon dioxide produced to heat up the reaction, at equilibrium temperatures of (d) 800 °C, (e) 900 °C, (f) 1000 °C and 25 bar, 10% O_2/CH_4 and 700 °C inlet temperature. Conversions lower than -1.0 are not shown for the sake of clarity.

Source: The author's.

the reactor is a priority over the conversion of process gas, then the heated reactor is not an adequate choice; otherwise, it may be a possible operational way to run a TRM reactor.

5.2.5 Syngas Ratio

Figure 21 shows the syngas ratio obtained by varying the water and carbon dioxide feed at three different temperatures.

The syngas ratio varies considerably, from values lower than 1.0 to above 3.0. As in adiabatic operation, the syngas ratio is mainly determined by the relation between water and carbon dioxide. Syngas ratio of 2.0, suitable for methanol production, for example, is obtained at a proportion of 2:1 between steam and carbon dioxide at 800 °C. Additionally, values around 1.0 are only obtained at a greater addition of carbon dioxide and less water, usually at 1:1.6. As expected, the water feed favors high syngas ratio whereas carbon dioxide, lower ones. As the temperature increases, the syngas ratio decreases due to the improvement in DMR reactions. For example, the steam for carbon dioxide proportion to obtain syngas ratio of 2.0 increases from 2: 1 at 800 °C to 2.7: 1 at 1000 °C.

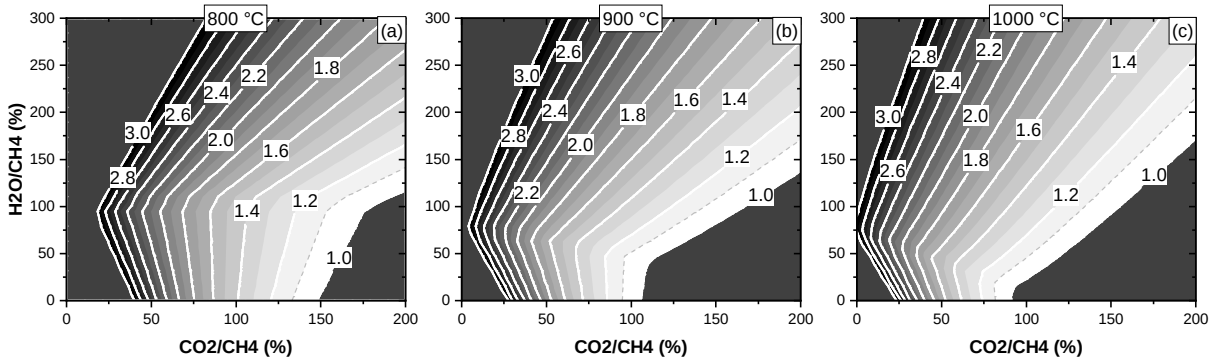

Figure 21 – Syngas ratio at equilibrium temperatures of (a) 800 °C, (b) 900 °C, (c) 1000 °C and 25 bar, 10% O_2/CH_4 and 700 °C inlet temperature. Values greater than 3.0 are not shown for the sake of clarity

.

Source: The author's.

5.2.6 Reaction Yield

The reforming reactions are improved by temperature, as shown in Figure 22. DMR, particularly, has a higher increase rate than SMR, going from negative values to more than 40% yield. Those results support the discussion in the sections about syngas yield, carbon dioxide, and syngas ratio, showing that: (i) since reforming reactions are improved by temperature, syngas is boosted as well, (ii) since DMR grows faster than SMR, conversion of CO_2 and syngas ratio decreases.

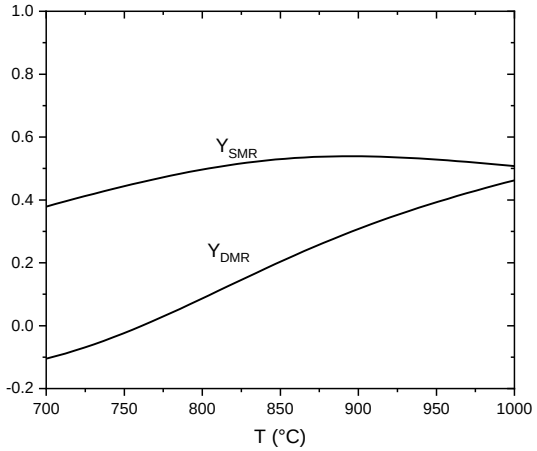

Figure 22 – Yield of SMR and DMR reactions as a function of temperature at 25 bar and composition of CH_4: H_2O: CO_2: O_2 = 1: 1.75: 0.5: 0.5

Source: The author's.

5.3 SUMMARY OF EQUILIBRIUM

Since the catalytic reactions closely follow the equilibrium data, as shown by Song and Pan(4), the simulations of reaction equilibrium give useful insights about TRM. The results presented in this chapter showed that performance attained at industrial pressure is lower than that in atmospheric conditions. For example, carbon dioxide conversion of 90% at 1 bar falls to a maximum of 50% at 25 bar. Moreover, since TRM can also operate adiabatically, the results showed a different behavior than isothermal, particularly regarding the dependence of oxygen feed. Therefore, the simulated equilibrium data shown in this section seems more appropriate for a comprehensive analysis of the applicability of TRM in the industry than at atmospheric pressure.

It is also important to analyze TRM comparing the metrics simultaneously to provide information on possible operations cases and its applicability for GTL industries. Figures 23 and 24 show the results of equilibrium simulation of TRM at adiabatic and isothermal conditions.

As discussed in the previous section, adiabatic TRM only performs reasonable yields when oxygen feed is greater than 45%. From Figure 23, note the region described by the range of 45% to 60% of oxygen feed. It also corresponds to the region free of coke deposition and high methane conversion. However, in this operational range, there is a **trade-off** between the syngas ratio and carbon dioxide conversion. A high syngas ratio means a low conversion of carbon dioxide. For example, the syngas ratio of 2, which is adequate to methanol and Fischer-Tropsch process, implies in negligible or even negative conversions of CO_2. Initial compositions that obtain CO_2 conversions of 20 and 40% also produce syngas at ratios of 1.6 and 1.4. If a proportion of oxygen lower than 45% is applied, the yield diminishes and CO_2 is not improved. Moreover, there is a risk of coke deposition. Therefore, the results indicate that adiabatic TRM requires a substantial amount of oxygen and produces the syngas ratio lower than 2.0. The adiabatic process requires an air separation unit and proper reactor configurations to avoid hot spots in the catalytic bed. GTL processes that avail low syngas ratios would benefit from TRM, such as DME and higher alcohols.

Figure 24 shows the performance of TRM at 900 °C, which is the equivalent of the adiabatic temperature attained at ca. 50% of oxygen. The obtained yields are greater than adiabatic, over 60% in the free coke region. The minimum steam to suppress coke in the feed is around 100% in relation to methane, due to the low level of oxygen (10%). As in adiabatic TRM, the opposing trends between syngas ratio and carbon dioxide conversion also exist. However, there is no trade-off between them. Syngas ratio of 2.0 can be obtained with a conversion of around 30% of CO_2. If the total conversion is considered, it drops to negative values similar to adiabatic. Clearly, since the CO_2 emission is an overall estimate, the overall conversion

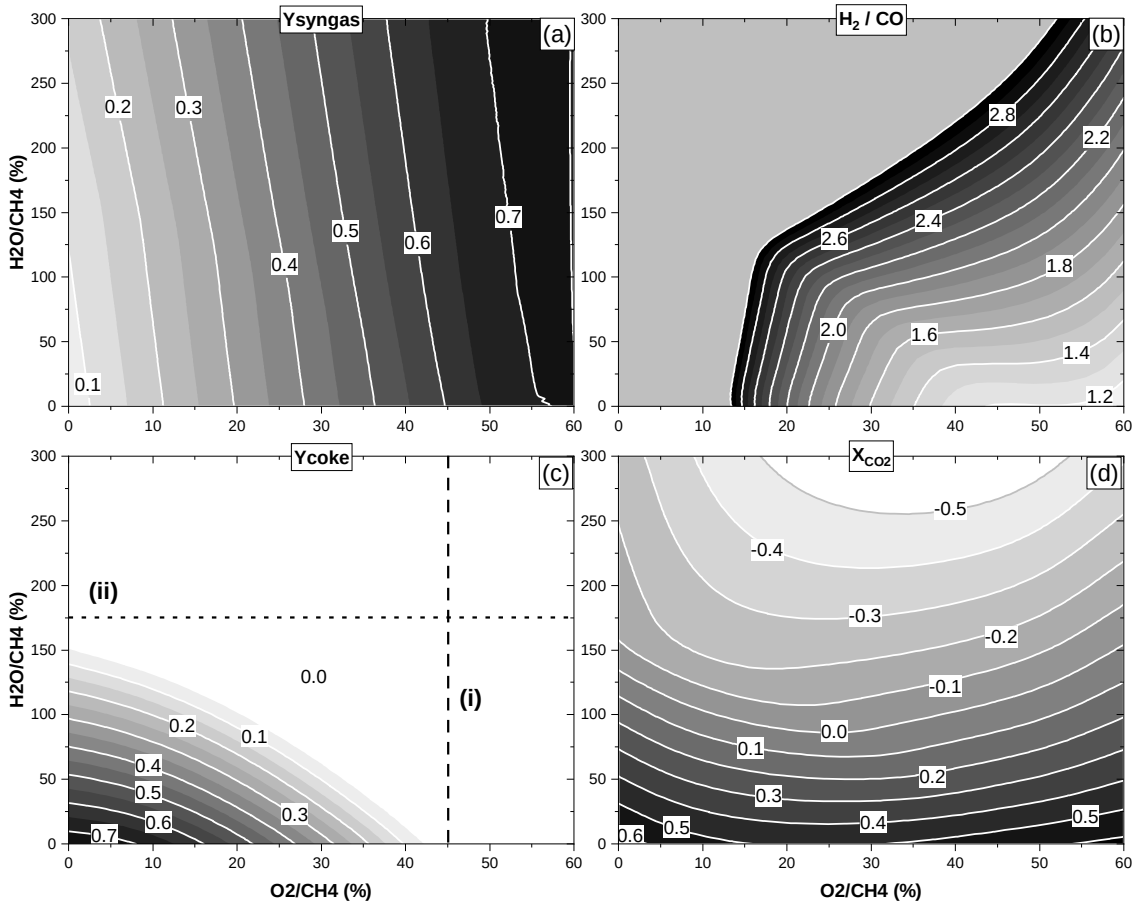

Figure 23 – Performance indexes of TRM at 50% of CO_2/CH_4, 700 °C and 25 bar. (a) syngas yield; (b) H_2/CO; (c) coke yield; (d) carbon dioxide conversion. In (b), values grater than 3.0 are not shown for the sake of clearness. (i) Represents the region free of coke independently of steam, (ii) independently of oxygen.

Source: The author's.

would be much smaller if the heat transfer is less efficient. Therefore, the results suggest that a heated TRM would be much more appropriate to process NG rich in CO_2 to the methanol process than adiabatic. However, to obtain a lower syngas ratio for DME and higher alcohols process, the load of CO_2 should be much greater.

To sum up, adiabatic conditions seem to be more appropriate to processes that demand lower syngas ratio whereas heated TRM, to methanol and usual Fischer-Tropsch plants. However, the adiabatic operation challenges the reactor design, due to a large amount of oxygen required. In the next sections, this issue will be addressed as well as a comparison among three reactor configurations.

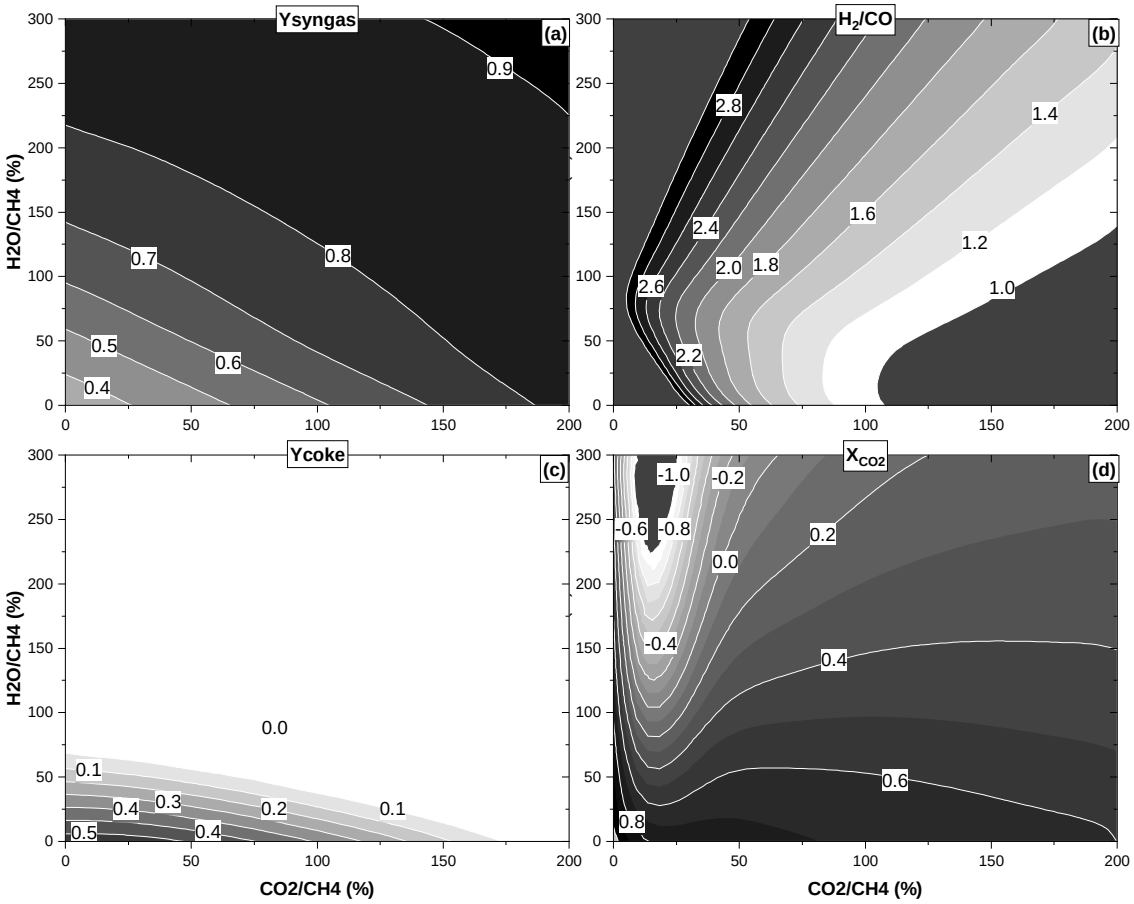

Figure 24 – Performance of TRM at 900 °, 25 bar and CH_4: O_2 = 1: 0.1 . Syngas yield (a), syngas composition (b), coke yield (c) and reformer carbon dioxide conversion (d) as function of water and carbon dioxide feed

.

Source: The author's.

6 REACTORS

6.1 MEMBRANE REACTOR

The last chapter discussed the adiabatic TRM, focusing on carbon dioxide conversion, coke, and syngas yield. As seen, TRM presents a trade-off between carbon dioxide conversion and syngas ratio. However, the most important feature for the design of the adiabatic reactor is the requirement of a large amount of oxygen due to the risk of dangerous temperatures and process safety. If oxygen is added with the feed in the conventional packed bed reactor, then a dangerous hot spot is produced, attaining a temperature of order 1400 °C, surely harming the catalyst and tubes. If the addition of oxygen is partitioned between the feed and a membrane, hot spots are mitigated, as reported by Rahimpour, Arab Aboosadi and Jahanmiri(23). However, a more detailed study must be done to explore the influence of oxygen partition in performance and also the limitations of a membrane reactor.

For this purpose, the section is divided into four subsections: (i) membrane reactor and equilibrium, (ii) oxygen partition, (iii) porous membrane reactor and (iv) membrane reactor and coke production. The first one discusses the relationship between reaction equilibrium in closed and open systems, particularly related to membrane reactors. The second one studies the influence of oxygen distribution and the third one analyzes a non-uniform flux in a porous membrane reactor. The last subsection investigates the problem of coke production. The base case of study is a feed composed of CH_4: CO_2: H_2O: O_2 = 1: 0.5: 1.75: 0.50 at 700 °C and 25 bar, which is thermodynamically free of coke and independent of oxygen feed (see section 5.1.4). The grid analysis for the mathematical model is shown in Appendix A.

6.1.1 Membrane Reactor and Equilibrium

In contrast to closed systems, such as batch and plug flow, membrane reactors transfer mass with its surroundings. Therefore, it is important to understand if the thermodynamic study for closed systems (as done in the last chapter) applies to systems whose mass is not constant. This subsection will address a number of analyses that will be used in the following discussions on the membrane reactor. Firstly, it will present two general conclusions on the reaction equilibrium and, secondly, it will discuss the general behavior of membrane reactors regarding closed equilibrium analysis.

6.1.1.1 Reaction Equilibrium

Recall from the modeling section, that the equilibrium state of adiabatic reactive closed system is calculated by:

$$min\, G(T,P,n_i) = \sum^{i} \mu(T,P,n_i)\cdot n_i \tag{6.1a}$$

s.t.:

$$\sum^{i} C_{ci}\cdot \delta n_i = \sum^{i} A_{ci}\cdot n_i - b_c = 0 \tag{6.1b}$$

$$\Delta P = 0 \tag{6.1c}$$

$$H_0 - H(T,P,n_i) = H_0 - \sum^{i} h_i(T,P,n_i)\cdot n_i = 0 \qquad \text{(adiabatic)} \tag{6.1d}$$

This set of equations describes a non-linear function (total Gibbs energy) of a multidimensional state variable (T,P, n_i) that belongs to a closed domain (restricted by equations 4.11b, 4.11c and 4.11d). From this perspective, two simple but important conclusions for membrane reactors can be addressed.

If there is a unique minimum to the minimization problem (no meta-stable states), then

I any non-equilibrium state, belonging to the fixed domain, evolves to the unique equilibrium state (global minimum), **regardless of initial temperature or composition** and

II if the mathematical space domain changes, another equilibrium (global minimum) state is possible. This process can be named as an equilibrium shift.

6.1.1.2 Adiabatic Membrane Reactors and Equilibrium Shift

Suppose an adiabatic closed homogeneous system *C* , static or in constant movement, free from external field forces in an initial non-equilibrium state Ω_0, similar to one described in the previous section (section 6.1.1.1). This system will evolve spontaneously to an equilibrium state Ω^f.

Now, suppose a similar system *M* with the same composition, enthalpy, and pressure divided into two subsystems by a perm-selective membrane (Figure 25). The subsystem (i) undergoes chemical reactions and the other system (ii) is inert. Only certain species can pass irreversible through the membrane , leaving or entering the subsystem (i) in relation to the subsystem (ii); in fact, the two subsystems are selectivity open to each other, though the overall system M is closed.

Additionally, suppose a membrane reactor composed by a reaction side and permeate/retentate side. The reaction side follows an 1D homogeneous reaction, without axial dispersion and pressure drop, and a uniform thermodynamic state in the sectional area (similar hypothesis of the membrane reactor). The reactive and permeate/retentate side are modeled as the subsystem (i) and (ii), respectively. The equilibrium state for comparison is the Ω_f.

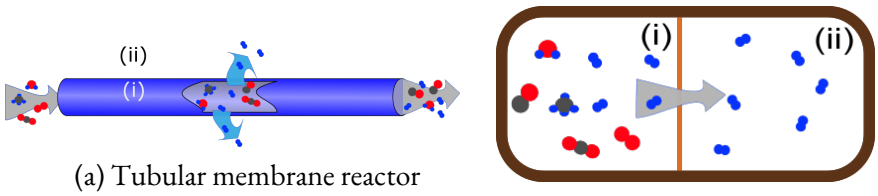

(a) Tubular membrane reactor

(b) Batch membrane reactor

Figure 25 – Removal membrane reactor, divided in two subsystems (of M) : (i) reactive retentade zone and (ii) inert permeate zone.

Source: The author's

From conclusion **II**, it follows that as long as the addition/removal of species is occurring, the equilibrium state Ω^f changes (is displaced). Since the mass and enthalpy restriction is continuously changing by addition/removal of species, the space domain changes, driving the minimization to another minimum. Therefore, membrane reactors shift the equilibrium expected along with addition/removal, and, consequently, new features may appear that were not predicted by the equilibrium analysis. Nevertheless, removal and addition membrane reactors differ on the overall approach to equilibrium. The membrane reactors for material removal have a reaction path that diverges from the expected overall equilibrium state whereas the addition reactors have a convergence approach.

Consider firstly the removal reactor (Figure 25). If the feed or initial state is Ω_0, then it would evolve spontaneously to Ω_f in the absence of a membrane. Instead, as chemical species are removed, the target equilibrium departs from Ω_f in a diverging path. As a consequence, the closed thermodynamic analysis presented in this work cannot predict the overall performance of such systems. Removal membrane reactors benefit reactions whose performance is restricted by equilibrium. Steam Methane Reforming, for example, is improved when hydrogen is withdrawn through a Palladium membrane, obtaining yields over the conventional operation. Additionally, in consecutive reactions, the removal of the final product prevents the undesired formation of intermediate species, improving selectivity[1].

The opposite behavior occurs in an **additive (distributive) membrane** (Figure 26). Consider the state Ω_0; if species are split between the subsystem (i) and (ii), and all species of (ii) are added[2]to (i), then the final state will spontaneously be Ω_f. Although the equilibrium

[1] It is supposed that the desired product is the final substance in the reaction chain and the undesirable ones are formed in the intermediate reactions.

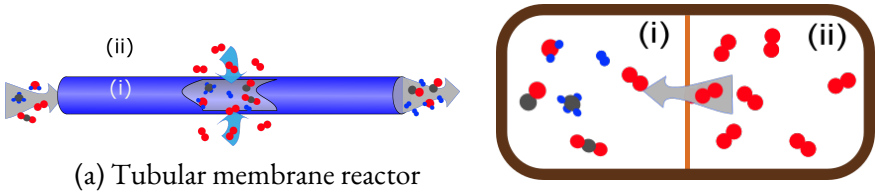

(a) Tubular membrane reactor

(b) Batch membrane reactor

Figure 26 – Additive membrane reactor, divided in two subsystems (of M) : (i) reactive permeate zone and (ii) inert retentade zone.

Source: The author's

is displaced during addition, the reactive system will tend towards Ω_f, in a convergence approach. This fact follows from conclusion **I** because the state after total addition belongs to the same domain as Ω_0 despite the difference in temperature and composition. As a result, such systems have the possibility of changing the reaction path (reaction rate) and the final/output state remains the predicted (designed) by equilibrium. Therefore, the final state may be predicted by the equilibrium analysis of this work but not the intermediate equilibrium states.

6.1.2 Oxygen Partition

The influence of oxygen partition (equation 4.14) on the performance of TRM is shown in Table 9 and Figure 27. Table 9 reveals that oxygen partition does not change the overall

Table 9 – Overall performance of the membrane reactor in different oxygen partitions. The feed is composed of CH_4: CO_2: H_2O: O_2 = 1: 0.5: 1.75: 0.50 (and 1e-4 of H_2 for kinetics issue) at 700 °C and 25 bar.

O_2 partition	equilibrium	0%	20%	40%	60%	80%	100%
O_2/ CH_4 (feed)	50%	50%	40%	30%	20%	10%	0%
J_{O_2} (mol/m^{2}s)	-	0.00	0.08	0.16	0.24	0.31	0.39
X_{CH_4}	94%	94%	94%	94%	94%	94%	94%
X_{CO_2}	-20%	-17%	-17%	-17%	-17%	-16%	-16%
Y_{syngas}	69%	69%	69%	69%	69%	69%	69%
H_2: CO	2.3	2.2	2.2	2.2	2.2	2.2	2.2

Source: The author's

performance. Conversions, yields, and syngas ratio hold almost constant despite the increase of oxygen permeation rate from 0 to 0.39 mol/m^2 s. Additionally, the output stream of the reactor model matched closely the equilibrium ones. The major difference was in the carbon dioxide conversion, where the equilibrium resulted in -20% and the model in -17%. The disagreement also occurred in other simulations and it is likely due to the adopted

[2] The addition occurs in a manner that the species enter with a molar enthalpy able to uphold the enthalpy constraint 4.11d and the same amount expected for Ω_0 . For example, if the specie enters with the same temperature and pressure as in Ω_0 . This is done in section 6.1.2.

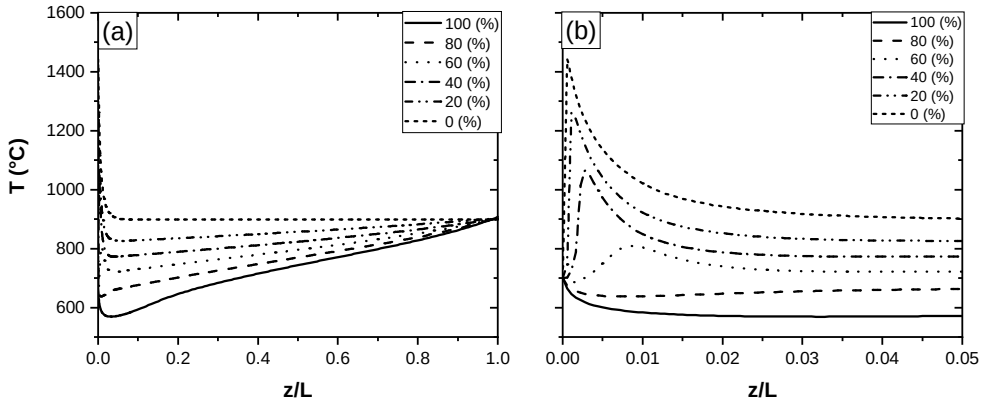

Figure 27 – Temperature profiles for different oxygen partitions, (a) is full zoom and (b) inlet zone.

Source: The author's.

kinetic model, which increases CO_2 conversion (24). Therefore, the results confirmed the conclusions about the addition of membrane reactors, addressed in section 6.1.1.2. The overall performance of additional membranes converges to equilibrium values after reactant addition. This effect could be observed in this simulation because the CCM reactions are very fast, driving TRM quickly to equilibrium.

Figure 27 shows the temperature profile at several oxygen partitions. The temperature varied from ca. 580 °C at 100% of partition to 1425 °C at 0% of partition. The inlet zone had a sharp temperature gradient, producing whether a hot or cold spot, which is common to all reformer reactors due to the extreme reaction enthalpies. After the steep profile at the entrance, the temperature attains the equilibrium smoothly.

The oxygen distribution impacts substantially the industrial application of TRM. As shown in Figure 27, in the case of the conventional reactor without the membrane, the reaction would attain temperatures above 1400 °C, which surpasses the melting point of Ni, damaging the catalyst and structural materials. The sharp increase occurs in a very short space, almost as a flame front. Therefore, a membrane reactor is indispensable for the adiabatic operation, unless a combustion chamber is present before the catalytic bed. The membrane reactor proved to be able to mitigate hot spots with partitions greater than 60% or oxygen feed below 20%.

6.1.3 Porous Membrane Reactor

A first-principle porous membrane of α-alumina, with a non-uniform flux, was simulated and the results are shown in Figure 28. Oxygen flux and temperature are shown in Figure 28 (a) and (b), indicators and molar compositions are depicted in Figure 28 (c) and (d).

In the membrane reactor, oxygen permeation grew from 0.27 to 0.40 mol/m^{2}s. It stems from

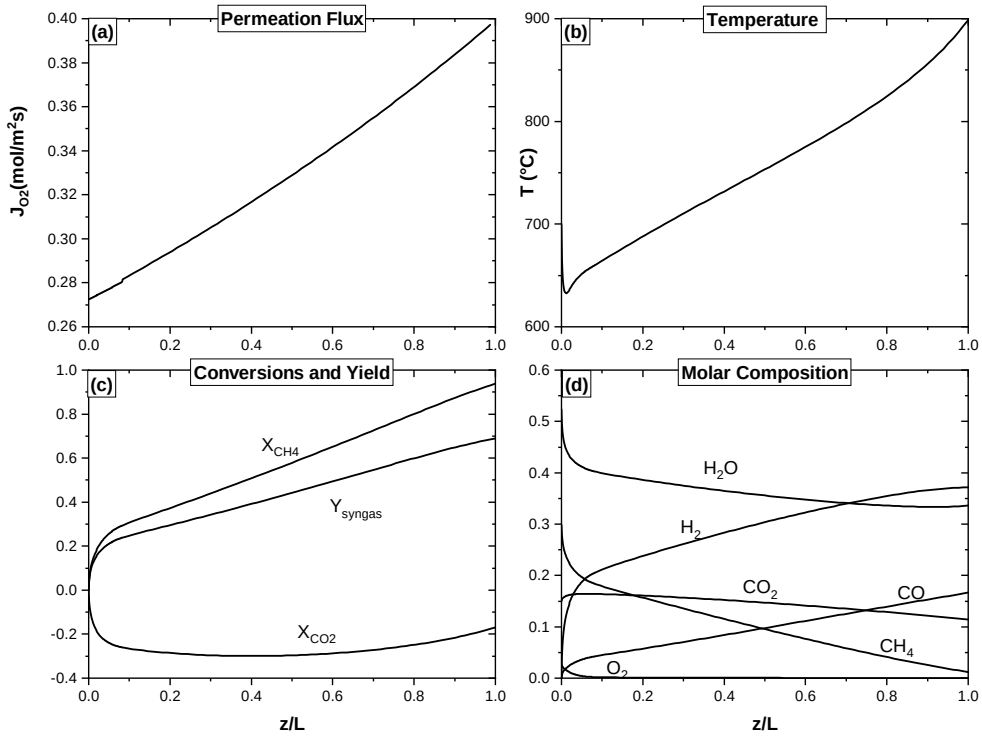

Figure 28 – Profile of the porous membrane reactor for 80% of oxygen partition, CH_4: CO_2: H_2O: O_2 = 1: 0.5: 1.75: 0.45 at 700 °C and 25 bar. (a) Oxygen permeation flux ,(b) temperature, (c) conversions and yields, (d) molar composition.

Source: The author's.

the fact that oxygen permeation is driven by the difference in pressure between retentate and permeate side, then, permeation grows with the pressure drop in the catalytic bed. As a result, an over-injection may occur at the outlet zone, consuming hydrogen instead of methane (which is almost depleted). Therefore, it is imperative the right control of distribution in the final section of the reactor. The reactor presented a cold spot at the inlet followed by a smooth increase, as already shown in the previous section. It varied from ca. 640 °to 900 °C. Reforming reactions were very fast at the inlet zone, dropping drastically the temperature, similar to conventional steam reformers.

Figure 28 (c) showed that methane conversion and yield grew similarly along the reactor bed but the distance between them increased due to the decrease of selectivity. TRM reactions attained more than 95% of conversion and ca. 70% of yield. However, carbon dioxide conversion had different behavior. It showed a steep fall at inlet followed by slow growth, attaining ca. -20%. The molar fraction of syngas increased up to 0.38 for hydrogen and 0.17 for carbon monoxide. Hydrogen had a slow decrease at the outlet, likely due to the RWSG reaction. Water and carbon dioxide decreased down to 0.34 and 0.11, respectively. Methane had a steep decrease, almost to depletion. It is important to note that oxygen had trace composition along the catalytic bed, as a result of its fast reaction with methane.

6.1.4 Membrane Reactor and Coke Production

The previous analysis of the membrane reactor used an initial state that was free of coke deposition, independently of how the oxygen was distributed. As a consequence, the carbon dioxide conversion was negative, i. e., TRM produced CO_2, instead of consuming it. The following analysis explores other initial states, verifying the coke production and the conversion of CO_2.

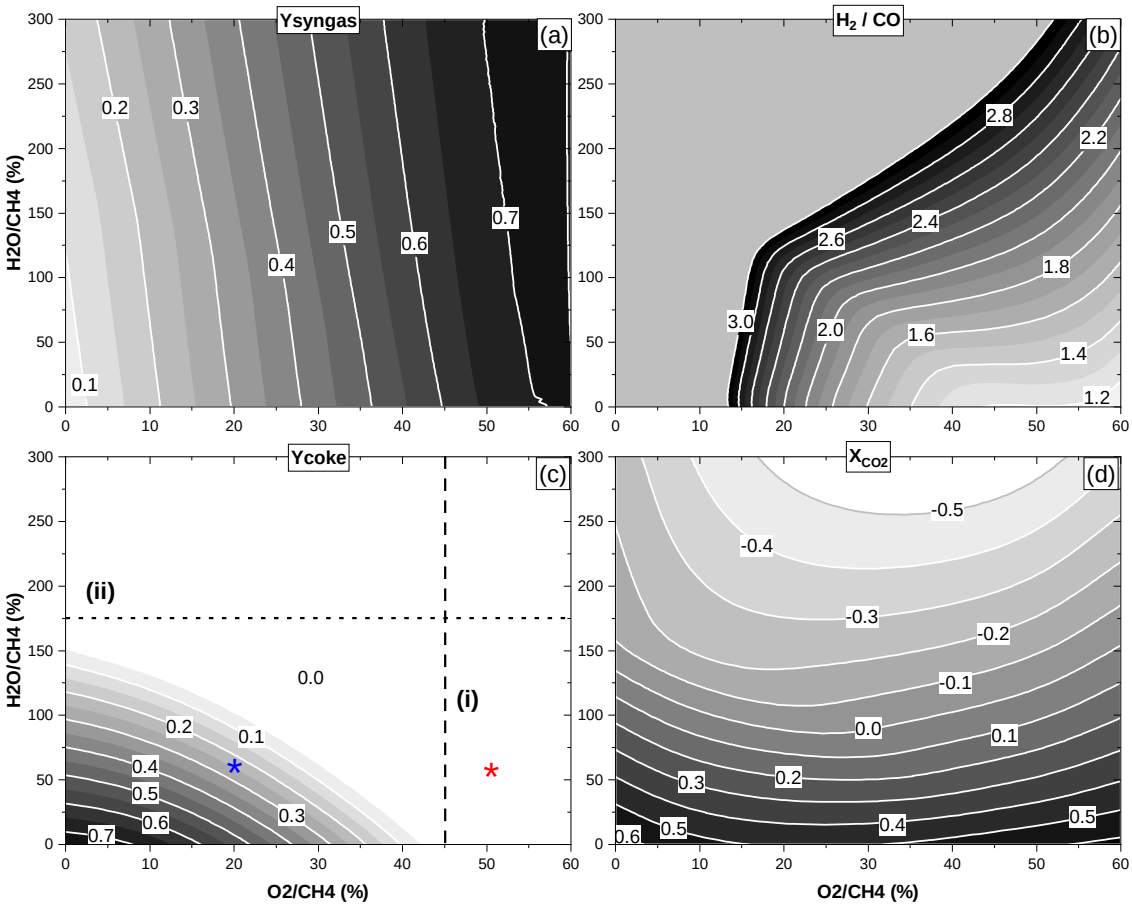

Figure 29 – Performance indexes of TRM at 50% of CO_2: CH_4, 700 °C and 25 bar. (a) syngas yield; (b) H_2: CO; (c) coke yield; (d) carbon dioxide conversion. In (b), values grater than 3.0 are not shown for sake of clearness. (i) represents the region free of coke independently of steam, (ii) independently of oxygen.

Source: The author's.

In Figure 29, note the results for initial states with water feed below 100%. The conversion of carbon dioxide is positive and the other indicators vary according to oxygen feed. Now, to obtain substantial yield and no coke in the reactor, the operational red asterisk was chosen. Apparently, if the membrane reactor is fed in these conditions, the performance indicators shown in red asterisk are obtained, as indicated by the previous sections (the reactor follows the equilibrium). However, recall from the discussion in section 6.1.1 that the membrane reactor presents a convergence behavior: it "seeks"' other equilibrium states during addition,

displacing equilibrium until it converges to the expected state. Applying the conditions of the red asterisk, coke may be produced if the partition is substantial because the low oxygen levels at the beginning displace red asterisk to the coke regions, for example, to the blue asterisk. Therefore, although the operation does not indicate overall coke production, in the membrane reactor it may occur, turning operation unsuitable to industry.

A trade-off appears between hot spot mitigation, coke deposition, and carbon dioxide conversion. They cannot be satisfied simultaneously. If a positive conversion is desired, water feed should be below 100%. At those conditions, oxygen higher than 45% is necessary for great yields and to avoid coke. However, large oxygen feed produces a hot spot in the catalytic bed. Then, a membrane reactor distributes oxygen but it forms solid carbon deactivating the catalyst. Therefore, the membrane reactor seems to be unsuitable to carry TRM, aiming for carbon dioxide conversion. Literature suggested that the membrane reactor is an alternative to carry out TRM but when coke and conversion of carbon dioxide are concerned, the results indicate the opposite.

6.2 AUTOTHERMAL REACTOR

As discussed in the reaction equilibrium section, adiabatic TRM demands large oxygen concentration to obtain high yields per pass, requiring a special reactor to manage the temperature. The first configuration proposed was the membrane reactor, which had the purpose of partitioning oxygen in the feed. Another configuration is the autothermal reactor, which has an especial refractory chamber to stand against high temperature caused by the methane oxidation. Cho et al.(56) proposed this configuration to carry TRM reactions, producing syngas for a DME plant. However, the performance still has not been compared to other configurations or studied for different syngas ratios.

For this reason, this section studies the main features of an autothermal reactor for TRM, using a first-principle approach (section 4.3.2). Two cases were analyzed, TRM producing syngas ratio of 2.0 (case 1) and 1.0 (case 2), which correspond to the demanded ratios for methanol/Fischer-Tropsch and DME processes, respectively. The feed conditions were determined by the maximization of carbon dioxide conversion, as described in the modeling chapter. A comparison of the combustion section model with literature is shown in Appendix A. The last part of the section analyses the effect of pressure on the reactor performance.

6.2.1 Reactor Performance

Autothermal configuration presented different trends when producing syngas ratio of 2.0 and 1.0, as shown in Tables 10 and 11. To produce the syngas ratio above 2.0, CO_2

conversion is lower or negative and the opposite trend is found for the syngas ratio of 1.0. The syngas yield and selectivity were similar, ca. 65% and 73%, respectively. The performance shifted from the expected equilibrium states, with methane conversion higher and the water conversion lower than expected. It stems from the combustion section where the equilibrium does not follow the model used in this work (it has more chemical species and reactions).

Table 10 – Performance of the autothermal configuration for case 01 (syngas ratio of 2.0). Feed at CH_4: CO_2: H_2O: O_2 = 1: 0.5: 1.17: 0.45, 700°C and 25 bar.

metrics	equilibrium	overall	combustion	catalytic
$\mathbf{X_{CH_4}}$	0.86	0.88	0.59	0.69
$\mathbf{X_{CO_2}}$	-0.03	-0.02	0.08	-0.10
$\mathbf{X_{H_2O}}$	0.02	-0.06	-0.33	0.21
$\mathbf{Y_{syngas}}$	0.64	0.63	0.34	0.70
$\mathbf{S_{syngas}}$	0.74	0.72	0.57	1.00
$\mathbf{H_2:CO}$	2.00	2.00	1.30	2.00
$\mathbf{T_{out}}$ **(°C)**	872	873	1,226	873

Table 11 – Performance of the autothermal configuration for case 02 (syngas ratio of 1.0). Feed at CH_4: CO_2: H_2O: O_2 = 1: 1.50: 0.82: 0.54, 700°C and 25 bar.

metrics	equilibrium	overall	combustion	catalytic
$\mathbf{X_{CH_4}}$	0.95	0.96	0.68	0.88
$\mathbf{X_{CO_2}}$	0.27	0.25	0.22	0.25
$\mathbf{X_{H_2O}}$	-0.65	-0.69	-0.96	0.14
$\mathbf{Y_{syngas}}$	0.68	0.65	0.37	0.89
$\mathbf{S_{syngas}}$	0.72	0.68	0.54	1.00
$\mathbf{H_2:CO}$	1.00	0.55	0.55	1.00
$\mathbf{T_{out}}$ **(°C)**	889	898	1203	898

The two sections performed differently. In the combustion section, total and partial oxidation prevailed, increasing the temperature. Since DMR is more reactive at high temperatures, in the refractory chamber, TRM preferentially converted CO_2 instead of steam. As a result, the combustion section produced syngas at a lower ratio, 1.3 (case 1) and 0.55 (case 2). In addition, the combustion section was also the major converter of methane. In turn, the catalytic bed was much more selective than the combustion chamber, and also preferentially converting water. Additionally, it was much more productive: in case 1, it yielded 70% against 34% of the combustion section; in case 2, yielded 89% against 37%. However, both sections are complementary to each other, the combustion section rises the temperature whereas, in the catalytic section, TRM reacts more selectively. Note that, only in the combustion chamber, the TRM converted carbon dioxide in both cases, even when the overall conversion was negative.

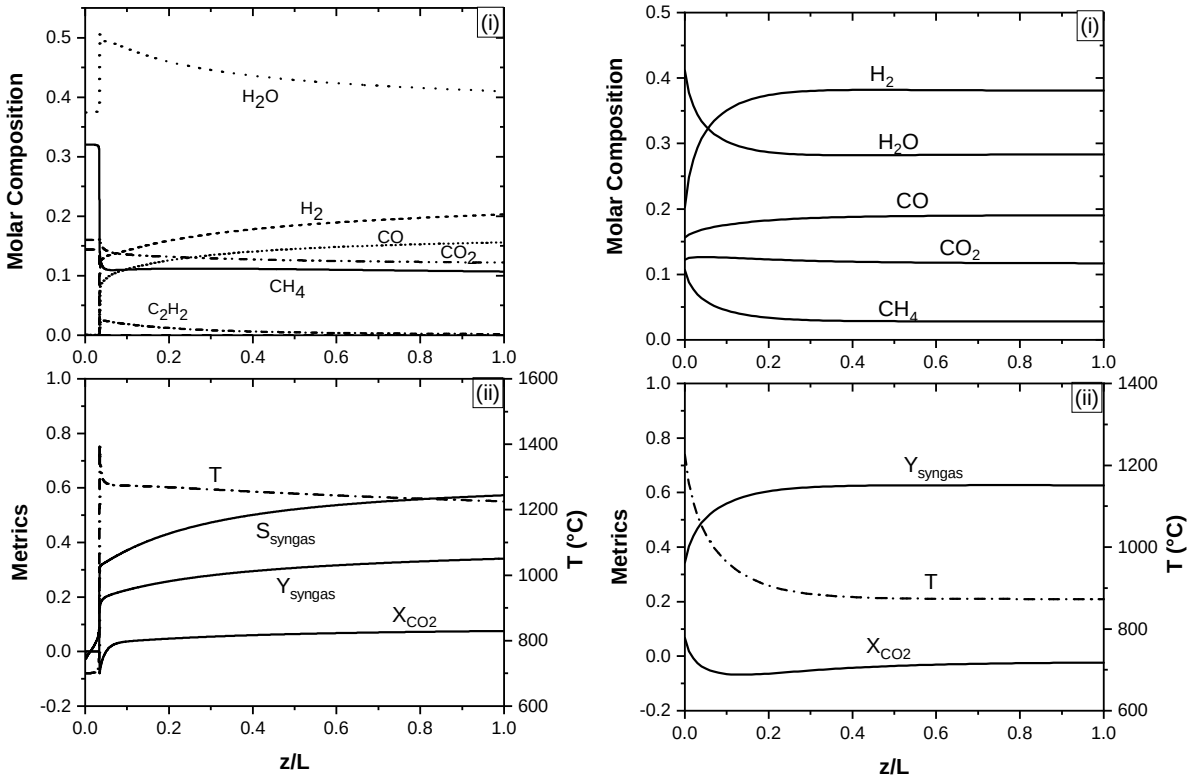

(a) Combustion section.

(b) Catalytic section.

Figure 30 – Profiles of the autothermal reactor producing syngas ratio of 2.0 (case 1).

Source: The author's.

The axial profiles of molar composition and metrics are shown in Figures 31 and 30, for case 1 and 2, respectively. The combustion section, simulated as an ignition problem, had a sharp profile before 5% of the reactor length followed by a smooth curve. Initially, the radical species were formed and, then, the extremely fast oxidation reactions took place at the ignition[3]. The ensuing reactions were much slower, yielding a smooth composition profile. At the ignition, methane and carbon dioxide were consumed while water, syngas, and light-saturated hydrocarbons were produced. This indicates that dry reforming reaction, which converts methane and carbon dioxide, is boosted by the heat from the quick oxidation reactions. It explains why in both cases there is carbon dioxide consumption, even though the overall conversion might be negative.

Note that the ignition temperature of 1400 °C is close to the values obtained in the packed bed without oxygen partition, suggesting that, in the catalyst, ignition also occurs. Since homogeneous TRM is less selective to syngas, as depicted by the yield and selectivity curves, it is disadvantageous to prolong residence time. It is important to note that light-saturated hydrocarbons, acetylene as the most expressive, were also produced at ignition, but con-

[3] Simulations in other conditions revealed that the ignition time is very sensitive to initial temperature and hydrogen concentration

verted afterward by the homogeneous reforming reactions. The catalytic section received the exhausted gases at a temperature of ca. 1200 °C, as usually occurs in industrial autothermal reformers. In the presence of the catalyst, the reforming reactions were much faster, converting the methane selectively to syngas and also reducing the temperature.

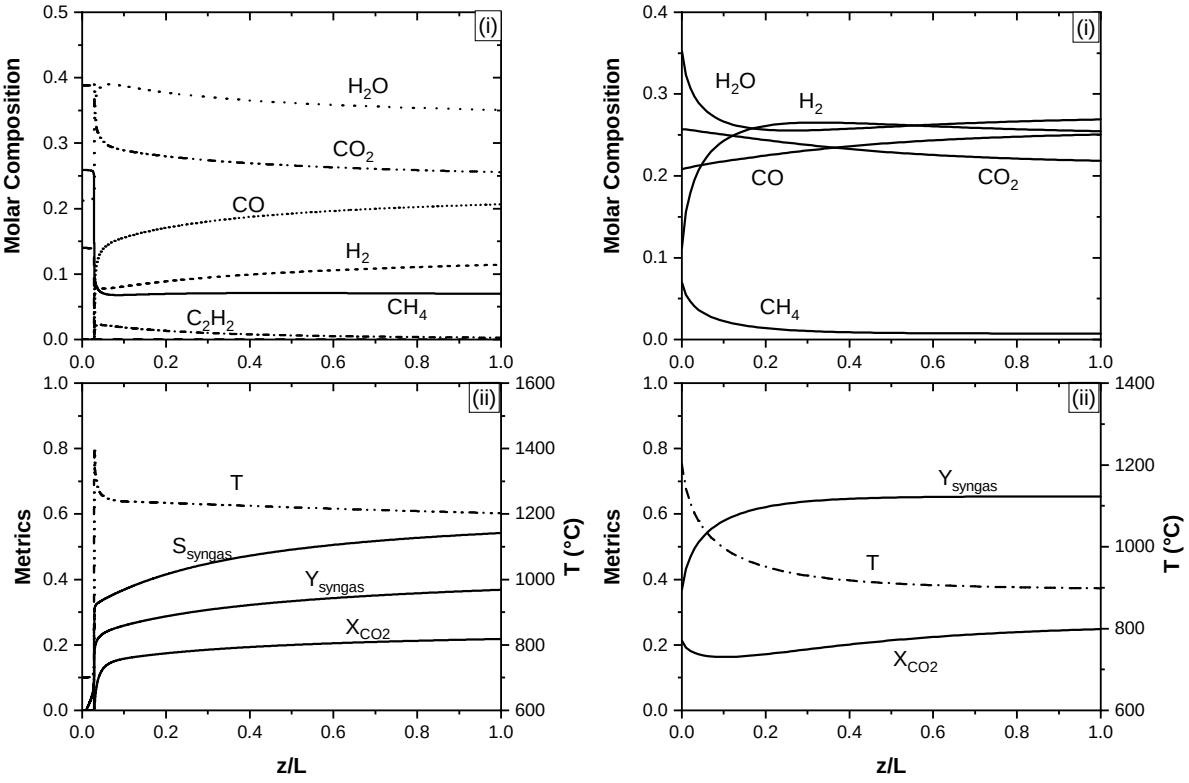

(a) Combustion section. (b) Catalytic section.

Figure 31 – Profiles of the autothermal reactor producing syngas ratio of 1.0 (case 2).

Source: The author's.

6.2.2 Pressure Effect

Although the increase of pressure reduces performance, it is advantageous, from the industrial point of view, to increase the gas density in order to reduce cost with equipment. In this sense, Figure 32 shows some performance indicators for TRM as a function of the pressure.

As pressure grows, methane conversion, syngas yield ratio, and syngas decrease. Methane conversion decreases from almost 1 to 0.9 and yield declines from 0.78 to 0.60, increasing the pressure from 1 to 40 bar. Conversely, the syngas ratio experiences an increase in CO production, reducing from 2.4 to 1.92. However, carbon dioxide conversion is the only indicator to benefit from pressure, increasing from -0.2 to almost 0. When pressure rises, in adiabatic operation two opposing forces act in TRM performance, one to reduce and another to improve performance. As mentioned previously, pressure hinders reforming reactions because they expand the reactive gas, but temperature improves them because they

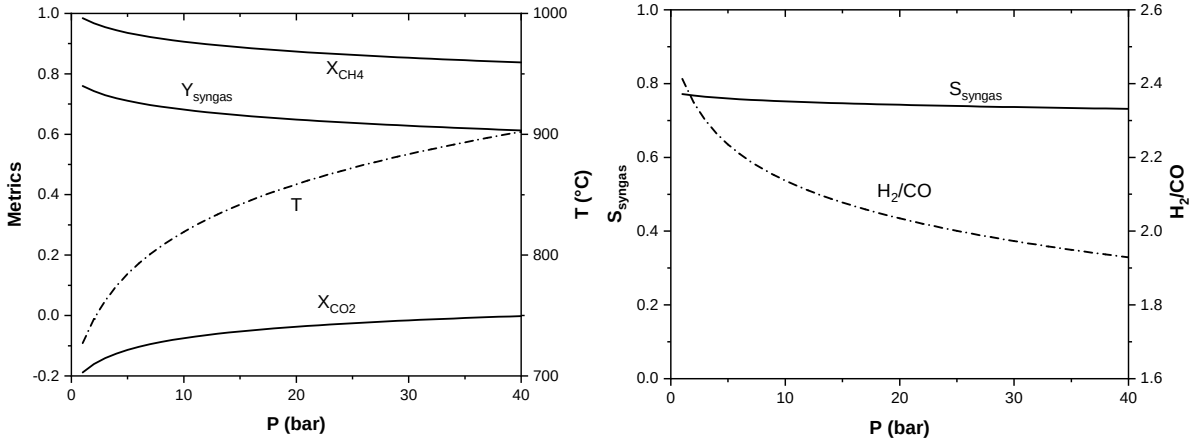

Figure 32 – Performance of adiabatic TRM on equilibrium as a function of pressure at feed composition of CH_4: CO_2: H_2O: O_2 = 1: 0.5: 1.167: 0.1. and 700 °C.

Source: The author's.

are endothermic. Therefore, since temperature also increases with the pressure in adiabatic conditions, carbon dioxide conversion also increases, consequently, falling the syngas ratio. These opposite trends explain why yield and methane conversion are less sensitive to pressure than in non-adiabatic conditions.

Table 12 – Pressure effect in ATR. The molar flow of syngas and residence time are relative to operation at 25 bar.

P (bar)	$\mathbf{F}^{rel}_{syngas}$	τ^{rel}	$\mathbf{T}_{equil}$ **(°C)**	$\mathbf{Y}_{syngas}$	$\mathbf{X}_{CO_2}$	$\mathbf{X}_{CH_4}$	$\mathbf{S}_{syngas}$
25	1.00	1.00	872	0.64	-0.03	0.86	0.74
30	1.17	1.18	884	0.63	-0.02	0.85	0.74
35	1.36	1.31	893	0.62	-0.01	0.85	0.73
40	1.53	1.47	902	0.61	0.00	0.84	0.73

Since performance is slightly affected in the range of 25 and 40 bar, it may be advantageous to operate adiabatic TRM in high pressures. Table 32 shows the effect of pressure in the autothermal model, relatively to an operation at 25 bar (restricted to a constant volumetric flow). The advantage of high pressure is that gas becomes denser, then more NG is processed. In the autothermal model, elevating pressure to 40 bar increases production volume by 53%, whereas yield diminishes slightly, less than 5%. The results strongly suggest that it is better to operate the adiabatic TRM at higher pressures, similarly to the conventional autothermal reformers.

6.3 HEATED REACTOR

Chapter 5 showed that TRM at non-adiabatic conditions outperforms the adiabatic operation. However, there is no report of simulations of heated reactors in the scientific literature for TRM. Song(55), for example, initially suggested a non-adiabatic operation of TRM, similar to conventional steam reformers, but the reactor was not simulated. In this scenario, the present section aims to provide information about non-adiabatic conditions, resembling the configuration of steam methane reformers. Two cases were analyzed at syngas ratio of 2.0 (case 1) and syngas ratio of 1.0 (case 2).

6.3.1 Reactor Performance

As shown in Table 13, the heated reactor substantially converted carbon dioxide, also producing a large amount of syngas. The carbon dioxide conversions were 40 and 52% and syngas yields were 74 % and 83% for cases 1 and 2, respectively. However, when the carbon dioxide produced in the furnace side was included, the total conversion severally dropped, particularly in case 1. The conversion decreased from 40% to - 40%, in case 1, and 52% to 17%, in case 2. The water conversion was 33% and -12% in case 1 and 2, respectively, as expected by the higher and lower syngas ratio produced. To produce a lower syngas ratio, more heat was necessary, 228.3 kW to 294.4 kW from case 1 to case 2, due to the prevalence of DMR which is more endothermic. The reactor followed the calculated equilibrium states, slightly outperforming.

Table 13 – Heated reactor performance metrics for case 1 and 2.

Metrics	**Case 1**		**Case 2**	
	equilibrium	**reactor**	**equilibrium**	**reactor**
$\mathbf{X_{CH_4}}$	0.78	0.78	0.87	0.88
$\mathbf{X_{CO_2}}$	0.39	0.40	0.51	0.52
$\mathbf{X_{CO_2}^{total}}$	-0.43	-0.42	0.16	0.17
$\mathbf{X_{H_2O}}$	0.33	0.33	-0.12	-0.12
$\mathbf{Y_{syngas}}$	0.73	0.74	0.82	0.83
$\mathbf{S_{syngas}}$	0.94	0.94	0.94	0.95
$\mathbf{H_2{:}CO}$	2.0	2.0	1.0	1.0
Q (kW)	228.3		294.4	

6.3.2 Pressure Effect

Unlike the adiabatic operation, the performance of the non-adiabatic reaction strongly declined, as shown in Figure 34. This effect was more pronounced at 800 °C than in 900 °C. Yield fell from ca. 0.90 to 0.4 at 800 °C and to 0.6 at 900 °C, when pressure was elevated up to 40 bar. Additionally, carbon dioxide conversion also decreased, unlike adiabatic operation,

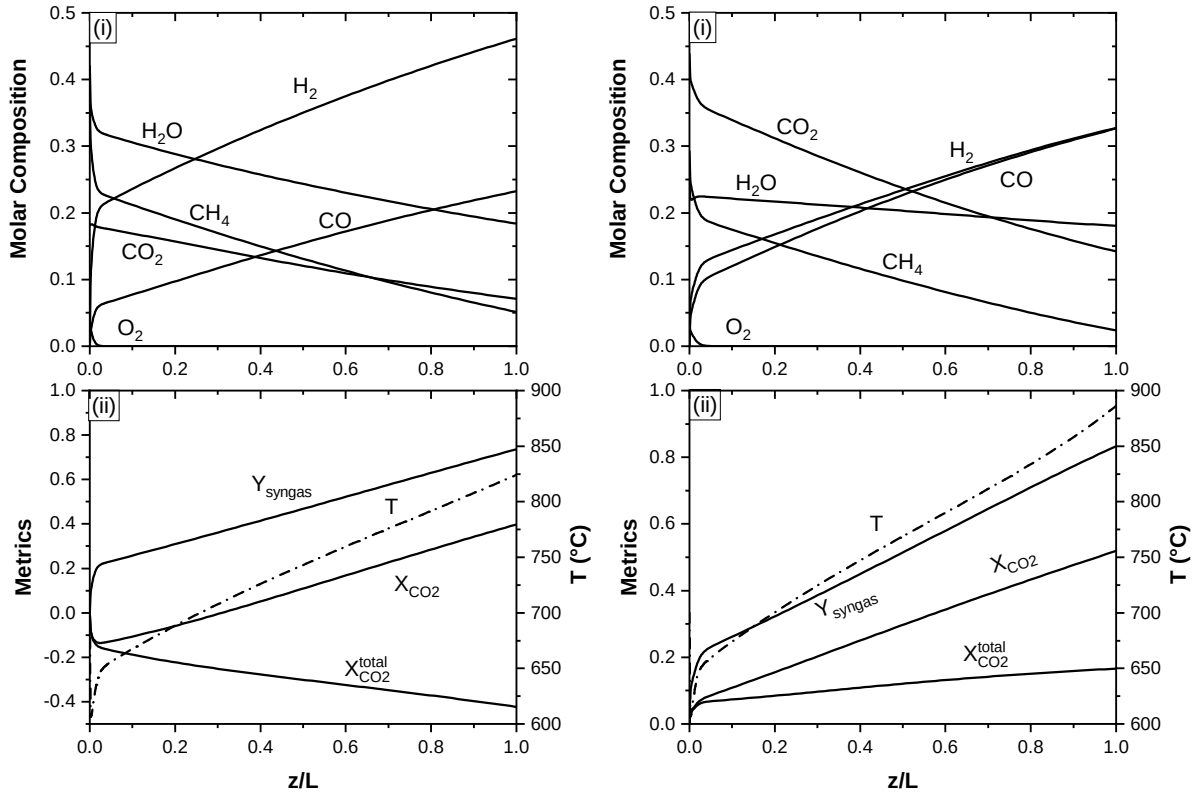

(a) Case 1. (b) Case 2.

Figure 33 – Profiles of molar composition and performance metrics of the heated reactor for the two cases simulated.

Source: The author's.

from 0.5 to 0.30. Syngas ratio and selectivity were less affected, particularly at 900°C. The difference between heated and adiabatic regarding pressure stems from the fact that, in adiabatic conditions, temperature also increases, compensating the less efficiency due to pressure increase.

In this sense, reducing the pressure may be an alternative to non-adiabatic conditions. Table 14 shows the relative volume of production and the residence time to 25 bar operation. The heated configuration at 10 bar produces half of the syngas volume at 25 bar. However, the residence time drops by one third, suggesting that an increase of reactor volume caused by a low density of the gas can be compensated by a faster reaction. Moreover, the syngas yield grows to 0.88 and methane conversion to 0.93. Carbon dioxide conversion inside the tubes increases to 0.47 but the total conversion in the reformer decreases proportionally.

6.4 COMPARISON OF HR AND ATR

Figures 35 and 36 compare the autothermal and heated reactors, concerning cases 1 and 2, respectively. The performance of the heated reactor was superior to autothermal in both

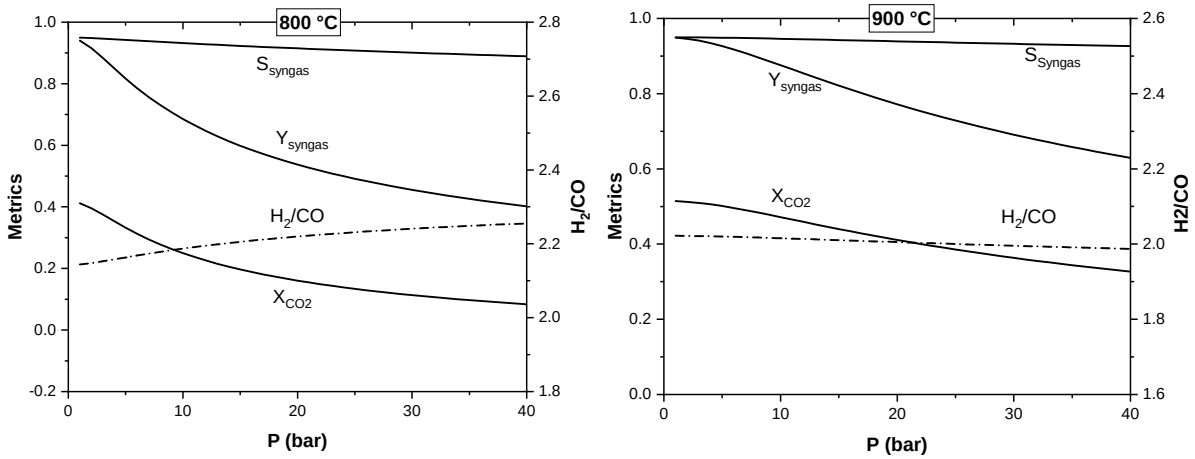

(a) at 800 °C (b) at 900 °C

Figure 34 – TRM performance on equilibrium as a function of pressure at feed composition of CH_4: CO_2: H_2O: O_2 = 1: 0.5: 1.16: 0.1. and 700 °C.

Source: The author's.

Table 14 – Pressure effect in HR. Molar flow of syngas and residence time are relative to the operation at 25 bar.

P (bar)	$\mathbf{F}_{syngas}^{rel}$	τ^{rel}	$\mathbf{Y}_{syngas}$	$\mathbf{X}_{CO2}$	$\mathbf{X}_{CO2}^{tot}$	$\mathbf{X}_{CH4}$
10	0.47	0.34	0.88	0.47	-0.52	0.93
15	0.67	0.62	0.82	0.44	-0.49	0.87
20	0.84	0.84	0.77	0.41	-0.46	0.82
25	1.00	1.00	0.73	0.39	-0.44	0.78

cases. It showed greater yield, selectivity and carbon dioxide conversion. Only the methane conversion was inferior to autothermal configuration.

In the case of syngas ratio of 2.0, HR outperformed ATR by ca. 10% in methane conversion and syngas yield. The selectivity in ATR was inferior to 22%, comparing to HR. The remarkable difference was in carbon dioxide conversion, 42%. The performance of the HR was much superior, consequently, the HR should be the technically preferred for syngas around 2.0. However, when the total conversion in HR is considered, the opposite occurs. While the carbon dioxide conversion of the process gas is 40%, the overall conversion including the furnace side is -42%. Therefore, if the overall abatement of carbon dioxide is aimed, ATR should be the choice, instead.

In the case of syngas ratio 1.0, HR also performs better than ATR. HR is 18% better in syngas yield, 27% in selectivity but worse 8% in methane conversion. HR still has a better carbon dioxide conversion than ATR, more than the double. When overall performance is considered, it is 8% less than the ATR. Again, HR performs better than ATR. The best

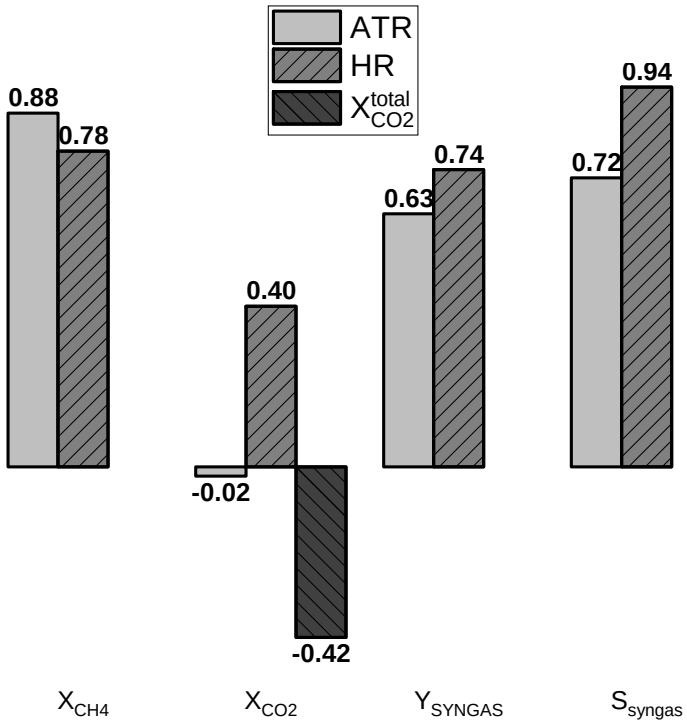

Figure 35 – Performance comparison between autothermal and heated reactor for case 1 (syngas ratio of 2.0).

Source: The author's.

performance of both reactors is at the syngas ratio 1.0. However, note that the proportion of CO_2 in the feed is 1.5 in relation to methane. This proportion can only be achieved in feed with recycles or from another concentrated stream from the process. Although the conversion is much higher than case 1, the remainder of carbon dioxide in the output stream is substantial.

6.5 SUMMARY OF REACTORS

The tri-reforming of methane is a suitable combination of reactions to convert methane and carbon dioxide into syngas. It can be operated in adiabatic or heated conditions. Many types of reactors were simulated in literature, most of them at adiabatic conditions and as packed bed configuration. The packed-bed reactor was incapable to prevent hot spots. Also, very few of the scientific papers concerned with carbon dioxide conversion. The adiabatic TRM challenges the reactor design due to the combination of fast and exothermic reaction with endothermic reforming reactions. To avoid hot spots, a membrane reactor was proposed, distributing oxygen slowly in the reactive mixture. The simulations presented in this chapter showed that the membrane reactor is efficient in preventing hot spots. Partitions higher than 60% were able to mitigate hot peaks in the catalytic bed. Otherwise, a temperature of the order of 1400 °C would damage the catalyst and tube materials. A special tuning should be done in the membrane permeability, to avoid over injection of oxygen, particularly at

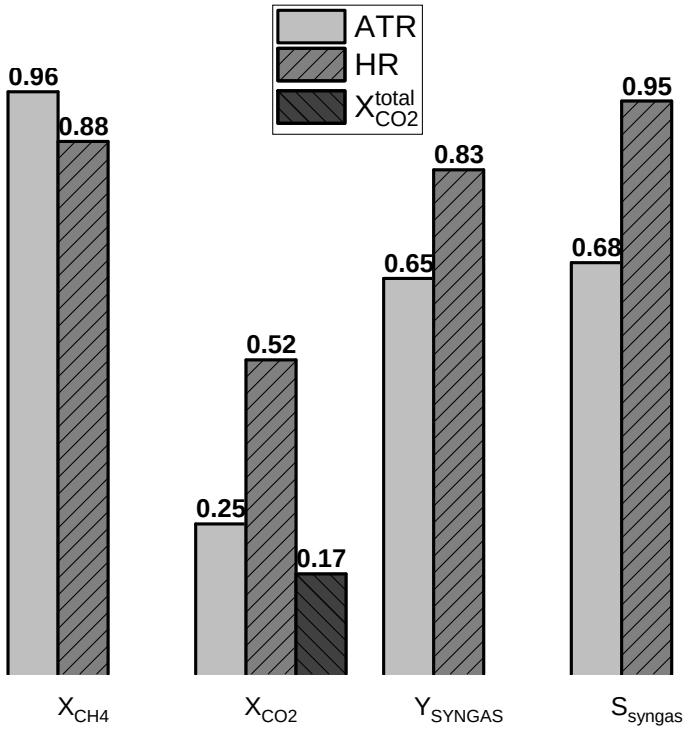

Figure 36 – Comparison of performance between autothermal and heated reactor for case 2 (syngas ratio of 1.0).

Source: The author's.

the final of the reactor where methane is in low concentrations. When investigating the behavior of membrane reactors, two important conclusions were addressed. The addition membranes have a convergent behavior: (i) it displaces equilibrium while addition occurs and (ii) after the addition, it converges to the expected equilibrium state. On one hand, the overall performance may be predicted by equilibrium simulations; on the other hand, during addition, it is difficult to predict to which equilibrium state the reaction is going. Therefore, the simulated results confirmed the overall performance despite oxygen partition. Concerning the displacement of equilibrium, the simulated data revealed a trade-off among hot spots, coke and carbon dioxide conversion. If the conversion of carbon dioxide is desired, it is necessary to lower the concentration of water. When the large oxygen feed is distributed to avoid hot spot, coke is produced in the catalytic bed. Therefore, membrane reactors seem to be unsuitable for industrial applications.

Two other configurations were studied to deploy the TRM reactions, autothermal (ATR) and heated reactor (HR). Those two types were less discussed in the literature of TRM. The autothermal consisted of a reactor divided between a refractory chamber and a catalytic bed, similar to industrial autothermal reformers. The heated reactor configuration comprised a tubular packed-bed heated by a furnace, similar to steam reformers. The advantage of the ATR is that it prevents damage in the catalyst bed concentrating the exothermic reactions at the refractory chamber. There, the homogeneous reactions take place, elevating the

temperature for the reforming reactions of the catalytic section. The results showed that the homogeneous section is much less selective and yields less syngas than the catalytic section. Due to the extreme temperatures reached, carbon dioxide was converted in the refractory chamber, despite negative overall conversions (case 01). Although reforming reactions are volume expansive, adiabatic TRM is much less sensitive to pressure. It stems from the fact that when pressure is increased, adiabatic temperature also grows; as a result, the temperature balances the negative effect caused by pressure. Therefore, it was shown that, for pressures of 30 and 40 bar, the autothermal reactor uses a larger volume of NG without losing performance. From the results of oxygen partition, it was suggested that oxygen feed around 20% in relation to methane was sufficient to provoke hot peaks in the catalytic bed. Therefore, the advantage of oxygen in reducing the energy demand compared to steam or bi-reforming may not be much explored in a conventional tubular packed-bed reactor. Conversely, HR performed much better than ATR, in terms of selectivity and yield. However, while the carbon dioxide conversion was ca. 40% in the catalytic bed, the overall conversion, including the furnace emission, was around -40%. Comparing both configurations, the HR was superior in both cases, producing syngas ratio of 2.0 or 1.0. Particularly, ATR did not perform very well at syngas of 2.0, with negative values of CO_2. It may be concluded that if TRM provides syngas for Methanol and Fischer-Tropsch, HR is more suitable and if syngas is used for DME or for higher alcohols both reactors can be used.

7 CONCLUSIONS

Tri-reforming of methane is a suitable reaction to produce syngas for GTL plants, using NG rich in carbon dioxide. When compared to DMR and BRM, it has the advantages of CO_2 conversion, coke prevention, and energy saving. In addition, it can also operate in adiabatic conditions, reducing the reactor size. Therefore, TRM can be used in natural gas resources such as biomethane and the Brazilian NG. Particularly in the Brazilian case, TRM could foster profitability of associated NG fields, reducing waste and re-injections, converting also the carbon dioxide present in the gas (between 8 and 18%, and sometimes up to 79% in volume).

The Review section showed that TRM is still a recent technology, without a mature industrial application, but with active research in the fields of catalysts, reactors and industrial processes. Regarding reaction equilibrium data, the scientific literature showed that TRM has good performance, with conversions and yield generally above 80%. Nevertheless, it evaluated the equilibrium at isothermal and atmospheric conditions. Syngas units, for example, apply pressures above 20 bar, at which the performance proved to be reduced. Moreover, the equilibrium literature has not considered adiabatic conditions. The studied reactors were mostly adiabatic and fixed-bed, which revealed dangerous hot spots. Other configurations were simulated but the literature still was not concerned about carbon dioxide conversion and coke deposition. In the midst of this background, the present work investigated the thermodynamics of TRM at 25 bar, included adiabatic conditions, and simulated three configurations of reactors, membrane, autothermal and heated reactors.

The equilibrium data showed that adiabatic TRM is intrinsically dependent on oxygen. Reasonable performance demands oxygen concentration greater than 45% to attain high yield, methane conversion, and prevention of coke deposition. The adiabatic operation has a trade-off between the syngas ratio and carbon dioxide conversion. For example, to produce syngas at a ratio of 2, the carbon dioxide conversion is negligible or negative (production instead of conversion). In order to convert carbon dioxide, TRM will produce syngas at lower ratios (around 1.5), instead.

At isothermal conditions, the equilibrium results showed that TRM has a better performance. TRM is very sensitive to the heat flux when the temperature is above 900 °C. It means that oscillations in the heat flux may drive the reaction to temperatures over 1000 °C, which is a risk for the tubular reactor. Carbon dioxide conversion was much greater than adiabatic, attaining values around 40 and 50%, and still producing syngas at a ratio of 2. Unlike adiabatic, there is no trade-off between the syngas ratio and carbon dioxide conversion.

As demonstrated, adiabatic reaction demands a large concentration of oxygen, around 45% to be suitable industrially. However, this amount challenges the reactor design, producing a hot peak in the conventional packed-bed reactor. Therefore, a membrane reactor was explored as an alternative to control the sharp temperature profile by slowly distributing oxygen. As discussed in the review section, the dense membranes, despite its perfect selectivity towards oxygen, still does not show stability and higher flux required by TRM. Porous membrane, instead, provided higher fluxes at the expense of selectivity. The developed model of the membrane reactor provided information about the influence of oxygen partition and permeation flux in TRM performance. Partitioning oxygen in the reactor proved to be a useful way to prevent hot peaks in the catalytic bed. It was indicated that concentrations of oxygen below 20% in the feed were sufficient to avoid hot spots. The simulations warned against an overoxidation in the outlet region due to an over-injection of oxygen, consuming hydrogen, instead of methane. As a consequence, a suitable tunning in the membrane permeation is necessary. Nevertheless, the thermodynamic study of the oxygen partition indicated that the membrane reactor is inappropriate to carry out adiabatic TRM. It showed a clear trade-off among carbon dioxide conversion, prevention of hot spot and coke formation; conditions that cannot be satisfied simultaneously.

Conversely, autothermal reactor can handle the fast and exothermic reactions within the refractory chamber, preventing dangerous temperatures in the catalytic bed and also coke formation. However, as already concluded in the equilibrium analysis, when the heat is provided outside the reaction, the performance of TRM is much superior. Thus, the comparison between the ATR and HR configurations showed that the HR outperformed. However, considering total carbon dioxide production, including the furnace emission, the CO_2 conversion was lower. For example, to produce a syngas ratio of 2.0, the HR converted 40% of the carbon dioxide whereas ATR, -2%. Regarding the pressure effect, the two reactors presented opposite trends. Adiabatic TRM is much less affected by the increase of pressure; consequently, raising to 30 or 40 bar would enhance the production volume at the expense of slightly inferior performance. Contrary, HR is very sensitive to pressure variation and, thus, a reduction in pressure should be considered to enhance performance.

In conclusion, TRM showed to be a suitable way to convert NG with CO_2. However, the performance at atmospheric pressure presented in the literature proved to be too optimistic concerning carbon dioxide conversion. Despite this fact, conversion of around 40% was attainable at industrial pressure reactors. Membrane reactor seems to be inadequate industrially. ATR is a suitable configuration to carry out adiabatic TRM, it is particularly adequate to lower the syngas ratio. HR has the best performance, concerning yield, selectivity, and carbon dioxide conversion which may be improved with proper heat integration in the process.

7.1 SUGGESTIONS

TRM still needs a comprehensive kinetic model, comprising the main reactions, SMR, DMR, and CCM simultaneously. This study explored three types of reactors, yet, many more reactors can be proposed to deploy tri-reforming. Moreover, it would be useful for a cost analysis in the syngas process, covering the cost of compressors, tube materials, utility and so on. In addition, more precise models would catch the especial features of the reactor, revealing localized hot spots or coke deposition, for example.

BIBLIOGRAPHY

1 ZHANG, Y. et al. Thermodynamic analyses of tri-reforming reactions to produce syngas. *Energy and Fuels*, v. 28, n. 4, p. 2717–2726, apr 2014. ISSN 15205029.

2 XU, J. G.; FROMENT, G. F. Methane Steam Reforming, Methanation and Water-Gas Shift .1. Intrinsic Kinetics. *Aiche J.*, v. 35, n. 1, p. 88–96, 1989. ISSN 0001-1541.

3 TRIMM, D. L.; LAM, C. W. The combustion of methane on platinum-alumina fibre catalysts-I. Kinetics and mechanism. *Chem. Eng. Sci.*, v. 35, n. 6, p. 1405–1413, 1980. ISSN 00092509.

4 SONG, C.; PAN, W. Tri-reforming of methane: A novel concept for catalytic production of industrially useful synthesis gas with desired H2/CO ratios. *Catal. Today*, v. 98, n. 4, p. 463–484, 2004. ISSN 09205861.

5 CONTI, J. et al. *International Energy Outlook 2016*. [S.l.: s.n.], 2016. v. 0484. 1–2 p. ISSN 0163660X. ISBN 2025866135.

6 U.S. Energy Information Agency. International Energy Outlook 2018. *Outlook 2018*, p. 312, 2018. ISSN 00162361.

7 SAHA, D. et al. *Postextraction Separation, On-Board Storage, and Catalytic Conversion of Methane in Natural Gas: A Review*. 2016. 11436–11499 p.

8 ANP. Exame e avaliação de dez descobertas e prospectos selecionadas no play do pré-sal em águas profundas na Bacia de Santos, Brasil. *Agência Nac. do Petróleo, Gás Nat. Bicombustíveis*, p. 105, 2010.

9 Agência Nacional do Petróleo Gas Natural e Biocombustíveis. Anuário Estatístico Brasileiro do Petróleo, Gás Natural e Biocombustíveis. 2018.

10 LIU, K.; SONG, C.; SUBRAMANI, V. *Hydrogen and Syngas Production and Purification Technologies*. [S.l.: s.n.], 2009. v. 2009. 528 p. ISBN 0470561246.

11 DYBKJAER, I. Tubular reforming and autothermal reforming of natural gas - an overview of available processes. *Fuel Process. Technol.*, ELSEVIER, v. 42, n. 2-3, p. 85–107, 1995. ISSN 03783820.

12 AMIN, M. H. et al. Tri-reforming of methane for the production of syngas: Review on the process, catalyst and kinetic mechanism. *APCChE 2015 Congr. Inc. Chemeca 2015*, n. SEPTEMBER, 2015.

13 WEI, J.; IGLESIA, E. Isotopic and kinetic assessment of the mechanism of reactions of CH 4 with CO2 or H2O to form synthesis gas and carbon on nickel catalysts. *J. Catal.*, v. 224, n. 2, p. 370–383, 2004. ISSN 00219517.

14 CHIN, Y.-H.; IGLESIA, E. Elementary Steps, the Role of Chemisorbed Oxygen, and the Effects of Cluster Size in Catalytic CH 4 ÀO 2 Reactions on Palladium. *J. Phys. Chem. C*, v. 115, p. 17845–17855, 2011.

15 DÍEZ-RAMÍREZ, J. et al. Kinetic, energetic and exergetic approach to the methane tri-reforming process. *Int. J. Hydrogen Energy*, v. 41, n. 42, p. 19339–19348, 2016. ISSN 03603199.

16 FARNIAEI, M. et al. Syngas production in a novel methane dry reformer by utilizing of tri-reforming process for energy supplying: Modeling and simulation. *J. Nat. Gas Sci. Eng.*, Elsevier B.V, v. 20, p. 132–146, 2014. ISSN 18755100.

17 GROOTE, A. M. D.; FROMENT, G. F. Simulation of the catalytic partial oxidation of methane to synthesis gas. *Appl. Catal. A Gen.*, v. 138, p. 245–264, 1996.

18 De Smet, C. R. H. et al. Design of adiabatic fixed-bed reactors for the partial oxidation of methane to synthesis gas. Application to production of methanol and hydrogen-for-fuel-cells. *Chem. Eng. Sci.*, v. 56, p. 4849–4861, 2001.

19 DASHLIBORUN, A. M.; FATEMI, S.; NAJAFABADI, A. T. Hydrogen production through partial oxidation of methane in a new reactor configuration. *Int. J. Hydrogen Energy*, v. 38, n. 4, p. 1901–1909, 2013. ISSN 03603199.

20 XU, J.; FROMENT, G. F. Methane steam reforming: II. Diffusional limitations and reactor simulation. *AIChE J.*, v. 35, n. 1, p. 97–103, 1989. ISSN 15475905.

21 PANTOLEONTOS, G.; KIKKINIDES, E. S.; GEORGIADIS, M. C. A heterogeneous dynamic model for the simulation and optimisation of the steam methane reforming reactor. In: *Int. J. Hydrogen Energy*. [S.l.: s.n.], 2012. v. 37, n. 21, p. 16346–16358. ISSN 03603199.

22 FARNIAEI, M. et al. Simultaneous production of two types of synthesis gas by steam and tri-reforming of methane using an integrated thermally coupled reactor: mathematical modeling. *Int. J. Energy Res.*, v. 38, p. 1260–1277, 2014. ISSN 12310956.

23 RAHIMPOUR, M. R.; Arab Aboosadi, Z.; JAHANMIRI, A. H. Synthesis gas production in a novel hydrogen and oxygen perm-selective membranes tri-reformer for methanol production. *J. Nat. Gas Sci. Eng.*, Elsevier B.V, v. 9, p. 149–159, 2012. ISSN 18755100.

24 Arab Aboosadi, Z.; JAHANMIRI, A. H.; RAHIMPOUR, M. R. Optimization of tri-reformer reactor to produce synthesis gas for methanol production using differential evolution (DE) method. *Appl. Energy*, Elsevier Ltd, v. 88, n. 8, p. 2691–2701, 2011. ISSN 03062619.

25 RAHNAMA, H. et al. Modeling of synthesis gas and hydrogen production in a thermally coupling of steam and tri-reforming of methane with membranes. *J. Ind. Eng. Chem.*, The Korean Society of Industrial and Engineering Chemistry, v. 20, n. 4, p. 1779–1792, 2014. ISSN 22345957.

26 OSTROWSKI, T. et al. Comparative study of the catalytic partial oxidation of methane to synthesis gas in fixed-bed and fluidized-bed membrane reactors Part I : A modeling approach. *Catal. Today*, v. 40, n. 2-3, p. 181–190, 1998. ISSN 09205861.

27 AL-DHFEERY, A. A.; JASSEM, A. A. Modeling and simulation of an industrial secondary reformer reactor in the fertilizer plants. *Int. J. Ind. Chem.*, v. 3, n. 1, p. 1–8, 2012. ISSN 22285547.

28 AL-DHFEERY, A. A.; JASSEM, A. A. Evaluation Performance of Different Types Catalysts of an Industrial Secondary Reformer Reactor in the Ammonia Plants. *Mod. Res. Catal.*, v. 01, n. 03, p. 43–51, 2012. ISSN 2168-4480.

29 AASBERG-PETERSEN, K. et al. Technologies for large-scale gas conversion. *Appl. Catal. A Gen.*, v. 221, n. 1-2, p. 379–387, 2001. ISSN 0926860X.

30 CHAUBEY, R. et al. A review on development of industrial processes and emerging techniques for production of hydrogen from renewable and sustainable sources. *Renew. Sustain. Energy Rev.*, Elsevier, v. 23, p. 443–462, 2013. ISSN 13640321.

31 TRAN, A. et al. CFD modeling of a industrial-scale steam methane reforming furnace. *Chem. Eng. Sci.*, v. 171, p. 576–598, nov 2017. ISSN 00092509.

32 FEPCO. *Catalytic Steam Reformers – FEPCO*. 2016.

33 LATHAM, D. *Mathematical Modelling of an Industrial Steam Methane Reformer*. Tese (Doutorado) — Queen's University, 2009.

34 WU, Z. et al. *CFD modeling and control of a steam methane reforming reactor*. [S.l.], 2016. v. 148, 78–92 p.

35 Haldor Topsoe. *SynCOR™ - Autothermal Reformer (ATR) | Steam Reformers | Products | Haldor Topsoe*. In: <https://www.topsoe.com/products/equipment/syncortm-autothermal-reformer-atr>.

36 Air Liquide Engineering & Construction. *Autothermal Reforming (ATR) - Syngas Generation | Air Liquide*. 2018. In: <https://www.engineering-airliquide.com/autothermal-reforming-atr-syngas-generation>.

37 Christian Friedrich Gottzmann, C. et al. *TUBE AND SHELL REACTOR WITH OXYGEN SELECTIVE ON TRANSPORT CERAMIC REACTION TUBES*. 2000.

38 PRASAD, R. et al. *SYNGAS PRODUCTION METHOD UTILIZING AN OXYGEN TRANSPORT MEMBRANE*. 2004.

39 REPASKY, J. M. et al. *STAGED MEMBRANE OXIDATION REACTOR SYSTEM*. 2008.

40 REPASKY, J. M. *OPERATION OF STAGED MEMBRANE OXIDATION REACTOR SYSTEMS*. 2011.

41 SUNARSOD, X. et al. Perovskite oxides applications in high temperature oxygen separation, solid oxide fuel cell and membrane reactor: A review. *Prog. Energy Combust. Sci.*, v. 61, p. 57–77, 2017.

42 FOY, K.; MCGOVERN, J. Comparison of Ion Transport Membranes. *Fourth Annu. Conf. Carbon Capture Sequestration*, p. 1–11, 2005.

43 Meredith Hashim, S.; Rahman Mohamed, A.; BHATIA, S. Current status of ceramic-based membranes for oxygen separation from air. *Adv. Colloid Interface Sci.*, v. 160, p. 88–100, 2010.

44 STEELE, B. C. Ceramic ion conducting membranes. *Curr. Opin. Solid State Mater. Sci.*, Elsevier, v. 1, n. 5, p. 684–691, oct 1996. ISSN 13590286.

45 TSAI, C.-y. et al. Dense Perovskite Membrane Reactors for Partial Oxidation of Methane to Syngas. *AIChE J.*, v. 43, n. 11, p. 2741–2750, 1997. ISSN 00011541.

46 TAN, X.; LI, K. Design of mixed conducting ceramic membranes/reactors for the partial oxidation of methane to syngas. *AIChE J.*, v. 55, n. 10, p. 2675–2685, oct 2009. ISSN 00011541.

47 HOANG, D.; CHAN, S.; DING, O. Kinetic Modelling of Partial Oxidation of Methane in an Oxygen Permeable Membrane Reactor. *Chem. Eng. Res. Des.*, v. 83, n. 2, p. 177–186, 2005. ISSN 02638762.

48 TAN, X.; LI, K. Modeling of air separation in a LSCF hollow-fiber membrane module. *AIChE J.*, v. 48, n. 7, p. 1469–1477, 2002. ISSN 00011541.

49 CHENG, Y.; PEÑA, M.; YEUNG, K. Hydrogen production from partial oxidation of methane in a membrane reactor. *J. Taiwan Inst. Chem. Eng.*, v. 40, n. 3, p. 281–288, 2009. ISSN 18761070.

50 CORONAS, J.; SANTAMARÍA, J. Catalytic reactors based on porous ceramic membranes. *Catal. Today*, v. 51, n. 3-4, p. 377–389, 1999. ISSN 09205861.

51 LAFARGA, D.; SANTAMARIA, J.; MENÉNDEZ, M. Methane oxidative coupling using porous ceramic membrane reactors-I. reactor development. *Chem. Eng. Sci.*, v. 49, n. 12, p. 2005–2013, 1994. ISSN 00092509.

52 DELTAPORE. *Technical datasheet ceramic membranes*. Beuningen, The Netherlands: [s.n.], 2018. 2 p.

53 MEMBRANE, P. et al. *Inorganic Membranes for Separation and Reaction*. [S.l.]: Elsevier, 1996. v. 3. 249–297 p. ISSN 1049-3867. ISBN 09339361.

54 GODINI, H. R. et al. Experimental and model-based analysis of membrane reactor performance for methane oxidative coupling: Effect of radial heat and mass transfer. *J. Ind. Eng. Chem.*, v. 20, n. 4, p. 1993–2002, 2014. ISSN 22345957.

55 SONG, C. Tri-reforming: A new process concept for effective conversion and utilization of CO2 in flue gas from electric power plants. *ACS Div. Fuel Chem. Prepr.*, v. 45, n. 4, p. 772–776, 2000. ISSN 05693772.

56 CHO, W. et al. Optimal design and operation of a natural gas tri-reforming reactor for DME synthesis. *Catal. Today*, v. 139, n. 4, p. 261–267, 2009. ISSN 09205861.

57 CHALLIWALA, M. S. et al. A combined thermo-kinetic analysis of various methane reforming technologies: Comparison with dry reforming. *J. CO2 Util.*, Elsevier, v. 17, p. 99–111, jan 2017. ISSN 22129820.

58 YAN, Y. et al. Thermodynamic Analysis on Reaction Characteristics of the Coupling Steam, CO ₂ and O ₂ Reforming of Methane. *J. Energy Resour. Technol.*, v. 140, n. 10, p. 102203, 2018. ISSN 0195-0738.

59 KHAJEH, S.; Arab Aboosadi, Z.; HONARVAR, B. Optimizing the fluidized-bed reactor for synthesis gas production by tri-reforming. *Chem. Eng. Res. Des.*, Institution of Chemical Engineers, v. 94, n. September, p. 407–416, 2015. ISSN 02638762.

60 CHEIN, R. Y.; HSU, W. H. Analysis of syngas production from biogas via the tri-reforming process. *Energies*, v. 11, n. 5, 2018. ISSN 19961073.

61 SMITH, G. P. et al. *GRI-Mech 3.0*. In: <http://www.me.berkeley.edu/gri_mech/>.

62 ZHANG, Y.; ZHANG, S.; BENSON, T. A conceptual design by integrating dimethyl ether (DME) production with tri-reforming process for CO2 emission reduction. *Fuel Process. Technol.*, Elsevier B.V., v. 131, p. 7–13, 2015. ISSN 03783820.

63 ZHANG, Y. et al. Process simulation and optimization of methanol production coupled to tri-reforming process. *Int. J. Hydrogen Energy*, v. 38, p. 13617–13630, 2013.

64 QIAN, Y. et al. Integrated Process of Coke-Oven Gas Tri-Reforming and Coal Gasification to Methanol with High Carbon Utilization and Energy Efficiency. *Ind. Eng. Chem. Res.*, v. 54, n. 9, p. 2519–2525, 2015. ISSN 0888-5885.

65 DAMANABI, A. T.; BAHADORI, F. Improving GTL process by CO2 utilization in tri-reforming reactor and application of membranes in Fisher Tropsch reactor. *J. CO2 Util.*, v. 21, p. 227–237, 2017. ISSN 2212-9820.

66 GRACIANO, J. E.; CHACHUAT, B.; ALVES, R. M. Conversion of CO2-Rich Natural Gas to Liquid Transportation Fuels via Trireforming and Fischer-Tropsch Synthesis: Model-Based Assessment. *Ind. Eng. Chem. Res.*, v. 57, n. 30, p. 9964–9976, 2018. ISSN 15205045.

67 ROSTRUP-NIELSEN, J. R. Catalytic Steam Reforming. In: *Catal. Sci. Technol. Vol. 5*. [S.l.: s.n.], 1984. cap. 1, p. 1–117.

68 GODINI, H. R. et al. Performance analysis of a porous packed bed membrane reactor for oxidative coupling of methane: Structural and operational characteristics. *Energy and Fuels*, v. 28, n. 2, p. 877–890, 2014. ISSN 08870624.

69 SALEHI, M. S. et al. Sustainable Process Design for Oxidative Coupling of Methane (OCM): Comprehensive Reactor Engineering via Computational Fluid Dynamics (CFD) Analysis of OCM Packed-Bed Membrane Reactors. *Ind. Eng. Chem. Res.*, v. 55, n. 12, p. 3287–3299, 2016. ISSN 15205045.

70 NIKOLAOU, Z. M.; CHEN, J. Y.; SWAMINATHAN, N. A 5-step reduced mechanism for combustion of CO/H2/H2O/CH4/CO2 mixtures with low hydrogen/methane and high H2O content. *Combust. Flame*, v. 160, n. 1, p. 56–75, 2013. ISSN 00102180.

71 ANDERSEN, J. et al. Global combustion mechanisms for use in CFD modeling under oxy-fuel conditions. In: *Energy and Fuels*. [S.l.: s.n.], 2009. v. 23, n. 3, p. 1379–1389. ISSN 08870624.

72 GOODWIN, D. G. et al. *Cantera: An object-oriented software toolkit for chemical kinetics, thermodynamics, and transport processes.* 2018.

73 E, J.; E, O.; P, P. *SciPy: Open Source Scientific Tools for Python*. 2001.

Appendix

APPENDIX A – COMPARISON OF MODEL AND LITERATURE

A.1 REACTION EQUILIBRIUM

The results of the thermodynamic equilibrium model were compared to literature data from 4 and 1, shown in Table 15 and Figure 37. The data of this work was indistinguishable from Zhang et al. and it approached the results of Song and Pan with differences below 3%.

Table 15 – Comparison of thermodynamic results of this (a) present work with (b) Song and Pan(4). Isothermal equilibrium at 850 °C and 1 atm.

Inlet Composition	$\mathbf{X}_{CH4}$		$\mathbf{X}_{CO2}$		$\mathbf{X}_{H2O}$		**H_2:CO**	
CH_4:CO_2:H_2O:O_2	(a)	(b)	(a)	(b)	(a)	(b)	(a)	(b)
1:0.475:0.475:0.1	98.00%	97.90%	87.20%	87.00%	76.90%	77.00%	1.67	1.67
1:0.45:0.45:0.2	99.00%	99.00%	75.50%	75.20%	55.70%	56.00%	1.68	1.69
1:0.375:0.375:0.5	99.80%	99.80%	29.30%	28.40%	-29.90%	-29.00%	1.7	1.71
1:1:1:0.1	99.80%	99.80%	53.60%	53.10%	26.20%	26.70%	1.47	1.48

Source: Own authorship and Song and Pan(4).

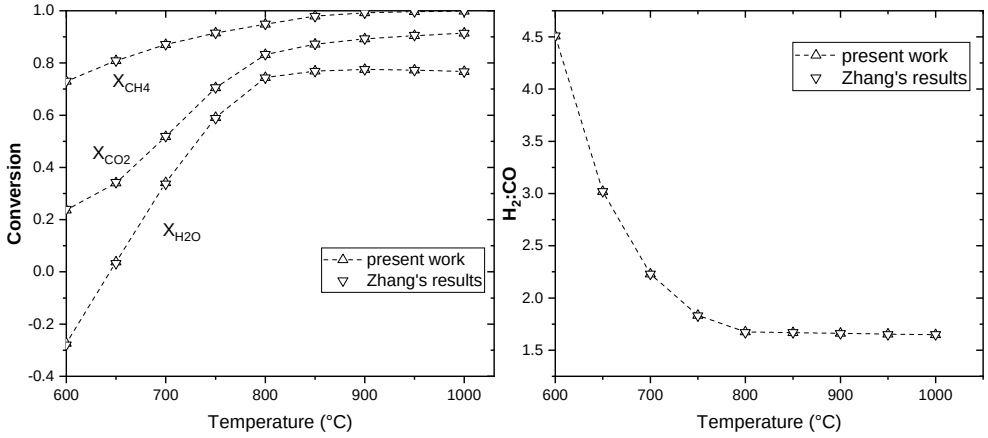

Figure 37 – Comparison of present model with data from (1).CH_4: CO_2: H_2O: O_2 = 1: 0.475: 0.475: 0.1

Source: Own authorship and Zhang et al.(1).

A.2 GRID ANALYSIS OF THE MEMBRANE REACTOR MODEL

Since the membrane reactor model was discretized, it is important to monitor the influence of the number of nodes in the results obtained. For this purpose, two variables were monitored in each section, temperature and methane molar flow. The relative difference

to the results from 300 nodes are shown in Figure 38. The case of comparison was for a 80% oxygen partition, feed temperature of 700 °C at 25 bar and composition of CH_4: CO_2: H_2O: O_2 = 1: 0.5: 1.75: 0.45 (and 1e-3 of H_2). The difference among different drops as the number of nodes increases and they were less than 3%.

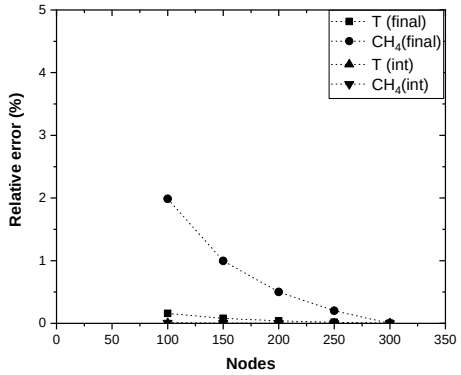

Figure 38 – Grid analysis for the membrane reactor model. The temperature and methane mole flow were monitored at 0.5 m (int) and 6 m (final) of reactor length.

Source: Own authorship.

A.3 COMBUSTION SECTION OF ATR

The results obtained by the homogeneous section of the autothermal model were compared to the results from Cho et al.(56). The present model followed closely the results showed by Cho et al. with maximum relative difference of 6%.

Table 16 – Literature comparison of outlet stream of a combustion section of an autothermal reactor for TRM. Feed is composed of CH_4: CO_2: H_2O: O_2 = 1: 1.08: 1.08: 0.644

		This work	**Cho**	**Relative difference**
CH_4	**(mol/s)**	2.12	2.20	0.04
H_2	**(mol/s)**	5.90	6.30	0.06
CO	**(mol/s)**	7.44	7.70	0.03
H_2: CO	–	0.79	0.82	0.04